AD-A189 644

APPLICATION OF EIGENSTRUCTURE ASSIGNMEN'
TECHNIQUES IN THE DESIGN OF A
LONGITUDINAL FLIGHT CONTROL SYSTEM

THESIS

Daniel G. Goddard

AFIT/GAE/AA/87S-2

DTIC
SELECTED
MAR 0 3 1988
E

DEPARTMENT OF THE AIR FORCE
AIR UNIVERSITY
# AIR FORCE INSTITUTE OF TECHNOLOGY

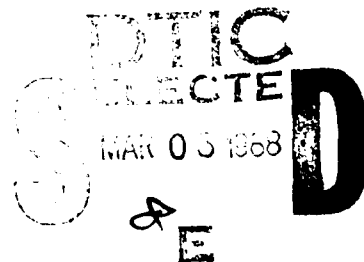Wright-Patterson Air Force Base, Ohio

88 3 01 04

AFIT/GAE/AA/87S-2

APPLICATION OF EIGENSTRUCTURE ASSIGNMENT
TECHNIQUES IN THE DESIGN OF A
LONGITUDINAL FLIGHT CONTROL SYSTEM

THESIS

Daniel G. Goddard

AFIT/GAE/AA/87S-2

AFIT/GAE/AA/87S-2

APPLICATION OF EIGENSTRUCTURE ASSIGNMENT TECHNIQUES
IN THE DESIGN OF A LONGITUDINAL FLIGHT CONTROL SYSTEM

THESIS

Presented to the Faculty of the School of Engineering
of the Air Force Institute of Technology
Air University
In Partial Fulfillment of the
Requirements for the Degree of
Master of Science in Aeronautical Engineering

Daniel G. Goddard

September 1987

Approved for public release; distribution unlimited

## Acknowledgements

There are several people whose support and guidance made
the completion of thesis project attainable. Capt. Dan
Gleason, my thesis advisor, was very helpful in pressing me
to stay on schedule and providing guidance when I needed it.
His hands-off approach made the project a better learning
experience for me. Mr Paul Blatt, my branch chief at
AFWAL/FIGD, allowed me to go to school full-time despite
whatever hardships my absense may have caused the branch. A
special thank-you to Mr Calvin Dyer, my immediate supervisor
and an exemplary engineer. His common sense approach to
engineering problems helped me over a number of hurdles.

Lastly, and most importantly, I would like to give my
deepest thanks to my wife and three children for their
support and understanding. Without question, my wife had the
tougher job during the last nine months.

Dan Goddard

# Table of Contents

## List of Figures

## List of Tables

# List of Symbols

| | | |
|---|---|---|
| $A$ | – | plant matrix |
| $\tilde{A}$ | – | augmented plant matrix ($A + BK$) |
| $\alpha$ | – | angle-of-attack |
| AR | – | Analog Reversion mode of the X-29A |
| ARG | – | indicates the phase angle of a transfer function |
| $\text{ARG}_{pc}$ | – | amount of phase lead or lag added by the pilot |
| $\text{ARG}_{ad}$ | – | amount of phase lead or lag added by the pilot in the simplified Neal-Smith criteria |
| $a_{z_{cg}}$ | – | normal acceleration at the center-of-gravity |
| $B$ | – | input matrix |
| $(BW)_{min}$ | – | minimum bandwidth |
| CAP | – | Control Anticipation Parameter |
| $\delta_s$ | – | strake deflection |
| $\delta_f$ | – | flaperon deflection |
| $\delta_c$ | – | canard deflection |
| $e^{-.3s}$ | – | pilot delay due to reaction time, neuromuscular delay, and other effects |
| FCDL | – | Flight Control Development Laboratory (AFWAL) |
| $g$ | – | acceleration due to gravity - 32.17 ft/sec$^2$ |
| HQ | – | Handling Qualities |
| HO | – | High-Order |
| HUD | – | Head-Up Display |
| $I$ | – | identity matrix |
| $K$ | – | feedback gain matrix |
| $K_p$ | – | pilot gain |
| LAMARS | – | Large Amplitude Multi-Mode Aerospace Research Simulator |
| $\lambda_i$ | – | eigenvalue |
| $\Lambda$ | – | eigenvalue matrix |
| LO | – | Low-Order |
| $M_u$ | – | dimensional aerodynamic derivative relating a change in forward speed to a change in pitching moment - 1/(sec·ft) |
| $M_\alpha$ | – | dimensional aerodynamic derivative relating a change in angle-of-attack to a change in pitching moment - 1/sec$^2$ |
| $M_{\dot{\alpha}}$ | – | dimensional aerodynamic derivative relating a change in angle-of-attack rate to a change in pitching moment - 1/sec |

$M_q$ — dimensional aerodynamic derivative relating a change in pitch-rate to a change in pitching moment - 1/sec

$M_\delta$ — dimensional control derivative relating a change in control surface deflection to a change in pitching moment - $1/sec^2$

MODES — Multi-Input/Multi-Output Designated Eigen-structure

$n/\alpha$ — normal acceleration change per unit angle-of-attack

$p_i$ — eigenvector

$p_A$ — achievable eigenvector

$p_D$ — desired eigenvector

$P$ — modal matrix

PR — Pilot Rating

PIO — Pilot Induced Oscillation

$q$ — pitch-rate

$\tau_{p_1}$ — pilot lead added

$\tau_{p_2}$ — pilot lag added

$\theta$ — pitch angle

$\theta/F_s$ — open-loop transfer function, no pilot model

$\theta/\theta_e$ — open-loop transfer function, with pilot model

$\theta/\theta_c$ — closed-loop transfer function, with pilot model

$u$ — forward velocity

$\bar{u}$ — control vector $(\delta_s, \delta_f, \delta_c)$

$U_.$ — steady-state forward velocity

$V_{TO}$ — total velocity

$w$ — normal velocity

$W_.$ — steady-state normal velocity

$\omega_n$ — undamped natural frequency

$\omega_{sp}$ — undamped natural frequency, short-period

$\omega_{ph}$ — undamped natural frequency, phugoid

$\bar{x}$ — state vector $(u, \alpha, q, \theta)$

$X_u$ — dimensional aerodynamic derivative relating a change in forward speed to a change in total drag - 1/sec

$X_\alpha$ — dimensional aerodynamic derivative relating a change in angle-of-attack to a change in total drag - $ft/sec^2$

$X_{\dot{\alpha}}$ — dimensional aerodynamic derivative relating a change in angle-of-attack rate to a change in total drag - ft/sec

$X_q$ — dimensional aerodynamic derivative relating a change in pitch-rate to a change in total drag - ft/sec

$X_\delta$ — dimensional control derivative relating a change in control surface deflection to a change in total drag - ft/(sec$^2$·rad)

$\xi_{sp i}$ — i$^{th}$ element of the short-period eigenvector pair

$\xi_{ph i}$ — i$^{th}$ element of the phugoid eigenvector pair

$Y_p$ — pilot model transfer function

$Z_u$ — dimensional aerodynamic derivative relating a change in forward speed to a change in total lift - 1/sec

$Z_\alpha$ — dimensional aerodynamic derivative relating a change in angle-of-attack to a change in total lift - ft/sec$^2$

$Z_{\dot\alpha}$ — dimensional aerodynamic derivative relating a change in angle-of-attack rate to a change in total lift - ft/sec

$Z_q$ — dimensional aerodynamic derivative relating a change in pitch-rate to a change in total lift - ft/sec

$Z_\delta$ — dimensional control derivative relating a change in control surface deflection to a change in total lift - ft/(sec$^2$·rad)

$\zeta$ — damping ratio

$\zeta_{sp}$ — damping ratio, short-period

$\zeta_{ph}$ — damping ratio, phugoid

## Abstract

The use of eigenstructure assignment techniques has received wide attention as a tool for designing flight control systems for aircraft with multiple control surfaces. One drawback for using this technique is a lack of handling quality guidelines to apply when selecting the eigenvalues and eigenvectors of the closed-loop system. This lack of specific eigenstructure requirements means that some uncertainty will remain as to whether the augmented control system will meet the MIL-F-8785C specifications.

. Therefore, development of a method for choosing the desired eigenstructure of the augmented, closed-loop system which would meet the handling qualities specifications was examined. This method consisted of forming an "optimal" plant matrix which possessed desirable dynamic characteristics and performing a spectral decomposition of this matrix. The resulting eigenstructure was used as the desired eigenvalues and eigenvectors during the full-state feedback, eigenstructure assignment process. The resulting feedback gain matrix was used in the control system.

As an example, this process was performed on a model of the X-29A using the canard, flaperon, and strake flap control surfaces. The resulting augmented system was evaluated using the Neal-Smith pilot-model analysis and also using an X-29A man-in-the-loop simulation. The results show that the method is very promising, although care must be taken that all anticipated control system dynamics are considered when forming the optimal A matrix.

# APPLICATION OF EIGENSTRUCTURE ASSIGNMENT TECHNIQUES
# IN THE DESIGN OF A LONGITUDINAL FLIGHT CONTROL SYSTEM

## I.  Introduction

### Background

Because of the increasing demands being placed on today's fighter aircraft, each aircraft system must be exploited to its fullest potential in order to yield superior performance and maneuverability. Engineers within the aerospace community are continually searching for innovative designs which will prove superior to present and future threats. One of the consequences of trying to increase the maneuverability of our aircraft is that inherent aerodynamic instabilities are being tolerated by aircraft designers in order to attain the quicker maneuvering response which static instabilities allow.

An unstable aircraft demands a closed-loop flight control system to maintain steady-state flight. Pilot reaction time and work-load restrictions demand that the aircraft exhibit predictable flying characteristics, at least from the pilot's perspective. In addition, multiple control surfaces per aircraft control axis are being used to decouple the characteristic modes or to allow for controlled flight in the post-stall regime [1:27,33]. Again, a flight control system is needed to deflect multiple control surfaces in the correct proportion so that the aircraft responds as the pilot has commanded through the cockpit controls.

The use of feedback to augment a control system is a well-known and accepted practice. It is done for a number of reasons including:  improving the stability of the system,

1

reducing sensitivity to modeling inaccuracies, and changing the response behavior of the system. In the design of an aircraft flight control system for an aerodynamically unstable aircraft for which only wind tunnel or other empirical data exists, all three of these reasons for feedback are pertinent.

The application of eigenstructure assignment techniques using full-state or output feedback has been developed and used in the last ten years to fulfill the three previously mentioned requirements, especially with the emergence of fly-by-wire control systems. Eigenstructure assignment also has advantages over classical design techniques for Multiple-Input/Multiple-Output (MIMO) systems. While application of the eigenstructure assignment techniques has progressed rapidly, there still exists some difficulty relating the choice of the desired eigenvalues and eigenvectors to the requirements of aircraft handling qualities. In the final analysis, the complete, augmented closed-loop system must behave in a manner acceptable to the pilot.

The MIL-F-8785C document "Military Specification-Flying Qualities of Piloted Airplanes" [2], along with its handbook "Background Information and User Guide for MIL-F-8785C" [3], currently contain the guidelines used by aircraft control system engineers to help insure that the resulting system will be acceptable to the pilot. However, the specifications of MIL-F-8785C were written when the classical frequency domain methods of control theory were used to design flight control systems. The control engineer using modern control theory cannot directly design the entire eigenstructure by these same specifications. One is, therefore, somewhat at a loss when choosing eigenvalues and especially eigenvectors,

2

for the augmented control system. In addition, the draft for the new flying qualities standard does not directly address eigenvalues or eigenvectors [4].

This lack of specific eigenstructure requirements means that despite the fact that eigenstructure assignment is a very powerful tool, some uncertainty will remain as to whether the augmented control system will meet the MIL-F-8785C specifications. Usually, this uncertainty leads to an iterative procedure involving analyzing a prospective control system using a manned simulation or pilot-model analysis tool, and then modifying the control system based on the results of the developmental studies. Ideally, given a reasonably accurate aircraft model, one would like to be able to make only one iteration in the design of a flight control system. This means having the capability of picking a realizable eigenstructure which will yield satisfactory handling qualities the first time.

## Problem

Development of a method for choosing the desired eigenstructure of the augmented, closed-loop system which would meet the handling qualities specifications and, furthermore, achieving this eigenstructure through the use of eigenstructure assignment would eliminate the uncertainty of using this design technique. This entails examining MIL-F-8785C and the associated Handbook and identifying key parameters which can be, either directly or indirectly, translated into a specification of the eigenstructure. This method should be proven by an appropriate example which includes the selection of the eigenstructure, application of eigenstructure assignment, and evaluation of the resulting closed-loop system by pilots.

3

## Summary of Current Knowledge

It is well known that a dynamic system and in particular, an aircraft's equations-of-motion, can be represented by n first-order, linear, time-invariant, differential equations of the form:

$$\dot{\bar{x}}(t) = A\bar{x}(t) + B\bar{u}(t) \tag{1.1}$$

where
$\bar{x}$ = nx1 state vector
$\bar{u}$ = mx1 control vector
A = nxn plant matrix
B = nxm input matrix

For the longitudinal axis of an aircraft, the **A** and **B** matrices are found by linearizing the vehicle's equations-of-motion about a trim condition and then writing the stability axis equations in matrix form. McRuer, et al. contains a rigorous treatment of aircraft equations-of-motion [5:Chap 5].

When full-state feedback is applied to a system, the knowledge of the state of the system is used to change the input in order to make the output behave in some desired manner. An example of a common feedback control system is the cruise control available on cars. In this application the speed of the car is the output of the system and is fed back to the input, the accelerator.

In multivariable systems, a feedback matrix **K** is formed and used to modify the control vector, $\bar{u}(t) = K\bar{x}(t)$ . The state space representation can now be written as:

$$\dot{\bar{x}}(t) = (A + BK)\bar{x}(t) \tag{1.2}$$

4

The quantity (A + BK) represents the closed-loop system, and the problem remains to determine K so that the system has desirable behavior.

As is well known, the dynamic response of a linear system is determined by the system's eigenvalues and eigenvectors. Elbert [6] or Reid [7] contain a thorough treatment of linear systems theory. The eigenvalues are simply the roots of the characteristic equation for the system:

$$\det(A + BK - \lambda I) = 0 \tag{1.3}$$

where I is the identity matrix and $\lambda$ are the n eigenvalues. The eigenvalues control the rate of decay or growth of the characteristic modes of response of the system. The eigenvectors are found by solving:

$$(A + BK)p_i = p_i \lambda_i \tag{1.4}$$

where $p_i$ is the eigenvector associated with the $i^{th}$ eigenvalue. The eigenvectors control the shape of the response for a given mode. The totality of the eigenvalues and eigenvectors is the eigenstructure of a system. By picking the eigenstructure for a system, one can control how the system will respond to inputs, disturbances, initial conditions, etc.

Eigenvalue placement has been used since the early 1960's, but placing the eigenvectors was not addressed until 1976 when B. C. Moore published a method for placing both the eigenvalues and eigenvectors [8]. He identified the necessary and sufficient conditions for simultaneous eigenvalue and eigenvector assignment. This early technique was restrictive in that it did not accommodate repeated eigenvalues, and it permitted only certain eigenvectors to be

5

placed. This restriction was characterized by G. Klein as a "class of generalized eigenvector chains" [9:140].

Around this time, many control system engineers realized that while full-state feedback permitted a good deal of flexibility in placing the eigenstructure, the necessity of measuring and feeding back the entire state was not practical. The types of measurement instrumentation needed for feedback are expensive, sensitive to disturbances, and require frequent calibration, making them prohibitive to use in the flight environment. Since the outputs are already a measured variable (all systems have some output or there would be no point to the system), there would be no additional measurements needed for the feedback signals. However, since the number of outputs is usually less than the number of states, the ability to control the eigenstructure placement is diminished.

Although this study used full-state feedback, it is interesting to briefly examine the emergence of output feedback. In 1978, S. Srinathkumar wrote the benchmark paper on eigenstructure assignment using output feedback. He defined the sufficient conditions under which the eigenvalues and eigenvectors can be assigned and set the stage for the second leap in the use of this design technique [10]. Srinathkumar determined the maximum number of eigenvalues and eigenvectors which can be placed for a given system. He concluded that "in addition to assigning min(n, m+r-1) eigenvalues (r-1) eigenvectors can be partially assigned with m entries in each vector arbitrarily chosen" [10:80]. In Srinathkumar's paper, m is the number of inputs and r is the number of outputs. For the state space model shown in Equation (1.1), Srinathkumar's argument would correspond to assigning n eigenvalues and a maximum of m elements of each

6

eigenvector. This number of eigenvalues and eigenvector elements assumes that the system is completely controllable, which is not always the case.

The Advanced Fighter Technology Integration (AFTI) F-16 aircraft was repeatedly used to demonstrate the advantages of output feedback. This aircraft has additional control surfaces which allow it to fly unlike any previous airplane. The additional control surfaces mean that the AFTI system's control matrix is of higher dimension than that for a conventional aircraft. For this design, control engineers had multiple inputs which would permit enhanced placement of the eigenstructure. Designing control laws for the AFTI F-16 became very popular as a means to display new thoughts and methods on output feedback for eigenstructure assignment. The designs successfully decoupled the characteristic modes of the aircraft and gave the engineers insight as to how the eigenvectors shaped the modes of a system [11,12].

A landmark paper was written by Andry, et al. in 1983 which summarized eigenstructure assignment including full-state and output feedback. An examination was also made into how the eigenvalues and eigenvectors affected the handling qualities of the aircraft; that is, how easy or difficult is it for the pilot to fly the aircraft under various conditions? They presented eigenvectors which would generally yield good handling qualities [13:719]. Still, many of the components of the eigenvectors were assigned arbitrarily and much of the eigenvector placement remains guesswork or based on experience.

There remains a good deal of research to be performed in defining the relationship between eigenstructure placement and aircraft handling qualities. Part of the difficulty in correlating aircraft handling qualities to flight control

7

system design is that handling quality ratings are, for the most part, the subjective evaluations of pilots. Therefore, one must always balance a pilot's ratings with his background and flying technique.

The specification document for aircraft handling qualities is written in parameters which are easily interpreted in classical control theory but which have less direct meaning in modern control theory. Further research into this relationship and more specifically, defining handling qualities parameters in terms of the eigenstructure, would make it much easier to apply this technique to aircraft control system design. Work by Stein and Henke [14] proposed a method for forming an optimal plant matrix which could subsequently be decomposed into its eigenvalues and eigenvectors. This eigenstructure could then be used in the eigenstructure assignment procedure. This procedure will be examined further in Section III.

## Scope

This study will accomplish each key step in the flight control design procedure in order to prove that the proposed eigenstructure selection process is applicable. The X-29A Advanced Technology Demonstrator was chosen as the study aircraft primarily because it is an aerodynamically unstable aircraft that requires stability augmentation, and also because it has three pitch control surfaces which will allow fuller assignment of eigenvector elements.

Extensive use will be made of the Flight Control Development Laboratory's simulation of the X-29A. This facility is located within the Flight Dynamics Laboratory at Wright-Patterson Air Force Base. The simulation is a high-fidelity, 6 degree-of-freedom simulation which drives

8

the Large Amplitude Multi-Mode Aerospace Research Simulator (LAMARS) motion-base simulator. This simulation was used extensively during the design and check-out of the X-29A prior to its first flight in 1984 and was used more recently to examine the X-29A's high angle-of-attack capabilities. The simulation incorporates the Grumman aerodynamic data and flight control systems and includes fourth-order actuator models on an analog computer. Sensor models are not used in this simulation. The equations-of-motion are nonlinear, and the simulation is valid in the entire X-29A flight envelope.

The longitudinal control law designed in this study will be used to replace the Analog Reversion mode longitudinal control path. The Normal Digital mode was not selected to be replaced due to the increased complexity of this control law which includes fault protection, automatic wing camber control, degraded modes, sensor failure contingencies, and other elements which must be taken into consideration when developing a flight-ready control system.

Full-state feedback will be used in the control system design. This method may not be practical for a flight-ready application because of the expense and difficulty of measuring the states, however, it is acceptable here since this study emphasizes the eigenstructure selection process and not how the feedback paths would be implemented on an actual aircraft.

A limited number of up-and-away flight conditions will be examined using an air-to-air pitch tracking task for the piloted portion of the evaluation. No sensitivity or surface failure analyses will be done. The center-stick feel system characteristics will not be altered from those of the actual aircraft.

## Approach

The development and evaluation of the control law for this study can be separated into five distinct steps:

1. Linearization of the X-29A airframe and the generation of the state space matrices

2. Selection of the desired eigenstructure by forming an ideal plant matrix and performing a spectral decomposition of this matrix

3. Utilization of eigenstructure assignment to obtain the feedback gain matrix

4. Generation of a pilot model to accomplish an off-line analysis of the closed-loop system

5. Implementation of the control law on the LAMARS and piloted evaluations of the aircraft

Each of these steps will be discussed briefly in the remainder of this section.

Linearization. A linearized model of the X-29A airframe was obtained. In order to include both the rigid body derivatives and flexible body increments in the linear model, and to have an accurate representation of the LAMARS simulation, the simulations's aerodynamic model was linearized rather than using existing Grumman or NASA linearized aerodynamic data. The state variables and control surfaces were perturbated about trim equilibrium conditions, and nondimensional stability and control derivatives were obtained. The longitudinal state variables used for this study were:

u - forward velocity (feet per second)

$\alpha$ - angle-of-attack (radians)

q - pitch rate (radians per second)

$\theta$ - pitch angle (radians)

10

The three pitch control surfaces are the close-coupled, all-moving canard; variable camber, trailing-edge flaps; and the strake flaps. The nondimensional stability and control derivatives were transformed into the dimensional derivatives used to calculate the elements of the **A** and **B** matrices of the linear, time-invariant system.

Eigenstructure Selection. Choosing the desired eigenvalues and eigenvectors of the augmented matrix was one of the most challenging parts of this study. Sufficient empirical data exists to choose eigenvalues which should yield good response decay rates. However, when picking the eigenvectors, in the past, one relied upon a few broad statements (such as orthogonality of the short period and phugoid modes, and the null participation of certain vectors in certain responses) and experience. This study generated the eigenvalues and eigenvectors by building an optimal **A** matrix based on knowledge about the relationship between aircraft response performance and the dimensional stability derivatives. This ideal matrix was then decomposed into its eigenvalues and eigenvectors, and these became the desired eigenstructure of the control law design.

Control Law Design. Eigenstructure assignment using full-state feedback was used to develop a feedback gain matrix, **K** . A computer program called MODES (see Ref. 15 for a description) was used to perform this task in a quick and efficient manner. Since all the states were available in the simulation, full-state feedback was easily accomplished. The closed-loop system matrix, (**A** + **BK**) , decomposed into the desired eigenstructure described in the previous section. In this case, the **A** and **B** matrices were the bare airframe X-29A plant and control matrices, respectively.

11

Off-line Analysis. A linear pilot model was used to
check that the pilot-aircraft dynamic system exhibited good
performance. The pilot model used was sufficient to account
for the capabilities and limitations of the pilot in the
closed-loop system. The form of the pilot model used in this
study is based on the Neal-Smith report [16]:

$$Y_p = \frac{K_p \, e^{-\tau s}(\tau_{p_1} s + 1)}{(\tau_{p_2} s + 1)} \tag{1.5}$$

where
$Y_p$ = pilot model transfer function
$K_p$ = pilot gain
$e^{-\tau s}$ = pilot's neuromuscular time delay, $\tau = 0.3$ sec
$\tau_{p_1}$ = pilot lead added
$\tau_{p_2}$ = pilot lag added


LAMARS Simulation. The final version of the control law
was integrated into the LAMARS simulation. Once the Analog
Reversion control system had been modified with the new
longitudinal control law, digitally controlled inputs into
the control system were used to generate time histories.
These were used to check for proper implementation of the
control law and for any additional time delay which may have
been introduced. An air-to-air tracking task was employed to
obtain Cooper-Harper handling quality ratings from the pilot
during the man-in-the-loop simulation runs. The
Cooper-Harper scale is an accepted pilot ratings tool that
has been used in flight testing for over 15 years [17]. A
correlation between Cooper-Harper ratings and flying quality
level is addressed in MIL-F-8785C. A sufficiently large test
matrix was used in the piloted sumulations in order to obtain
bias-free pilot ratings.

## Equipment

The primary resources necessary to accomplish this study were contained within the LAMARS simulation facility. The X-29A simulation uses a Gould/SEL 32/77 and 32/97 digital computer, as well as an EAI 781 analog computer connected by an EAI Hyshare system. A CSPI MAP multi-array processor is used for the aerodynamic table look-ups. The LAMARS itself is a five degree-of-freedom, beam-type motion simulator. The 20-foot-diameter dome contains a single-seat fighter cockpit and spherical dome display with a target projector. The cockpit was configured as a generic fighter for this study with a head-up display, center stick, throttle quadrant, and standard front-panel instrumentation. The center-stick was programmed to have the X-29A's feel system characteristics such as the stick force gradient and break-out forces. The head-up display presented a fixed reticle for the pilot as well as the pitch command tracking bar.

The interactive design program TOTAL, hosted on the ASD Cyber system, was used to manipulate transfer functions and obtain preliminary Nichol's plots. Also, as previously mentioned, the MODES program was used to find the feedback matrix. This program is available either on an AFIT minicomputer, or it can be used on a personal computer.

13

## II.  Linearization of the X-29A

One of the basic elements needed to perform eigenstructure assignment is a mathematical model of the unaugmented system in state-space form.  Since pilot handling quality ratings were to be taken from the LAMARS man-in-the-loop simulation of the X-29A supplemented with the control law designed in the course of this project, it was necessary to obtain an accurate model of the LAMARS simulation, rather than using existing NASA or Grumman linearized data.  This was necessary since models of the X-29A aerodynamics used by the various agencies varied in the level of sophistication and the revision level implemented. The aerodynamic model used on the LAMARS is referred to as AERO7B by the X-29A community.  It is a six degree-of-freedom nonlinear model which includes flexibility increments and contains over 60,000 data points.  It is valid in the entire X-29A envelope and is modified to handle high aircraft angles-of-attack (-50 to + 90 degrees AOA).  For this study, four flight conditions were examined and feedback gain matrices were found for each.  The elements of the gain matrices were then curve fit between the flight conditions to provide a piecewise linearization.  The flight conditions studied were Mach = 0.6, 0.8 and altitude = 10K, 30K feet.

## Formulation of the Linearized Equations of Motion

The linearized, perturbation equations-of-motion were taken from Reference 5.  The equations-of-motion were needed in the body reference frame for the X-29 linearization but also were needed in the stability axis frame for use in the development of the optimal eigenstructure, discussed in Section III.  Only the body axis equations will be discussed

14

here and the body axis frame is shown in Figure 1. A number
of assumptions were made during the formulation of the
equations and are listed below:

1) The airplane is a rigid body.
2) The earth is fixed in space.
3) The airplane has constant mass and mass distribution.
4) The XZ plane is a plane of symmetry.
5) All angles are small.
6) Steady-state lateral trim conditions are $P_o = R_o = V_o = \Phi_o = 0$.
7) The flow is quasisteady.
8) Variations of atmospheric properties are negligible for small altitude perturbations.
9) The earth is flat.

The resulting equations, in the body axis frame, are shown
below:

$$\dot{u} - X_{\dot{\alpha}}\, \dot{\alpha} = X_u\, u + X_\alpha\, \alpha + (X_q - W_o)q - g \cos \theta_o\, \theta$$
$$+ X_{\delta_s} \delta_s + X_{\delta_r} \delta_r + X_{\delta_c} \delta_c \qquad (2.1)$$

$$(U_o - Z_{\dot{\alpha}})\dot{\alpha} = Z_u\, u + Z_\alpha\, \alpha + (Z_q + U_o)q - g \sin \theta_o\, \theta$$
$$+ Z_{\delta_s} \delta_s + Z_{\delta_r} \delta_r + Z_{\delta_c} \delta_c \qquad (2.2)$$

$$-M_{\dot{\alpha}}\, \dot{\alpha} + \dot{q} = M_u\, u + M_\alpha\, \alpha + M_q\, q + M_{\delta_s} \delta_s + M_{\delta_r} \delta_r + M_{\delta_c} \delta_c \qquad (2.3)$$

$$\dot{\theta} = q \qquad (2.4)$$

In these equations, $\delta_s$ , $\delta_r$ , and $\delta_c$ are the strake flap,
symmetric flaperon, and canard surface deflections,
respectively. These control surfaces are shown in Figure 2.

The equations-of-motion were needed in state-space form
for the eigenstructure assignment process. This was quickly
accomplished and Equation (2.5) is the resulting form.

15
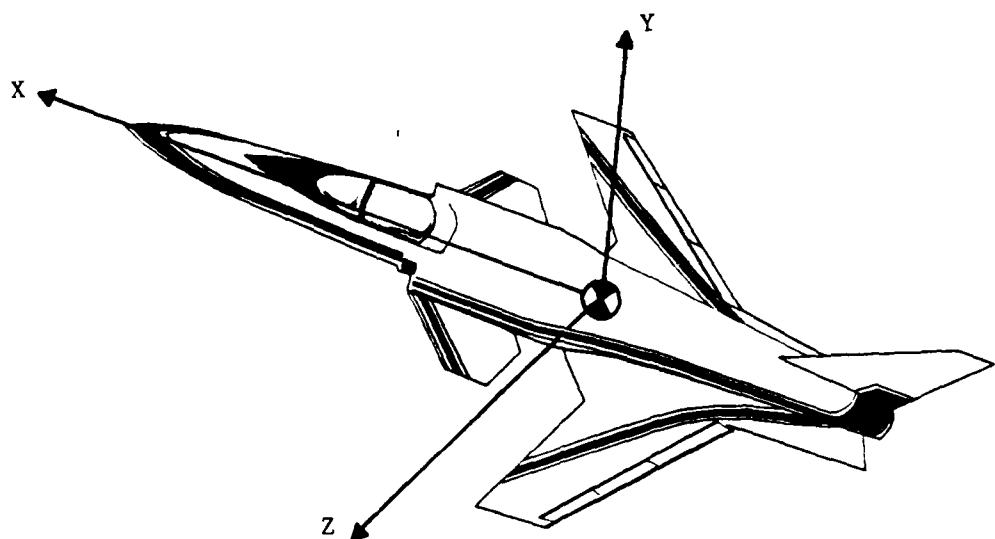
X-axis out nose
Y-axis out right wing
Z-axis completes orthogonal
right-hand system

Figure 1.  X-29A Body Axis Reference Frame

16

Figure 2. X-29A Control Surface Definition

17
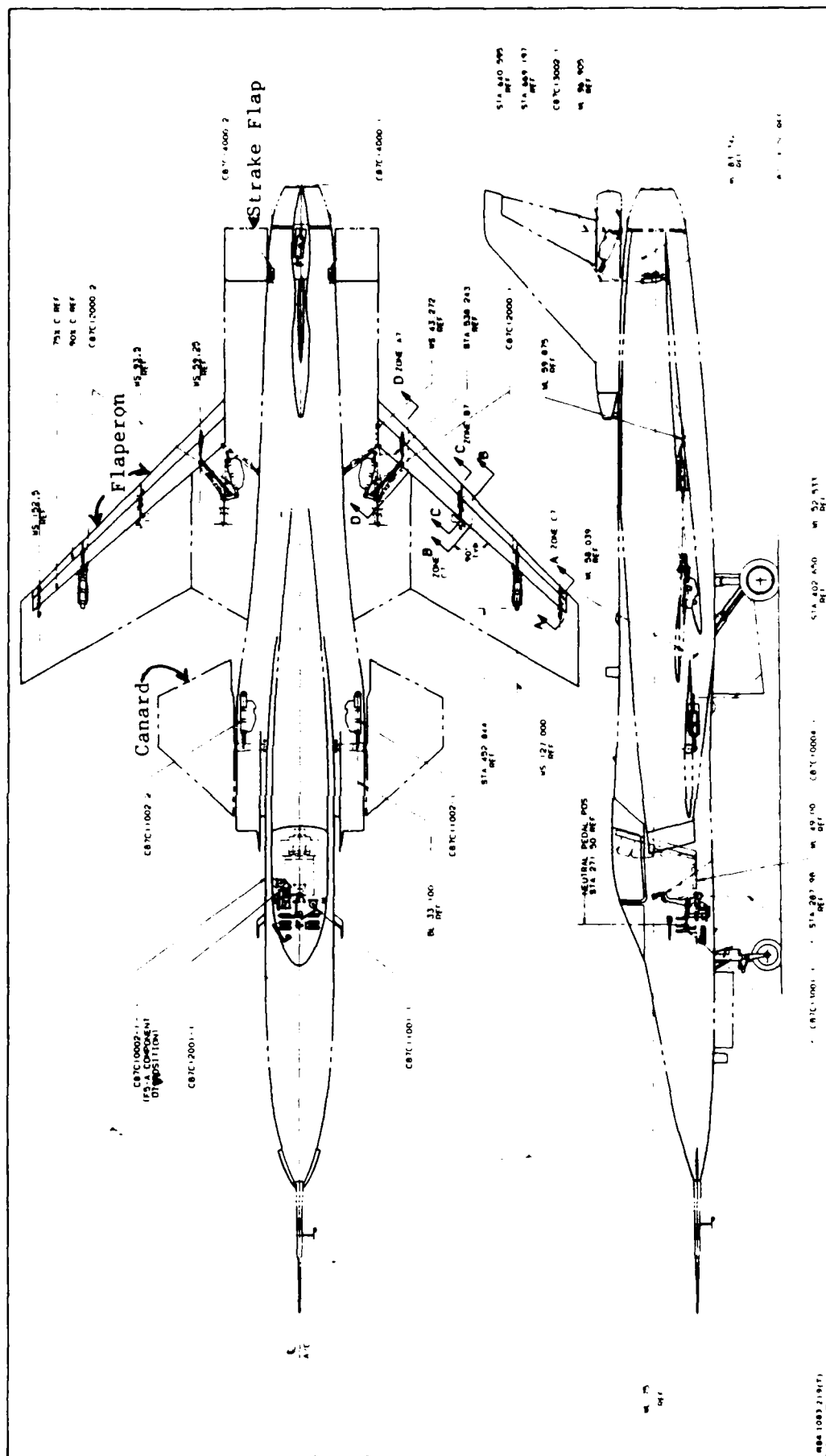
$$
\begin{bmatrix} \dot{u} \\ \dot{\alpha} \\ \dot{q} \\ \dot{\theta} \end{bmatrix} = \begin{bmatrix} A_{11} & A_{12} & A_{13} & A_{14} \\ A_{21} & A_{22} & A_{23} & A_{24} \\ A_{31} & A_{32} & A_{33} & A_{34} \\ A_{41} & A_{42} & A_{43} & A_{44} \end{bmatrix} \begin{bmatrix} u \\ \alpha \\ q \\ \theta \end{bmatrix} + \begin{bmatrix} B_{11} & B_{12} & B_{13} \\ B_{21} & B_{22} & B_{23} \\ B_{31} & B_{32} & B_{33} \\ B_{41} & B_{42} & B_{43} \end{bmatrix} \begin{bmatrix} \delta_s \\ \delta_r \\ \delta_c \end{bmatrix}
$$

(2.5)

where

$$A_{11} = X_u + Z_u \frac{X_{\dot{\alpha}}}{(U_o - Z_{\dot{\alpha}})} \qquad A_{12} = X_\alpha + Z_\alpha \frac{X_{\dot{\alpha}}}{(U_o - Z_{\dot{\alpha}})}$$

$$A_{13} = (X_q - W_o) + (Z_q + U_o) \frac{X_{\dot{\alpha}}}{(U_o - Z_{\dot{\alpha}})}$$

$$A_{14} = -g \cos \theta_o - g \sin \theta_o \frac{X_{\dot{\alpha}}}{(U_o - Z_{\dot{\alpha}})}$$

$$A_{21} = \frac{Z_u}{(U_o - Z_{\dot{\alpha}})} \qquad A_{22} = \frac{Z_\alpha}{(U_o - Z_{\dot{\alpha}})}$$

$$A_{23} = \frac{(Z_q + U_o)}{(U_o - Z_{\dot{\alpha}})} \qquad A_{24} = \frac{-g \sin \theta_o}{(U_o - Z_{\dot{\alpha}})}$$

$$A_{31} = M_u + \frac{M_{\dot{\alpha}} Z_u}{(U_o - Z_{\dot{\alpha}})} \qquad A_{32} = M_\alpha + \frac{M_{\dot{\alpha}} Z_\alpha}{(U_o - Z_{\dot{\alpha}})}$$

$$A_{33} = M_q + \frac{M_{\dot{\alpha}} (Z_q + U_o)}{(U_o - Z_{\dot{\alpha}})} \qquad A_{34} = - \frac{M_{\dot{\alpha}} g \sin \theta_o}{(U_o - Z_{\dot{\alpha}})}$$

$$A_{41} = A_{42} = A_{44} = 0 \qquad A_{43} = 1$$

$$B_{11} = X_{\delta_s} + Z_{\delta_s} \frac{X_{\dot{\alpha}}}{(U_o - Z_{\dot{\alpha}})} \qquad B_{12} = X_{\delta_r} + Z_{\delta_r} \frac{X_{\dot{\alpha}}}{(U_o - Z_{\dot{\alpha}})}$$

$$B_{13} = X_{\delta_c} + Z_{\delta_c} \frac{X_{\dot{\alpha}}}{(U_o - Z_{\dot{\alpha}})}$$

$$B_{21} = \frac{Z_{\delta_s}}{(U_o - Z_{\dot{\alpha}})} \qquad B_{22} = \frac{Z_{\delta_r}}{(U_o - Z_{\dot{\alpha}})} \qquad B_{23} = \frac{Z_{\delta_c}}{(U_o - Z_{\dot{\alpha}})}$$

$$B_{31} = M_{\delta_s} + Z_{\delta_s} \frac{M_{\dot{\alpha}}}{(U_o - Z_{\dot{\alpha}})} \qquad B_{32} = M_{\delta_r} + Z_{\delta_r} \frac{M_{\dot{\alpha}}}{(U_o - Z_{\dot{\alpha}})}$$

$$B_{33} = M_{\delta_c} + Z_{\delta_c} \frac{M_{\dot{\alpha}}}{(U_o - Z_{\dot{\alpha}})} \qquad B_{41} = B_{42} = B_{43} = 0$$

## Linear Analysis

A computer program was written which quickly and efficiently computed the dimensional derivatives and formed the **A** and **B** matrices for the LAMARS X-29A simulation. First the aircraft was trimmed in one of the four flight conditions of interest. In the analog reversion mode, the strakes and canards are set to zero and only the flaperons are used to balance the forces when trimming. From the trimmed condition, one of the states was changed first through a small positive perturbation, then through an equal negative perturbation and the total aerodynamic nondimensional coefficients ($C_X$, $C_Z$, $C_M$) were determined from the X-29A simulation's aerodynamic model at each perturbation step. Once this was accomplished, the nondimensional stability derivatives were calculated ($C_{x_\alpha}$, $C_{z_u}$, $C_{m_q}$, etc) based on the difference between the aerodynamic coefficients for the positive and negative perturbations and the size of the perturbation. The variables perturbated were: alpha, alpha-dot, pitch-rate, Mach number, strake, flaperon, and canard. It should be noted that these coefficients were measured in the body axis frame.

Next the dimensional derivatives were formed from the nondimensional derivatives using the following equations:

$$X_u = \frac{\rho S U_o}{m} \left( \frac{M}{2} C_{x_M} + C_X - \frac{W_o}{2U_o} C_{x_\alpha} \right) \qquad \text{1/sec} \qquad (2.6)$$

$$X_\alpha = \frac{\rho S U_o^2}{2m} \left( C_{x_\alpha} + 2\frac{W_o}{U_o}(C_X + \frac{M}{2} C_{x_M}) \right) \qquad \text{ft/sec}^2 \qquad (2.7)$$

$$X_{\dot\alpha} = \frac{\rho S c\, U_o^2}{4m\ V_{TO}} C_{x_{\dot\alpha}} \qquad \text{ft/sec} \qquad (2.8)$$

$$X_q = \frac{\rho S c\, U_o^2}{4m\ V_{TO}} C_{x_q} \qquad \text{ft/sec} \qquad (2.9)$$

$$X_\delta = \frac{\rho S V_{TO}^2}{2m} C_{x_\delta} \qquad \text{ft/sec}^2/\text{rad} \qquad (2.10)$$

where $V_{TO}$ is the total velocity in ft/sec

And similarly for the Z and M derivatives.

With the dimensional derivatives in hand, the **A** and **B** matrices were formed using Equation (2.5). This process was repeated for each flight condition. The **A** and **B** matrices for Mach = 0.6 and altitude = 10k feet are shown below:

$$A = \begin{bmatrix} -.1262E-01 & .3680E+02 & -.3451E+02 & -.3213E+02 \\ -.8438E-04 & -.1048E+01 & .9906E+00 & -.2657E-02 \\ -.5757E-03 & .1687E+02 & -.4844E+00 & .1553E-03 \\ .0000E+00 & .0000E+00 & .1000E+01 & .0000E+00 \end{bmatrix}$$

$$B = \begin{bmatrix} .1590E+01 & .5594E+01 & -.7027E+01 \\ -.4534E-01 & -.3359E+00 & -.6440E-01 \\ -.2990E+01 & -.5455E+01 & .8449E+01 \\ .0000E+00 & .0000E+00 & .0000E+00 \end{bmatrix}$$

The computer program also accessed a subroutine which determined the eigenvalues of the **A** matrix. The dynamic characteristics for the characteristic modes were calculated from the eigenvalues. For the above flight condition , the eigenvalues and dynamic characteristics for the bare airframe are

$\lambda_1 = 3.334 + j(0.0)$            Unstable Short Period

$\lambda_2 = -4.865 + j(0.0)$

$\lambda_{3,4} = -.007138 \pm j(0.06258)$      Phugoid

          $\zeta = .11332$       $\omega_n = .06299$ rad/sec

20

While it has taken only a short section to describe the linearization process used to obtain the unaugmented **A** and **B** matrices of the X-29A, it should be noted that this was a very critical and laborious portion of the project. The importance of having an accurate state-space model has already been discussed.

The accuracy of the linearization process was checked by comparing the elements of the **A** and **B** matrices developed here to those appearing in a NASA X-29A linear analysis report [18]. The correlation was very good and the next step in the project was to develop a method to select desired eigenvalues and eigenvectors for the closed-loop system.

## III. Development of Optimal Eigenstructure

### Background

As has been previously argued in Section I, there is
little in the current handling quality specification which
can guide the control system designer wanting to use
eigenstructure assignment. Desirable eigenvalues can be
computed based on specifications of the system damping and
natural frequency, however there is no information in the
specifications which can be used to directly compute the
desired eigenvectors. One of the major challenges of this
effort was to derive a desirable eigenstructure from the
handling quality specifications.

Stein and Henke proposed a design procedure using
quadratic optimal control theory and a handling quality
oriented cost function for flight control systems. They used
data from MIL-F-8785 to define a system of differential
equations having the same form and desirable handling
qualities of the augmented aircraft [14: Sec II]. The
portion of their work of interest here is how they formed a
plant matrix possessing desirable handling qualities. Stein
and Henke applied their design procedure to the lateral-
directional axis. The following discussion extends their
work to the longitudinal axis, with the intent of using
full-state feedback.

### Handling Quality Model

The beginning point for generating the handling quality
model is the A (plant) matrix for the rigid-body, longi-
tudinal equations-of-motion, written in the stability axis
system. We want an A matrix which, when placed in the

$\dot{\bar{x}} = A\,\bar{x}$ system, will yield desired handling qualities as defined by the current MIL-PRIME Standard. This A matrix will provide the desired eigenstructure which will be used in the full-state eigenstructure assignment.

Since the elements of the A matrix are composed of the dimensional derivatives, the problem of forming the optimal matrix reduces to assigning values to these derivatives such that the optimal matrix results. If the dimensional derivatives can be related to handling quality specifications, then the optimal values of the dimensional derivatives can be solved for.

There are twelve longitudinal, aerodynamic dimensional derivatives. In order to solve explicitly for these twelve variables, one would need twelve linearly independent equations. Fortunately, four of the derivatives can be assummed zero:

$X_{\dot{\alpha}}$ - is primarily due to the change in drag on the pitch control surface which is small in comparison to the total drag [5:273]

$Z_{\dot{\alpha}}$ - is due to the change in lift on the pitch control surface primarily as a result of an aerodynamic time lag [5:274]

$X_q$ - again, the increased drag is negligible to the first approximation [5:275]

$Z_q$ - again, the increased lift has little effect and is neglected [5:277]

This leaves eight dimensional derivatives which must be solved for from eight as yet unknown equations. The approach taken to identify the eight equations was to sift through the MIL-PRIME Handbook and other handling quality sources and identify specifications which could be related to an

23

expression involving the dimensional derivatives. After
several passes through the documents, eight equations were
found and are discussed below, along with the handling
quality specification which corresponds to each equation.
When examining specifications from the literature, the flight
phase considered was Category A (air-to-air combat) and the
aircraft type was Class IV (high-maneuverability).

The MIL-PRIME Handbook provides recommended values for
the phugoid mode damping ratio, $\zeta_{ph}$ [4:186]. McRuer gives an
approximate form for the phugoid damping [5:336]:

$$2\zeta\omega_{ph} \cong -X_u - \frac{M_u(X_\alpha - g)}{\frac{1}{U_\circ}Z_\alpha M_q - M_\alpha} \qquad (3.1)$$

The MIL-PRIME Handbook doesn't address the natural
frequency of the phugoid, but a review of various aircraft's
dynamic characteristics can provide good values. The
approximate form for the phugoid natural frequency is [5:336]

$$\omega_{ph}^2 \cong \frac{g(M_\alpha Z_u - M_u Z_\alpha)}{Z_\alpha M_q - U_\circ M_\alpha} \qquad (3.2)$$

Recommended values for the short period damping are
found in MIL-F-8785C [2:13] and the short-period
approximation gives [5:336]

$$2\zeta\omega_{sp} \cong -(\frac{1}{U_\circ}Z_\alpha + M_q + M_{\dot\alpha}) \qquad (3.3)$$

The short-period natural frequency is partially
restricted by allowable values for the Control Anticipation
Parameter (CAP) which is directly proportional to $\omega_{sp}^2$
[4:192]. Also Etkin gives a range of values for $\omega_{sp}$ based on
experiments using a variable stability aircraft [19:513].
The short-period approximation for $\omega_{sp}$ is [5:336]

24

$$\omega_{sp}^{2} \cong \frac{1}{U_{o}} M_{q} Z_{\alpha} - M_{\alpha} \qquad (3.4)$$

Allowable values for the normal acceleration change per unit angle-of-attack, $n/\alpha$, are given in MIL-F-8785C [2:14]. An approximate form for $n/\alpha$ is given by Roskam [20:538]:

$$n/\alpha \cong -Z_{\alpha}/g \qquad (3.5)$$

The modal response ratios have a direct bearing on the eigenvectors. For the phugoid mode, Etkin [19:324] and McRuer [5:350] both state that there is a 90° phase difference between speed, $u$, and the pitch angle, $\theta$. This angle can be approximated by [5:350]

$$ARG \left(\frac{-\theta}{u}\right) \cong \tan^{-1} \frac{\omega_{ph}\sqrt{1 - \zeta_{ph}^{2}}}{\zeta\omega_{ph} + (g M_{u}/M_{\alpha})} \qquad (3.6)$$

For the short-period mode, Etkin [19:324] shows that the phase difference between $\alpha$ and $\theta$ is small and the angle can be approximated by [5:347]

$$ARG \left(\frac{\theta}{\alpha}\right) \cong \tan^{-1} \frac{Z_{\alpha}}{U_{o}\omega_{sp}}\sqrt{1 - \zeta_{sp}^{2}} \qquad (3.7)$$

The static to short-period gain ratio must be greater than allowable limits, as indicated in Reference 1, page 66. This corresponds to defining a minimum low-frequency gain margin. The static to short-period gain ratio can be be expressed as [5:424]

$$\frac{1}{\omega_{ph}^{2} T_{\theta_{1}} T_{\theta_{2}}} \cong \frac{Z_{\alpha}X_{u} - X_{\alpha}Z_{u}}{-g Z_{u}} \qquad (3.8)$$

These are the eight equations in eight unknowns that are required. When $\omega_{sp}$, $\omega_{ph}$, $\zeta_{sp}$, or $\zeta_{ph}$ appeared on the

25

right-hand side of an equation, they were replaced by the appropriate approximation expression.

Three sets of data were chosen for the handling quality parameters (the left-hand side of the equations): one set to yield good handling qualities, one to yield fair, and one to yield poor. These three sets correspond to Level 1, 2, and 3 respectively, as defined in the MIL-PRIME Handbook [4:96]. The values chosen for the handling quality parameters are shown in Table I.

Table I
Handling Quality Parameter Values

| Model Parameter | Good | Fair | Poor |
|---|---|---|---|
| $2\zeta\omega_{ph}$ | 0.007 | 0.002 | -0.004 |
| $\omega_{ph}^2$ | 0.0025 | 0.0025 | 0.0025 |
| $2\zeta\omega_{sp}$ | 4.90 | 1.50 | 0.40 |
| $\omega_{sp}^2$ | 12.25 | 4.0 | 1.0 |
| $n/\alpha$ | 30.00 | 20.00 | 20.0 |
| $ARG(\frac{-\theta}{u})_p$ | 85.00 | 70.00 | 45.0 |
| $ARG(\frac{\theta}{\alpha})_s$ | 15.00 | 24.00 | 45.0 |
| $\frac{1}{\omega_{sp}^2 T_{\theta_1} T_{\theta_2}}$ | 3.0 | 1.0 | 0.01 |

$\underline{2\zeta\omega_{ph}}$ & $\underline{\omega_{ph}^2}$ . A value of 0.05 was chosen for the phugoid natural frequency based on a survey of fighter aircraft. This value was used in all three sets of data in order to isolate the effect of changing the damping ratio in the phugoid mode. The MIL-PRIME directive was consulted in picking values for $\zeta_{ph}$ of 0.07, 0.02, and -0.04. Note that the last value will produce an unstable phugoid with a time-to-double of 347 seconds, which falls within the Level 3 criteria. Since the phugoid mode characteristics are

26

unlikely to be noticed by the pilot in an air-to-air tracking task, the three different sets of values may have no effect on pilot comments and handling quality ratings.

$2\zeta\omega_{sp}$ & $\omega_{sp}^2$ . MIL-F-8785C gives a range of acceptable values for the short-period damping ratio. The Level 1 value picked was 0.7, Level 2 was 0.375 (this also falls within the lower range of acceptable Level 1 values but was felt to be low enough that when coupled with other Level 2 parameters would not give Level 1 handling qualities), and Level 3 was 0.2. The values for the short-period undamped natural frequency were selected to yield appropriate values for Control Anticipation Parameter (CAP), which range between 0.28 and 1.0 rad/g·s$^2$ for fine tracking. The values for $\omega_{sp}$ were 3.5 for Level 1, 2.0 for Level 2, and 1.0 for Level 3.

n/α . Values were selected from Figure 13 of the MIL-PRIME Handbook using the $\omega_{sp}$ selected for each level.

Modal Phase Angles . The angles were chosen based on generalizations about how the vectors in the Argand diagram behave in the short-period and phugoid modes. Since these angles have a direct influence on the eigenvectors, the choices for the angles are likely to have a strong effect during the eigenstructure assignment.

Static to Short-Period Gain Ratio . Values were selected to give 9 db of low-frequency gain for Level 1, 0 db for Level 2, and -40 db for Level 3.

Simultaneous Solution for HQ Model

The eight non-linear equations were solved simultaneously using a routine from the International Mathematical & Statistics Libraries (IMSL) software package. The routine uses the secant method for finding the roots to an equation and requires the user to provide an initial guess for each of

27

the design variables (the dimensional derivatives for this application). Choosing the initial conditions proved to be a difficult task when trying to solve all eight equations simultaneously. If the algorithm converged at all, the roots were usually unreasonably large (the algorithm converged on an unacceptable local minimum). Often the algorithm iterated a design variable to the wrong sign (for instance a positive $M_\alpha$) and an error would result for trying to take the square root of a negative number. Due to these difficulties, it was decided to reduce the number of equations being solved simultaneously and, as valid solutions were found, to add back equations one or two at a time until all the equations were being solved together.

Using the solution for a given dimensional derivative as the initial guess for that design variable the next iteration, allowed swift and valid convergence of the algorithm. Unfortunately, there is not a subset of the eight equations which would give two equations in two unknowns (or three in three). Therefore, Equations (3.3), (3.4), and (3.7) were chosen to be solved simultaneously and values for $M_{\dot{\alpha}}$ were supplied in order that only three unknowns remained ($M_\alpha$, $M_q$, & $Z_\alpha$). $M_{\dot{\alpha}}$ was chosen to be given a constant value because, as indicated in Table 5-6 of Reference 5, it has the least widespread effect on the dynamics. The three equations were solved several times with different values of $M_{\dot{\alpha}}$ to insure that the solutions found weren't overly sensitive to variations in $M_{\dot{\alpha}}$.

The values found for $M_\alpha$, $M_q$, and $Z_\alpha$ were used as the initial guess when another equation (3.6) was added to the system (adding only one more unknown). This process was continued until values were found for all eight variables at four separate flight conditions and for each HQ level. In

28

the end, only seven of the equations were solved simultane-
ously; Equation (3.5) was not used. $M_{\dot{\alpha}}$ was not allowed to
optimize for the reasons stated earlier. The four flight
conditions examined were Mach = 0.6, 0.8 and altitude = 10K,
30K. The results for the dimensional derivatives are shown
in Table II. It is pleasing to see that some of the
dimensional derivatives are nearly constant with flight
conditions. Hopefully, this will lead to a feedback gain
matrix which will require limited gain scheduling with flight
condition (dynamic pressure typically).

## Optimal A Matrix and Eigenstructure

With the necessary dimensional derivatives in hand now,
the optimal A matrices were formed for each of the twelve
sets of data. The matrix for M = 0.6, Alt = 10K for each
handling qualtity level is shown below (in stability axis):

### Level 1

$$A = \begin{bmatrix} -.7200E-02 & 0.2200E+02 & 0.0000E+00 & -.3217E+02 \\ -.1276E-03 & -.1315E+01 & 0.1000E+01 & 0.0000E+00 \\ -.2053E-05 & -.7537E+01 & -.3587E+01 & 0.0000E+00 \\ 0.0000E+00 & 0.0000E+00 & 0.1000E+01 & 0.0000E+00 \end{bmatrix}$$

### Level 2

$$A = \begin{bmatrix} -.1000E-01 & 0.1605E+02 & 0.0000E+00 & -.3217E+02 \\ -.5972E-03 & -.9616E+00 & 0.1000E+01 & 0.0000E+00 \\ -.1841E-02 & -.3482E+01 & -.5393E+00 & 0.0000E+00 \\ 0.0000E+00 & 0.0000E+00 & 0.1000E+01 & 0.0000E+00 \end{bmatrix}$$

Table II

Optimal Dimensional Derivatives

| Level | Alt | Mach | $M_q$ | $Z_\alpha$ | $M_\alpha$ | $M_u$ | $Z_u$ | $X_\alpha$ | $X_u$ | $M_{\dot\alpha}$ |
|---|---|---|---|---|---|---|---|---|---|---|
| 1 | 10K | 0.6 | -1.49 | -849.0 | -10.30 | -.00027 | -.082 | 22.00 | -.007 | -2.1 |
|   |     | 0.8 | -1.49 | -1132.0 | -10.30 | -.00027 | -.110 | 22.00 | -.007 | -2.1 |
|   | 30K | 0.6 | -1.49 | -783.8 | -10.30 | -.00027 | -.076 | 22.00 | -.007 | -2.1 |
|   |     | 0.8 | -1.49 | -1045.0 | -10.30 | -.00027 | -.101 | 22.00 | -.007 | -2.1 |
| 2 | 10K | 0.6 | -0.29 | -621.0 | -3.72 | -.00199 | -.386 | 16.05 | -.010 | -0.3 |
|   |     | 0.8 | -0.29 | -828.0 | -3.72 | -.00199 | -.514 | 16.05 | -.010 | -0.3 |
|   | 30K | 0.6 | -0.29 | -573.3 | -3.72 | -.00199 | -.356 | 16.05 | -.010 | -0.3 |
|   |     | 0.8 | -0.29 | -764.4 | -3.72 | -.00199 | -.475 | 16.05 | -.010 | -0.3 |
| 3 | 10K | 0.6 | -0.63 | -659.8 | -0.36 | -.00058 | -1.21 | -11.64 | -.021 | 1.3 |
|   |     | 0.8 | -0.63 | -879.8 | -0.36 | -.00058 | -1.61 | -11.64 | -.021 | 1.3 |
|   | 30K | 0.6 | -0.63 | -609.2 | -0.36 | -.00058 | -1.11 | -11.64 | -.021 | 1.3 |
|   |     | 0.8 | -0.63 | -812.2 | -0.36 | -.00058 | -1.48 | -11.64 | -.021 | 1.3 |

Level 3

$$
A = \begin{bmatrix}
-.2130E-01 & -.1164E+02 & 0.0000E+00 & -.3217E+02 \\
-.1868E-02 & -.1022E+01 & 0.1000E+01 & 0.0000E+00 \\
-.2914E-02 & -.1635E+01 & 0.6208E+00 & 0.0000E+00 \\
0.0000E+00 & 0.0000E+00 & 0.1000E+01 & 0.0000E+00
\end{bmatrix}
$$

It was important to establish that these matrices did indeed
have the dynamic characteristics to place them in the
handling quality level for which they were designed.  For
this reason, the eigenvalues were found for each matrix.  It
was verified that two characteristic modes were present and
the damping ratio and natural frequancy were calculated.  In
addition, several other handling quality criteria were used
to check the optimality of each matrix:

1) Check CAP vs $\zeta_{sp}$ from Figure 3 [4:193]

where: CAP $= \dfrac{\omega_{sp}^2}{n/\alpha}$  $(g^{-1} \cdot s^{-2})$

$n/\alpha = -Z_\alpha/g$  $(g \cdot rad^{-1})$

2) Check $\omega_{sp}T_{\theta_2}$ vs $\zeta_{sp}$ from Figure 4 [4:211,386]

where: $T_{\theta_2} = \dfrac{V}{g\ n/\alpha}$  (sec)

3) Check $\omega_{sp}$ vs $n/\alpha$ from Figure 5 [4:214]

4) Check that $1/T_{\theta_2}$ is greater than 0.38 for Level 1 and
0.24 for Level 2 [4:385]

5) Check that $\dfrac{d\gamma}{du}$ is less than 0.06 for Level 1, 0.15 for
Level 2, and 0.24 for Level 3

where: $\dfrac{d\gamma}{du} = \dfrac{1}{g}\left[X_u - (X_\alpha - g)\dfrac{Z_u}{Z_\alpha}\right]$  $(deg \cdot knot^{-1})$

6) Check $\dfrac{n/\alpha}{\omega_{sp}}$ vs $\zeta_{sp}$ from Figure 6 [18:514]

31

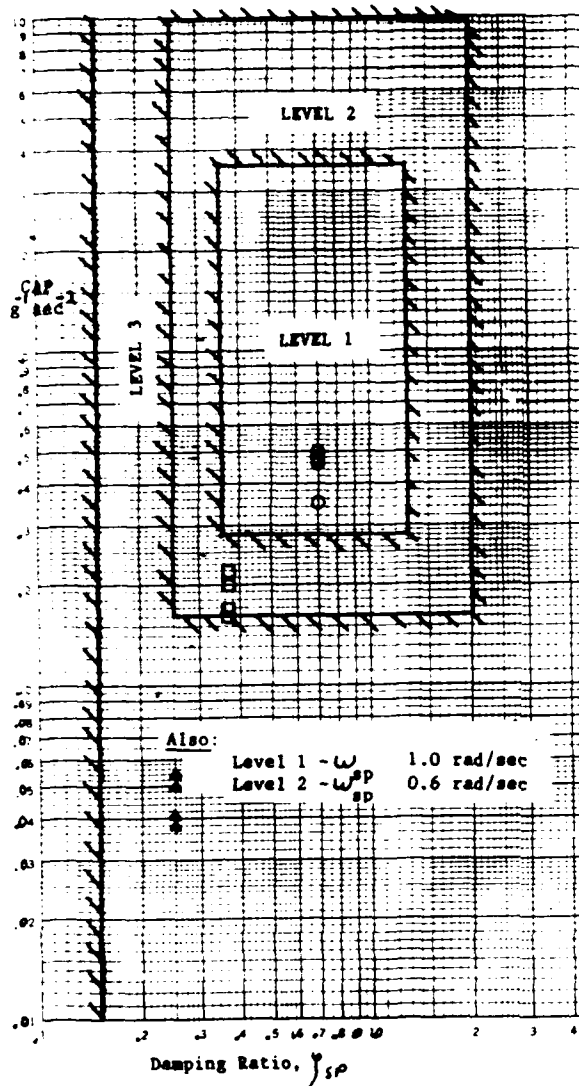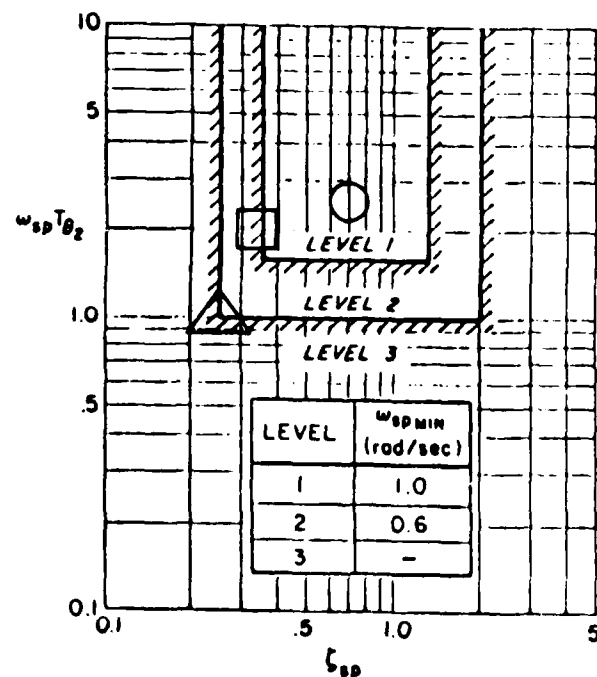Figure 3. Control Anticipation Parameter Versus Short-Period Damping Ratio

O – Cases 1-4
□ – Cases 5-8
△ – Cases 9-12

Figure 4. Comparison of $\omega_{sp}T_{\theta_2}$ Versus Short-Period Damping Ratio
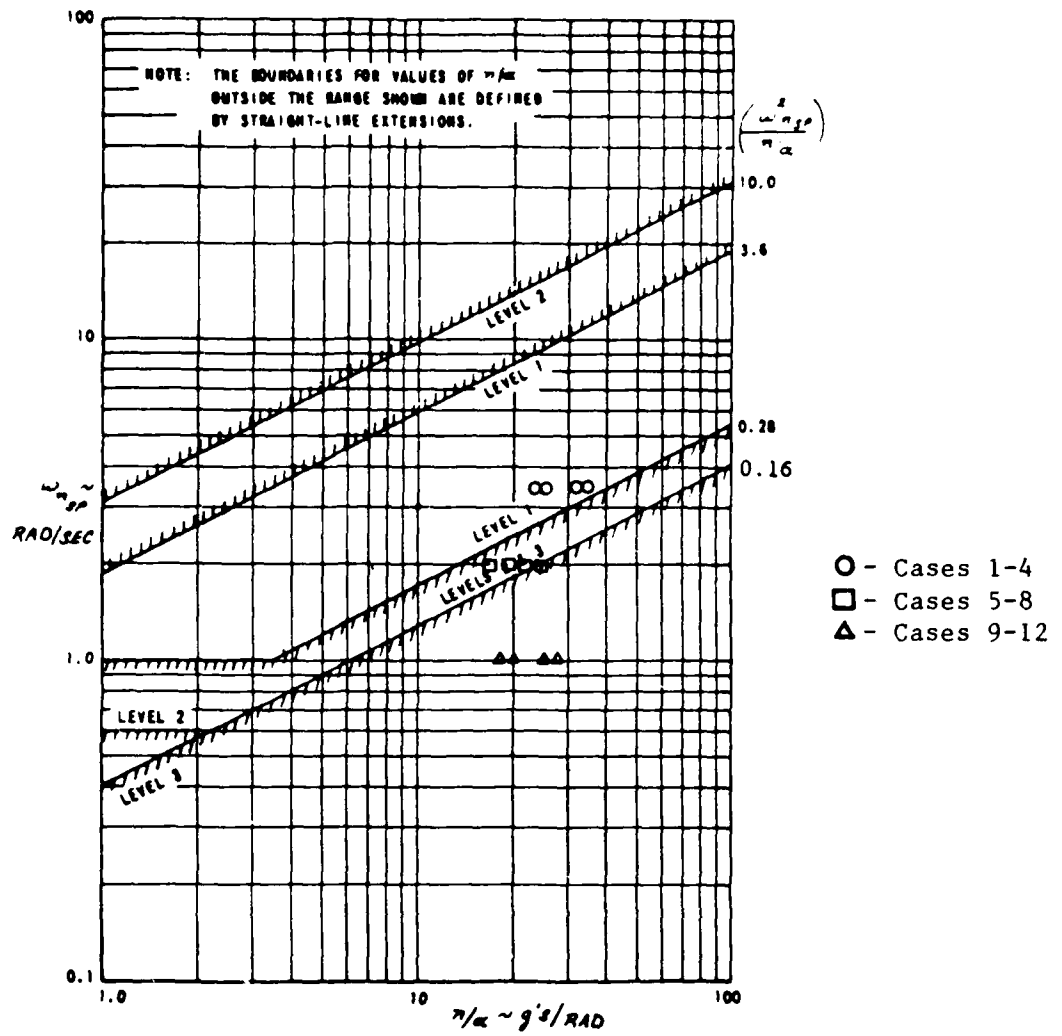
O – Cases 1-4
□ – Cases 5-8
△ – Cases 9-12

32

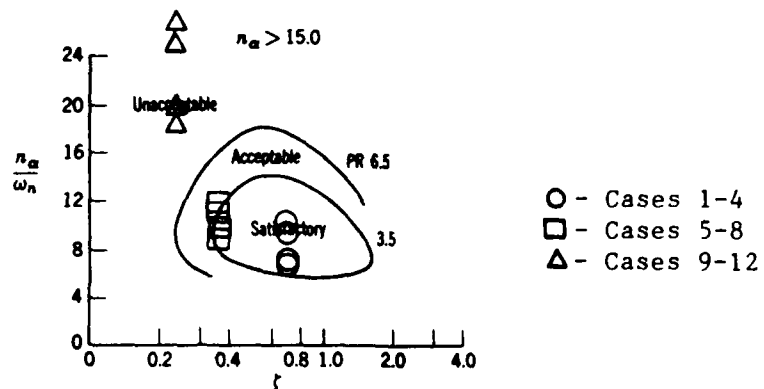Figure 5. MIL-F-8785C Short-Period Requirements



Figure 6. Variable-Stability Aircraft Handling
Qualities Results

33

The dynamic characteristics of all 12 matrices are summarized in Table III.

Most of the data falls fairly well into the handling quality level for which its matrix was designed. The $\omega_{sp} T_{\theta_2}$ vs $\zeta_{sp}$ check gives borderline Level 1/Level 2 handling qualities for data sets 5-8, and borderline Level 2/Level 3 for data sets 9-12. Also, for all cases $\frac{d\gamma}{du}$ falls within Level 1 criteria. Again, it is felt that this criteria will not be a factor in the air-to-air tracking task.

The damping ratio for the Level 3 data sets were unanticipated. By the phugoid approximation we should have a damping ratio of -0.04; what was produced was $\zeta_{ph}$ = -0.9404. Clearly Equation (3.1) was not a good approximation in this case. This is substantiated by the fact that the condition for validity for the approximation was erroneously violated [5:336]. The resulting time-to-double of 15 seconds is too fast for Level 3 and would probably be considered uncontrollable. However, it was decided that it would be interesting to leave the damping ratio as is for these cases to see if the pilot would notice the poor phugoid damping.

The **A** matrices were considered to be optimal at this point and a spectral decomposition was performed to get the eigenvalues and eigenvectors. Again for Mach = 0.6, Alt = 10K, the eigenstructure for each level is shown in Table IV. The next step in the control system design process was to find the feedback gain matrix given the bare airframe X-29A **A** & **B** matrices, and the just obtained optimal eigenstructure.

Table III

Optimal Matrices' Dynamic Characteristics

| Level | Case | $\zeta_{sp}$ | $\omega_{sp}$ | $\zeta_{ph}$ | $\omega_{ph}$ | CAP | $n_\alpha$ | $T_{\theta_2}$ | $\dfrac{d\gamma}{du}$* | $(\frac{\theta}{\alpha})$ | $(\frac{\theta}{u})$ | Bode Gain |
|---|---|---|---|---|---|---|---|---|---|---|---|---|
| 1 | 1 | 0.700 | 3.5 | 0.070 | 0.050 | 0.464 | 26.39 | 0.762 | -1.93 | 15. | 85. | 3.00 |
| | 2 | 0.700 | 3.5 | 0.070 | 0.050 | 0.348 | 35.19 | 0.762 | -1.93 | 15. | 85. | 3.00 |
| | 3 | 0.700 | 3.5 | 0.070 | 0.050 | 0.503 | 24.36 | 0.762 | -1.93 | 15. | 85. | 3.00 |
| | 4 | 0.700 | 3.5 | 0.070 | 0.050 | 0.377 | 32.48 | 0.762 | -1.93 | 15. | 85. | 3.00 |
| 2 | 5 | 0.376 | 2.0 | 0.029 | 0.050 | 0.207 | 19.30 | 1.042 | 4.08 | 24. | 70. | 1.00 |
| | 6 | 0.376 | 2.0 | 0.029 | 0.050 | 0.155 | 25.74 | 1.042 | 4.08 | 24. | 70. | 1.00 |
| | 7 | 0.376 | 2.0 | 0.029 | 0.050 | 0.224 | 17.82 | 1.042 | 4.08 | 24. | 70. | 1.00 |
| | 8 | 0.376 | 2.0 | 0.029 | 0.050 | 0.168 | 23.76 | 1.042 | 4.08 | 24. | 70. | 1.00 |
| 3 | 9 | 0.250 | 1.0 | -.940 | 0.049 | 0.051 | 20.51 | 0.980 | 1.83 | 45. | 45. | 0.00 |
| | 10 | 0.250 | 1.0 | -.940 | 0.049 | 0.038 | 27.35 | 0.980 | 1.83 | 45. | 45. | 0.00 |
| | 11 | 0.250 | 1.0 | -.940 | 0.049 | 0.055 | 18.94 | 0.980 | 1.83 | 45. | 45. | 0.00 |
| | 12 | 0.250 | 1.0 | -.940 | 0.049 | 0.041 | 25.25 | 0.980 | 1.83 | 45. | 45. | 0.00 |

\* Note: for Level 1, $\dfrac{d\gamma}{du} = -1.93 \times 10^{-4}$

Level 2, $\dfrac{d\gamma}{du} = 4.08 \times 10^{-7}$

Level 3, $\dfrac{d\gamma}{du} = 1.83 \times 10^{-6}$

## Table IV

### Optimal Eigenstructure
### (Mach = 0.6, Alt = 10k)

| Level | Short-Period | Phugoid |
|-------|-------------|---------|
| 1 | $\lambda_{sp} = -2.45 \pm 2.4994$ | $\lambda_{ph} = -.0035 \pm .0501$ |
| | $\xi_{sp1} = -.925 \pm -1.805$ | $\xi_{ph1} = -618.7 \pm 307.8$ |
| | $\xi_{sp2} = 0.084 \pm -.8021$ | $\xi_{ph2} = 0.0232 \pm -.012$ |
| | $\xi_{sp3} = 1.909 \pm 1.1221$ | $\xi_{ph3} = -.0480 \pm 0.251$ |
| | $\xi_{sp4} = -.153 \pm -.6138$ | $\xi_{ph4} = 0.5659 \pm 0.919$ |
| 2 | $\lambda_{sp} = -0.75 \pm 1.8573$ | $\lambda_{ph} = -.0015 \pm .0498$ |
| | $\xi_{sp1} = -5.03 \pm 2.7050$ | $\xi_{ph1} = -852.8 \pm -111.$ |
| | $\xi_{sp2} = -0.48 \pm 0.4326$ | $\xi_{ph2} = 0.4617 \pm .0577$ |
| | $\xi_{sp3} = -0.91 \pm -.7988$ | $\xi_{ph3} = -.0689 \pm .0122$ |
| | $\xi_{sp4} = -0.20 \pm 0.5687$ | $\xi_{ph4} = 0.2853 \pm 1.377$ |
| 3 | $\lambda_{sp} = -.257 \pm 0.9828$ | $\lambda_{ph} = 0.0456 \pm .0165$ |
| | $\xi_{sp1} = -29.3 \pm 15.257$ | $\xi_{ph1} = -3996. \pm -807.$ |
| | $\xi_{sp2} = -.323 \pm 0.5842$ | $\xi_{ph2} = 7.1925 \pm 1.509$ |
| | $\xi_{sp3} = -.876 \pm 0.1583$ | $\xi_{ph3} = 0.1891 \pm 0.232$ |
| | $\xi_{sp4} = 0.369 \pm 0.7948$ | $\xi_{ph4} = 5.2952 \pm 3.170$ |

# IV.  Eigenstructure Assignment

Once the unaugmented aircraft model and the optimal eigenstructure were found in Sections II and III, respectively, the feedback gain matrices could be calculated. This was accomplished using the MODES software package [15].

## Theory Behind MODES

MODES calculates the feedback gain matrix  K  which will cause the closed-loop, linear, time-invariant system

$$\dot{\bar{x}}(t) = [A(t) + B(t)K(t)]\bar{x}(t) \qquad (4.1)$$

to have the desired eigenstructure selected in Section III. Since the number of inputs (3) did not equal the number of states (4) for this problem, there was no exact solution to the problem

$$K = B^{-1}[P_D \Lambda P_D^{-1} - A] \qquad (4.2)$$

where

$P_D$ is the matrix of desired eigenvectors
$\Lambda$ is the diagonal matrix of desired eigenvalues
and $\tilde{A} = A + BK = P_D \Lambda P_D^{-1}$

Therefore, the eigenvectors picked in Section III were not fully realizable and some projection of these eigenvectors was needed.  Singular value decomposition was used to find the range space of the achievable eigenvectors of the augmented matrix  $[A - \lambda_i I | B]$ , where $\lambda_i$ is a desired eigenvalue.  Once the range space was found, singular value decomposition was used again to find the projection of the desired eigenvector into the range space of achievable eigenvectors, $p_A$.  This projection generated the eigenvectors which, in a least squares sense, came closest to matching the desired eigenvectors.

37

In this manner, an acievable eigenvector was found corresponding to each desired eigenvalue, and the $P_\Delta$ matrix, consisting of columns of eigenvectors, was formed. Naturally, having to use projected eigenvectors instead of the desired eigenvectors caused some deviation from the optimal handling qualities designed for in Section III. This was unavoidable since the number of inputs was less than the number of states.

Once the projected eigenvectors were found, the MODES program executed a straight-forward, full-state feedback eigenstructure assignment algorithm. The matrix

$$\tilde{A} = P_\Delta \Lambda P_\Delta^{-1} \tag{4.3}$$

has already been found. Each column of $P_\Delta$, considered as a vector $\bar{p}_i$, must satisfy the basic eigenvalue problem

$$\tilde{A} p_i = \lambda_i p_i \tag{4.4}$$

or since $\tilde{A} = A + BK$

$$[A + BK]p_i = \lambda_i p_i \tag{4.5}$$

Rearranging this equation leads to

$$[A - \lambda_i I]p_i + BKp_i = 0 \tag{4.6}$$

or, in matrix partitioned form

$$[A - \lambda_i I \mid B] \begin{bmatrix} p_i \\ \hline Kp_i \end{bmatrix} = 0 \tag{4.7}$$

This is tantamount to requiring that $\begin{bmatrix} p_i \\ \hline Kp_i \end{bmatrix}$ lie in the null space of $[A - \lambda_i I \mid B]$. This has already been taken care of earlier by the eigenvector projection process and the lower partition of the projected eigenvector determines $KP_\Delta$.

38

It remained only to postmultiply this by the inverse of $P_\Delta$
to obtain the unique feedback gain matrix K.

## Application of MODES

A total of twelve feedback matrices were found using the
MODES program. Three sets of desired eigenvalues and
eigenvectors corresponding to good, fair, and poor handling
qualities were used at each of the four flight conditions.

For use in the simulation it was necessary to calculate
the feedback gain matrices in the body axis frame. The bare
airframe X-29A A and B matrices calculated in Section II ,
were already in this frame. However, the optimal handling
quality A matrices from which the desired eigenstructure
were obtained were found in the stability axis frame (this
frame was necessary since most of the handling quality
specifications are expressed in this frame [3]). Therefore,
it was necessary to transform the stability axis dimensional
derivatives found in Section III into the body axis,
reformulate the A matrix, and decompose the new optimal
matrix into the desired eigenvalues and eigenvectors.

Again, a computer program was written to facilitate
this. The program allowed the user to enter dimensional
derivatives in either of the reference frames. The A and
B matrices were then formed in whichever frame was desired.
The optimal matrix was then decomposed into its eigenvalues
and eigenvectors using an IMSL routine.

Using MODES, it was a relatively quick process to
formulate the twelve feedback gain matrices. The personal
computer version of MODES was used on both an IBM PC and IBM
AT. For the Mach = 0.6, altitude = 10k ft flight condition,
and the eigenstructure corresponding to good handling
qualities, the feedback gain matrix calculated by MODES is

39

shown below:

$$K = \begin{bmatrix} -2.5642E-03 & -8.0207E+00 & 2.4117E+00 & -7.1717E-03 \\ 5.4848E-04 & 2.6434E+00 & -3.9755E-01 & 1.6116E-03 \\ -3.8463E-04 & -4.0206E+00 & 2.2998E-01 & -8.5830E-04 \end{bmatrix}$$

As an aid to understanding this matrix, the following example
is given:

$$\delta_{strake} = - 2.5642E-03 * u_{pert} - 8.0207E+00 * \alpha_{pert}$$
$$+ 2.4112E+00 * q_{pert} - 7.1717E-03 * \theta_{pert}$$

and similarly row 2 provides the flaperon command and row 3
provides the canard command.

MODES also formulated the $\tilde{A}$ matrix:

$$\tilde{A} = \begin{bmatrix} -1.0926E-02 & 6.7087E+01 & -3.4515E+01 & -3.2126E+01 \\ -1.2758E-04 & -1.3133E+00 & 9.9998E-01 & -2.8178E-03 \\ 8.4952E-04 & -7.5379E+00 & -3.5836E+00 & 5.5559E-03 \\ 0.0000E+00 & 0.0000E+00 & 1.0000E+00 & 0.0000E+00 \end{bmatrix}$$

Of course, the critical issue was whether the $\tilde{A}$ matrix
still possessed the dynamic characteristics designed for it.
A comparison of the eigenvalues of the $\tilde{A}$ matrix to those of
the original optimal A matrix of Section III revealed

Achievable $\tilde{A}$ Matrix
Eigenvalues

$$\lambda_{1,2} = -2.447761E+00 \pm j(2.504523E+00)$$
$$\lambda_{3,4} = -6.168339E-03 \pm j(7.340013E-02)$$

Optimal A Matrix
Eigenvalues

$$\lambda_{1,2} = -2.447769E+00 \pm j(2.504519E+00)$$
$$\lambda_{3,4} = -6.212100E-03 \pm j(7.334608E-02)$$

As can be seen, a very good match was made. As expected, the
eigenvectors did not compare numerically, however they still

40

may contain the same approximate mode shapes for which they were designed. From the $\tilde{A}$ matrix, an approximate value was found for $Z_\alpha = 848.14$. This was used to calculate values for $n/\alpha$ and CAP for the augmented system:

|       | $\tilde{A}$ | Optimal A |
|-------|-------|-----------|
| $n/\alpha$ | 26.36 | 26.39 |
| CAP   | 0.465 | 0.464 |

Again, a very good match was made. It appears as though the desired eigenstructure came through the eigenstructure assignment process in good shape.

## Feedback Matrix Preparation

In order for the pilot to be able to maneuver the aircraft throughout the envelope, the elements of the feedback gain matrices for each of the handling quality levels were curve fit together as a function of aircraft dynamic pressure. A third-order equation was found to be sufficient and yielded an error of less than 2% between the exact value and the curve fit value. The twelve equations were evaluated every 25 msec in the digital simulation to provide the feedback gains. The implementation of the modified control system into the X-29A simulation will be described in Section VI. First, in Section V, a pilot-model analysis will be described which was used to predict the handling qualities of the closed-loop, augmented system.

## V.  Pilot Model Analysis

### Background

With the feedback matrices developed in the last
section, the complete closed-loop system was ready to be
tested.  However, before the new flight control system was
evaluated on the man-in-the-loop simulator, an attempt to
predict the handling qualities of the aircraft was made.  To
accomplish this, a pilot-model analysis was performed and the
Neal-Smith criteria was used to predict pilot handling
quality ratings [16].

In the early 1970's, Neal and Smith published a report
which investigated the effects of control system dynamics on
the longitudinal flying qualities of fighter aircraft.  They
used the USAF NT-33 variable stability aircraft to evaluate
57 different combinations of flight condition, control system
dynamics, and short-period dynamics.  One of the important
products of this study was a pilot-model analysis tool which
enables the control system designer to predict what the pilot
handling quality ratings will be [16: Sec VI].

To apply the Neal-Smith technique, one needs the
closed-loop aircraft system, as well as an outer loop which
the pilot will close (usually a theta command loop).  A
typical configuration is shown in Figure 7.  The pilot model
was briefly discussed in Section I.  Once again, $K_p$ is the
pilot gain, or how much he moves the stick; $e^{-.3s}$ is the
time delay due to pilot reaction time, neuromuscular delay,
and other effects; $\tau_{p_1}$ and $\tau_{p_2}$ are the pilot lead and lag
time constants, respectively.  The pilot will adjust $K_p$,
$\tau_{p_1}$, and $\tau_{p_2}$ to attain certain performance standards,
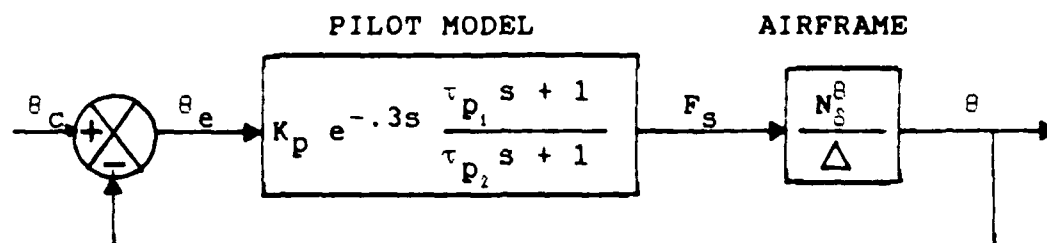described later in this section.

42

Figure 7. Block Diagram of Pitch Attitude Tracking

Nichol's charts are used extensively in the pilot-model analysis to relate the open-loop transfer function, $\theta/\theta_e$, to closed-loop performance. Using the model in Figure 7, the following design criteria were proposed.

Bandwidth (BW) . Bandwidth, by the Neal-Smith definition, is the frequency for which the closed-loop Bode phase is equal to -90 degrees. It is a measure of how quickly the pilot can move the airplane's nose toward the target. For high-speed flight, Neal-Smith recommend a minimum bandwidth, $(BW)_{min}$, of 3.5 rad/sec. The pilot will adjust his gain $(K_p)$ to attain this bandwidth.

Droop . Droop is defined as the maximum excursion of closed-loop Bode amplitude, $\left|\theta/\theta_c\right|_{max}$ , below the 0 db line for frequencies less than $(BW)_{min}$ . For a reasonable amount of damping, droop is a measure of how slowly the nose settles down on the target (steady-state tracking error). The amount

43

of droop which the pilot will allow, according to Neal-Smith, is 3 db below the 0 db line.

PIO Tendency . The tendancy to oscillate, or to generate Pilot Induced Oscillations, is defined in terms of the Bode magnitude of any closed-loop resonant peak, $\left|\theta/\theta_c\right|_{max}$ , which results from the pilot trying to meet the performance standards. The pilot will add lead to decrease the resonance peak, however droop will increase. As resonance grows, the pilot will complain first of overshoot, then oscillations, and finally PIO for high resonance values, $\left|\theta/\theta_c\right|_{max}$ > 11 db.

Pilot Compensation . The pilot's workload is related to the amount of phase lead or lag he is adding to the system. If the pilot must add too much lead, he will state that the aircraft response is sluggish, while too much lag generates comments about having to fly the aircraft smoothly. Pilots prefer to add a little lead rather than lag. The amount of pilot compensation is defined by

$$ARG_{pc} = ARG \left( \left. \frac{j\omega\tau_{p_1} + 1}{j\omega\tau_{p_2} + 1} \right) \right|_{\omega = (BW)_{min}} \tag{5.1}$$

In summary, one needs to determine the values of $K_p$ , $\tau_{p_1}$ , and $\tau_{p_2}$ which will minimize $\left|\theta/\theta_c\right|_{max}$ while maintaining a minimum bandwidth of 3.5 rad/sec and a maximum droop of 3 db. The values of $ARG_{pc}$ and $\left|\theta/\theta_c\right|_{max}$ which result can be used to predict the pilot's handling quality rating as shown in Figure 8. This figure is based on the experimental results of the Neal-Smith study.
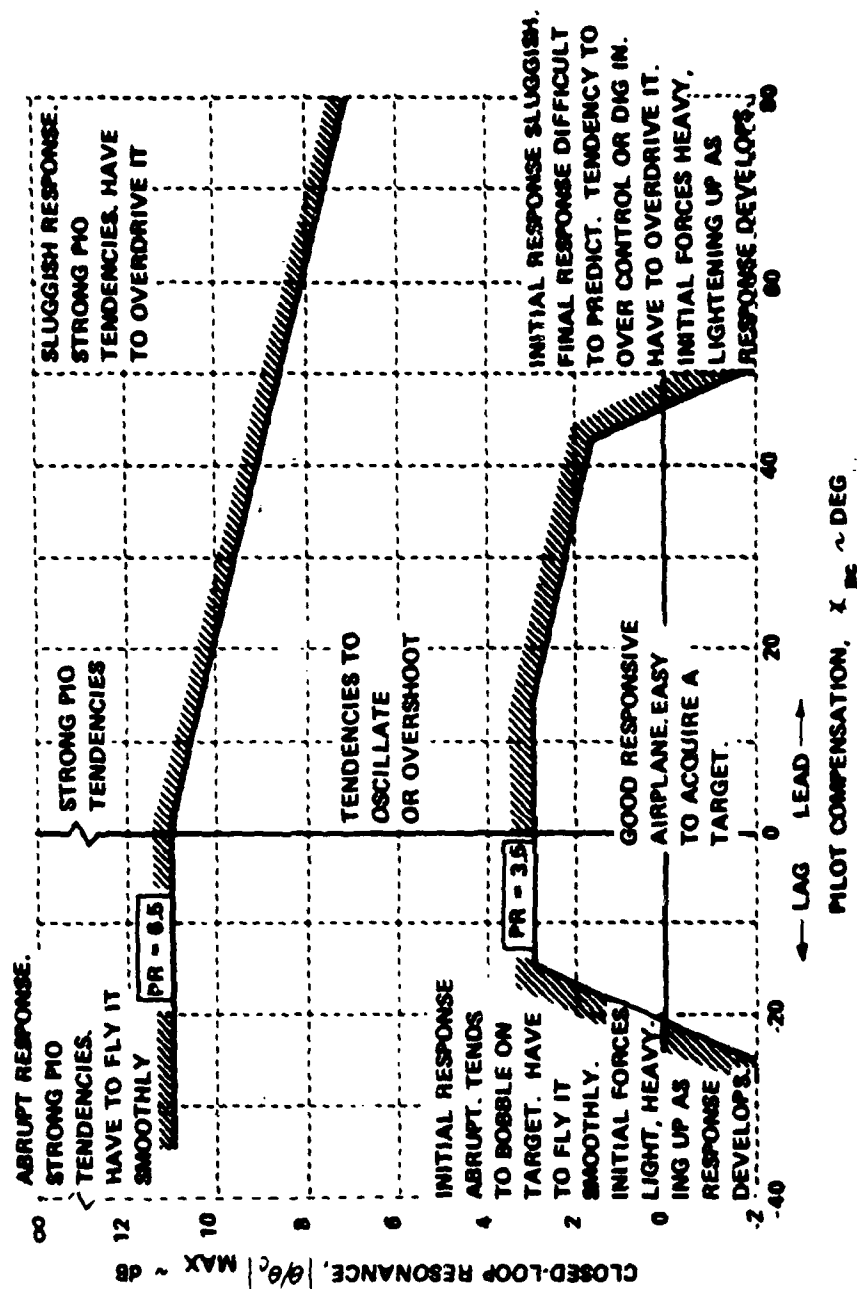
44

Figure 8. Neal-Smith Criterion for Fighter Maneuvering Dynamics

The methology to determine $K_p$, $\tau_{p_1}$, and $\tau_{p_2}$ will be shown by example later in this section. First, a simplified criteria developed by Neal-Smith will be discussed [16: Sec 8.2]. This method for predicting handling qualities does not require finding the values for $K_p$, $\tau_{p_1}$, and $\tau_{p_2}$. The method takes advantage of the fact that the amount of pilot compensation added, $ARG_{ad}$, is related to the open-loop phase of the uncompensated pilot plus airplane at $\omega = (BW)_{min}$. Also, the slope of the compensated amplitude-phase curve in the neighborhood of $\omega = (BW)_{min}$ is an approximate measure of how large the closed-loop resonance will be. Therefore, a rough guess to the amount of pilot compensation required and the closed-loop resonance are determined by the parameters $ARG_{ad}$ and $(\frac{dA}{dARG})_{ad}$. Equations for these two parameters are presented below [16: 117,118]:

$$ARG_{ad} = \left[ \; ARG(\frac{\theta}{F_s}) \Big|_{BW_{min}} - 17.2(BW)_{min} \; \right] , deg \qquad (5.2)$$

$$(\frac{dA}{dARG})_{ad} = \left[ \frac{\left[ d\left|\frac{\theta}{F_s}\right| \Big/ d(\log \omega) \right]_{(BW)_{min}}}{\left[ d(ARG\frac{\theta}{F_s}) \Big/ d(\log \omega) \right]_{(BW)_{min}} - 39.6(BW)_{min}} \right] \qquad (5.3)$$

The parameters are compared on Figure 9 to obtain the pilot ratings. One of the objectives of this part of the study was to compare the predictions of the handling qualities of the same system by using the simplified criteria and the full pilot model analysis. It will be seen that it became necessary to use the simplified criteria for certain high-order systems.
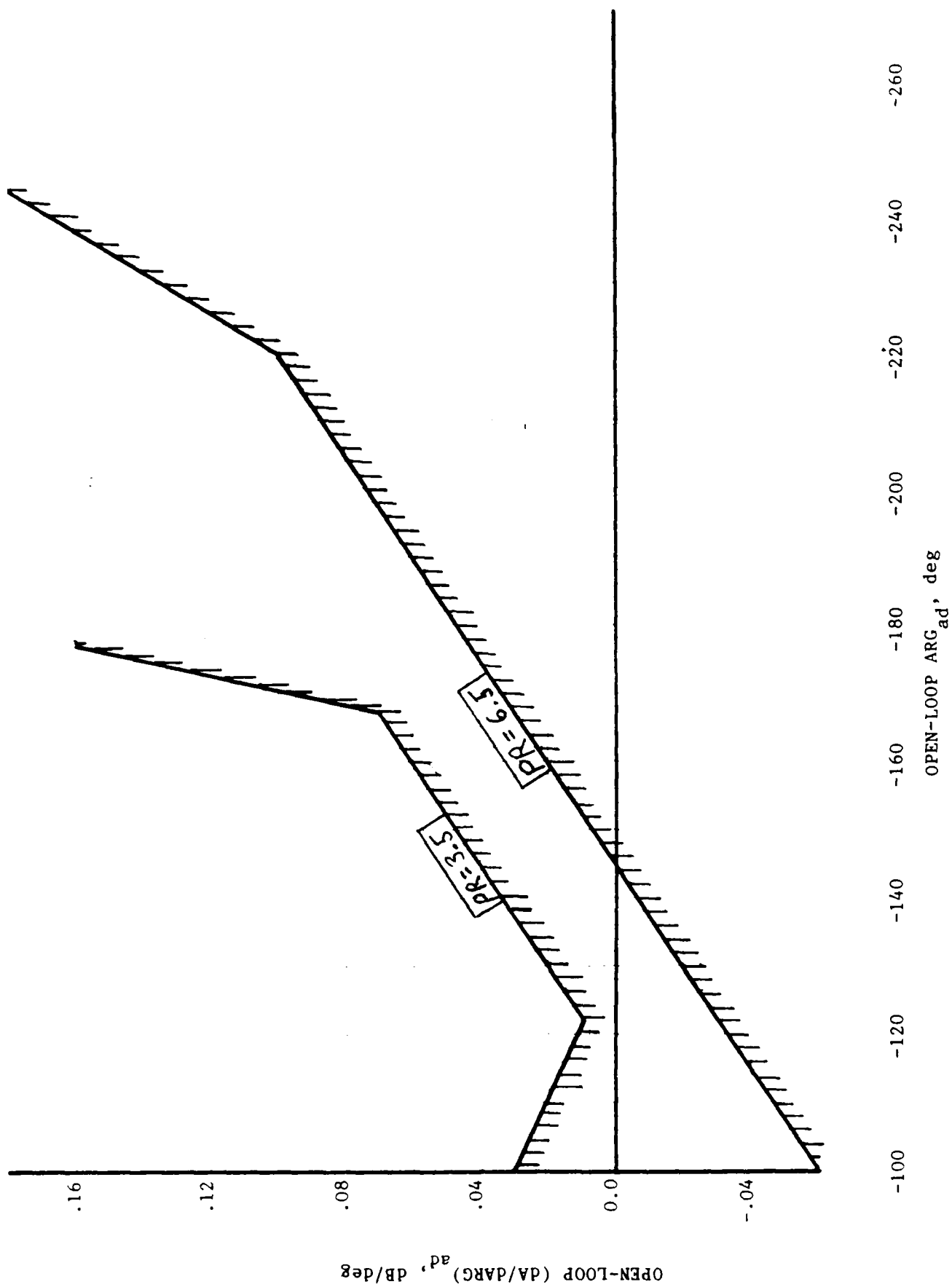
Figure 9. Neal-Smith Simplified Criterion

47

## X-29A Flight Control System

As a reminder, the primary purpose of using the Neal-Smith criteria in this study was to predict the pilot ratings which would be given when evaluations were made using the man-in-the-loop simulation. Therefore, it was necessary to duplicate the control system which would be used on the LAMARS during this phase of the study.

For the LAMARS simulation, the basic design used in the actual X-29A Analog Reversion (AR) mode would be kept, the major changes being the deletion of the proportional plus integral compensator and the addition of full-state feedback. For the Neal-Smith pilot analysis, the control system used is shown in Figure 10. This will be referred to as the high-order system. As can be seen, a number of first-order lags, as well as fourth-order actuator models were included. A second-order Pade' approximation was used to model the pilot time delay, $e^{-.3s}$. These higher-order effects were not taken into account when the feedback matrices were developed and will likely degrade the system performance. When the high-order system open-loop transfer function ($\theta/\theta_e$) was formed using TOTAL, it contained a $23^{rd}$ order numerator and a $29^{th}$ order denominator. However, what became a more difficult problem was that the coefficients for the polynomials were of the power $10^{20} - 10^{28}$. Due to the large coefficients of the high-order system and the fact that the exponential notation used by TOTAL provided only 4 significant digits in its output (i.e. 0.1234E+28), accurate Nichol's charts could not be obtained for these large transfer functions (specifically, the lower frequency part of the curve was lost). For this reason, it was decided to apply the simplified Neal-Smith criteria to the high-order $\theta/F_s$ transfer function, and apply the full Neal-Smith
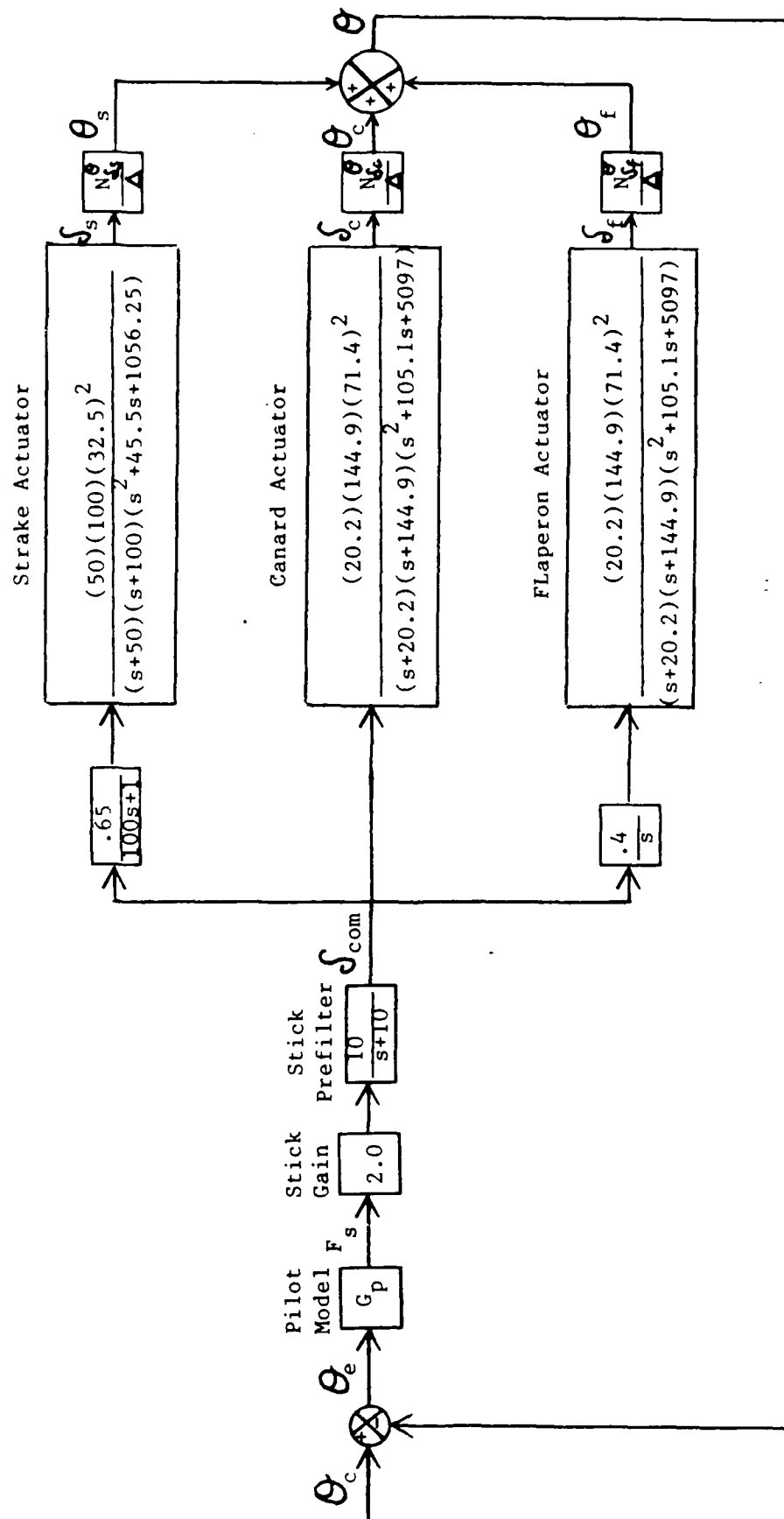
48

Figure 10. X-29A Higher-Order Mathematical Model

analysis to the low-order system, shown in Figure 11.

The Nichol's charts drawn by TOTAL were not adequate to apply the Neal-Smith criteria in that they did not display the constant M and N curves. Therefore, a program was written which drew a complete Nichol's chart using the DISSPLA graphics package and which emphasized the Neal-Smith criteria of 90 degrees phase for bandwidth and 3 db for low-frequency droop.

### Neal-Smith Analysis

Recall that feedback matrices were formed for four flight conditions in each of three handling quality levels (Good, Fair, and Poor). The flight conditions corresponding to M = .6, Alt = 10K for each level (Cases 1, 5, & 9) were selected to be evaluated using the Neal-Smith criteria.

Case 1. The $\theta/\delta$ transfer functions were found by using the resolvent matrix for the A + BK system and were provided by the MODES program, discussed in Section IV. It remained only to use TOTAL to combine the series and parallel paths into the open-loop transfer functions $\theta/F_s$ and $\theta/\theta_e$. The Bode plots for the lower-order (LO) and higher-order (HO) systems are shown in Figures 12 and 13. From tabular printouts, it was found that the phase margin degraded from 95° for lower-order $\theta/F_s$, to 58° when the pilot pure time delay was added - $\theta/\theta_e$ (LO). Similarly, the gain margin went from 15 db to 4.25 db. When the higher-order effects were taken into account, the phase margin for $\theta/F_s$ dropped to 65°, and for $\theta/\theta_e$ to 18°. Likewise, the gain margin was 7.5 db for $\theta/F_s$ and 1.09 for $\theta/\theta_e$. Clearly the stability margins for the higher-order transfer function were decreasing.
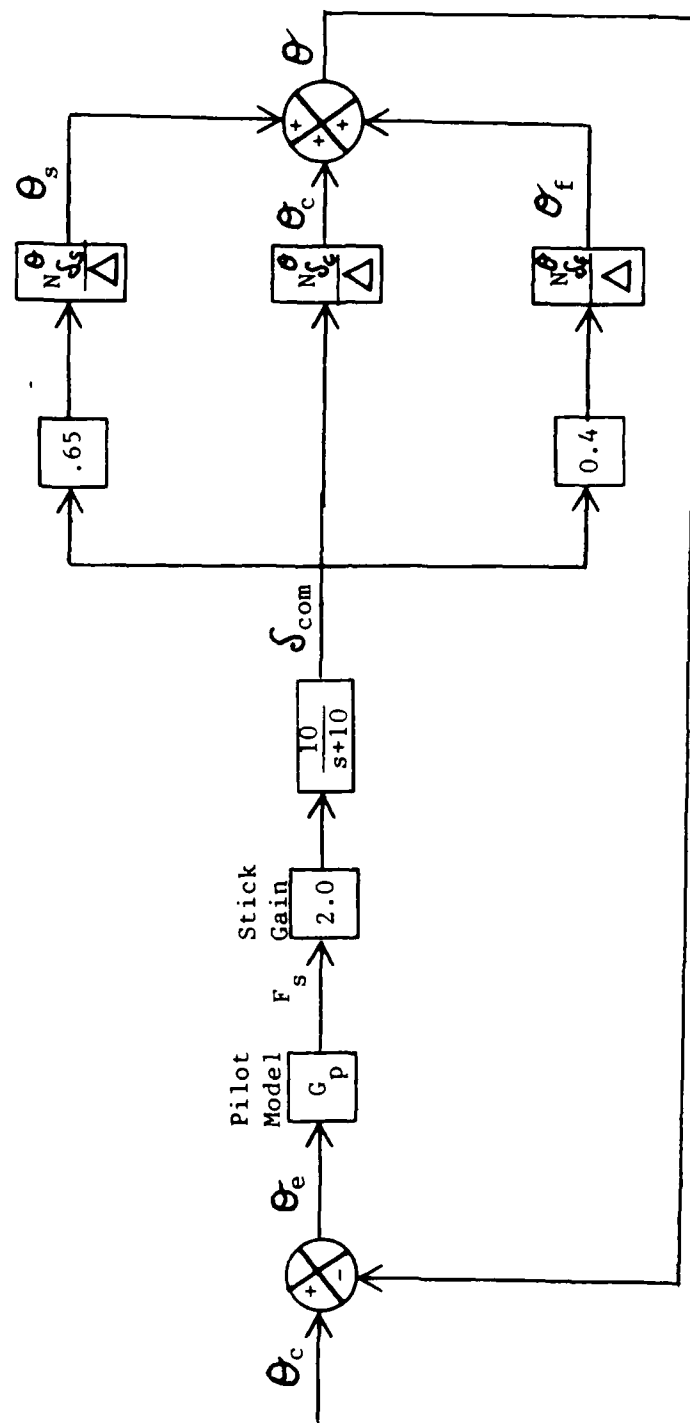
Figure 11. X-29A Lower-Order Mathematical Model

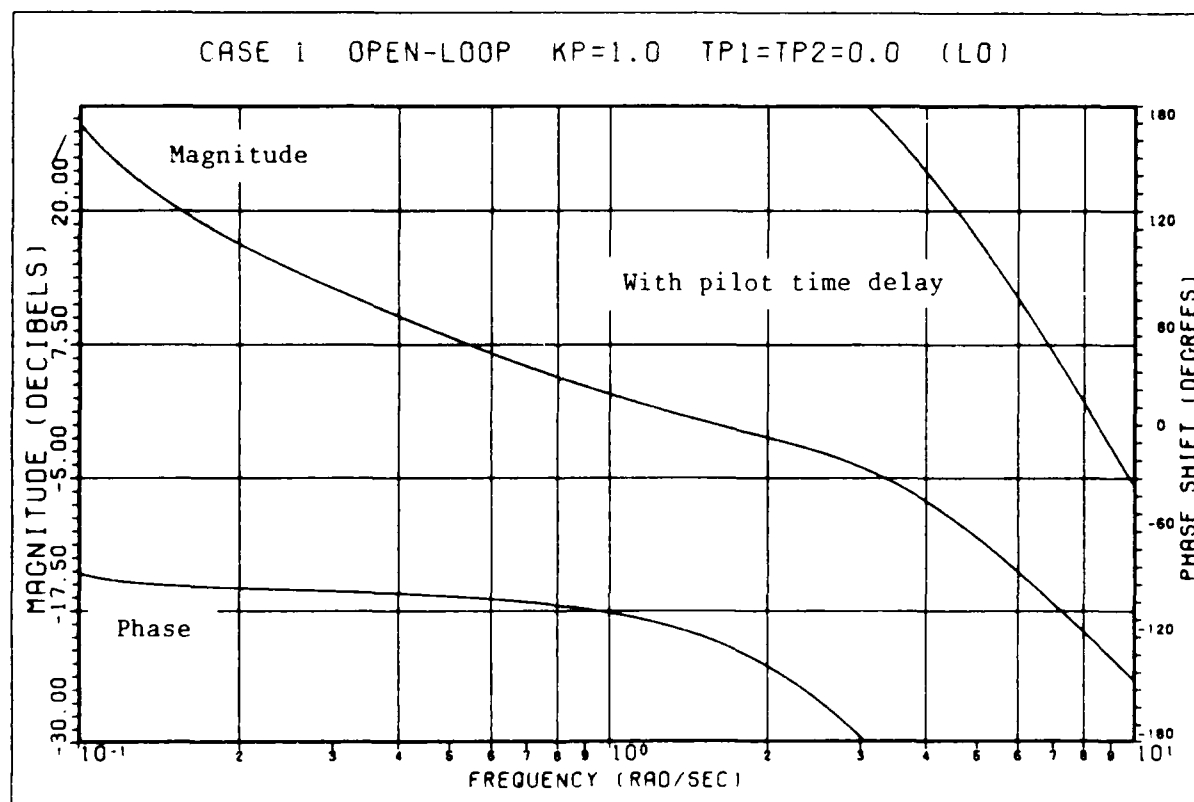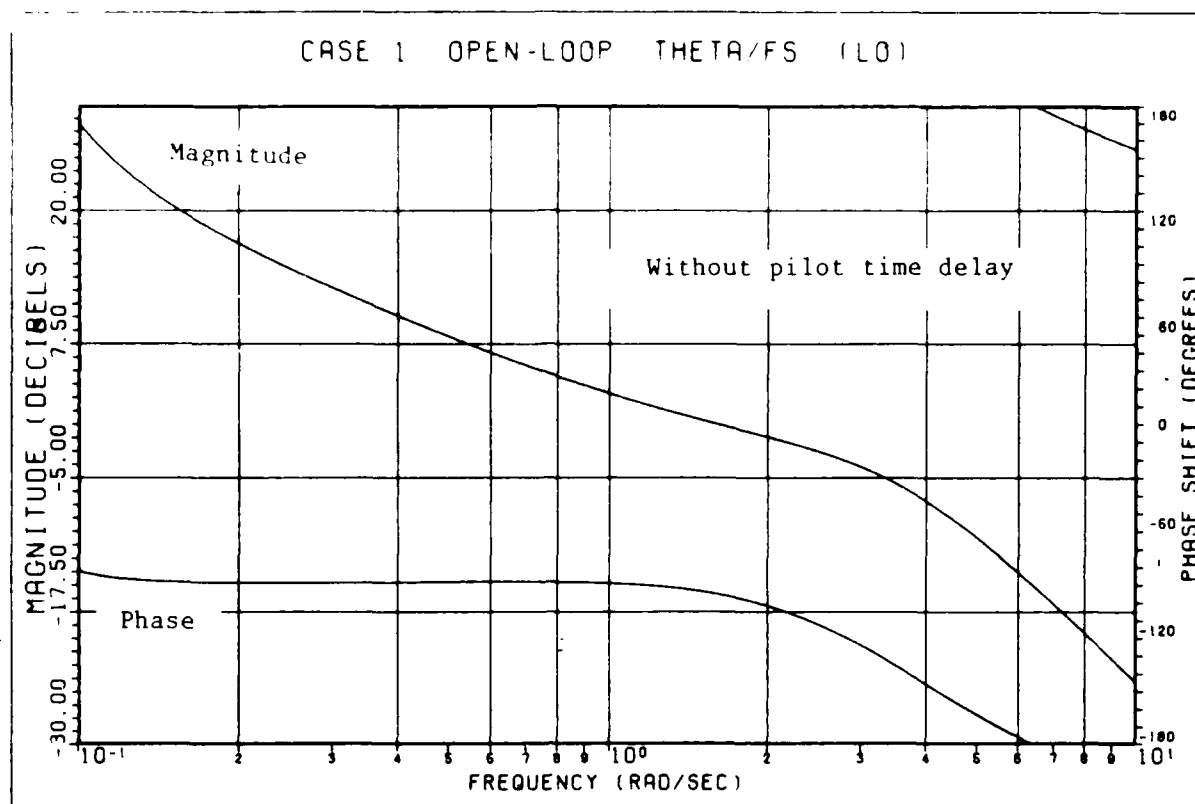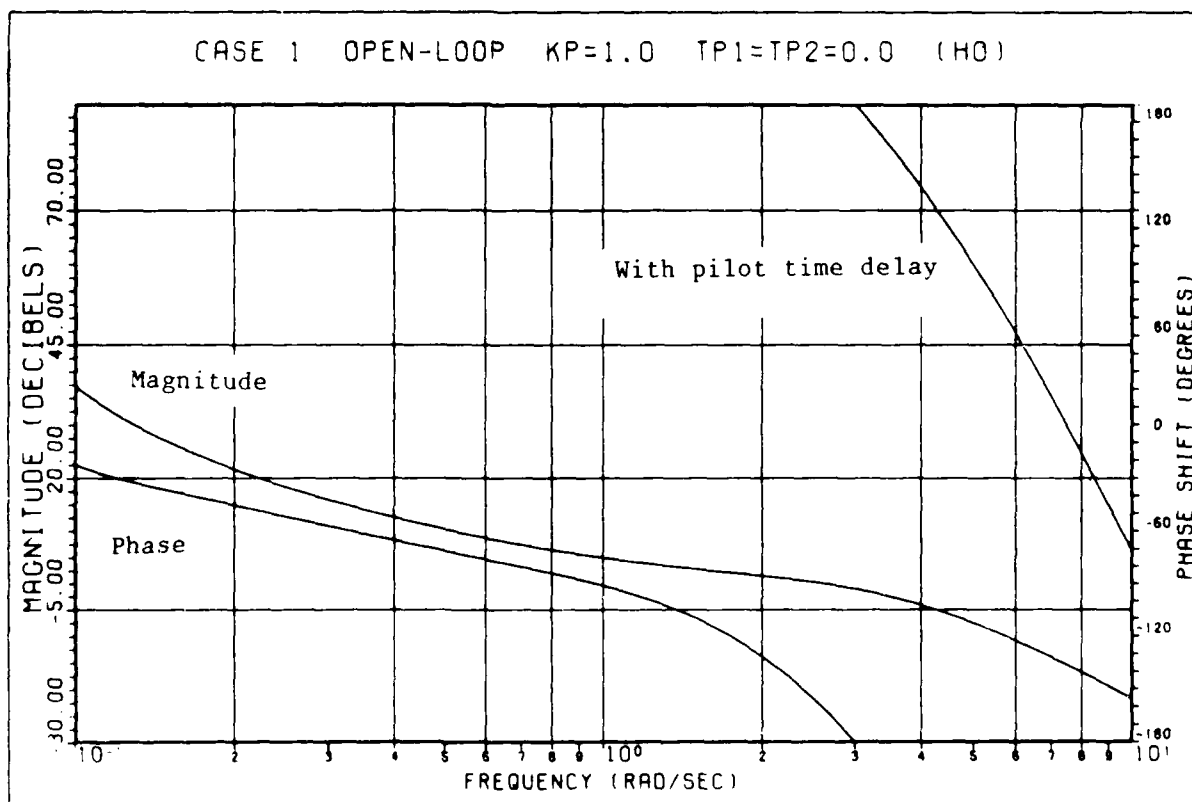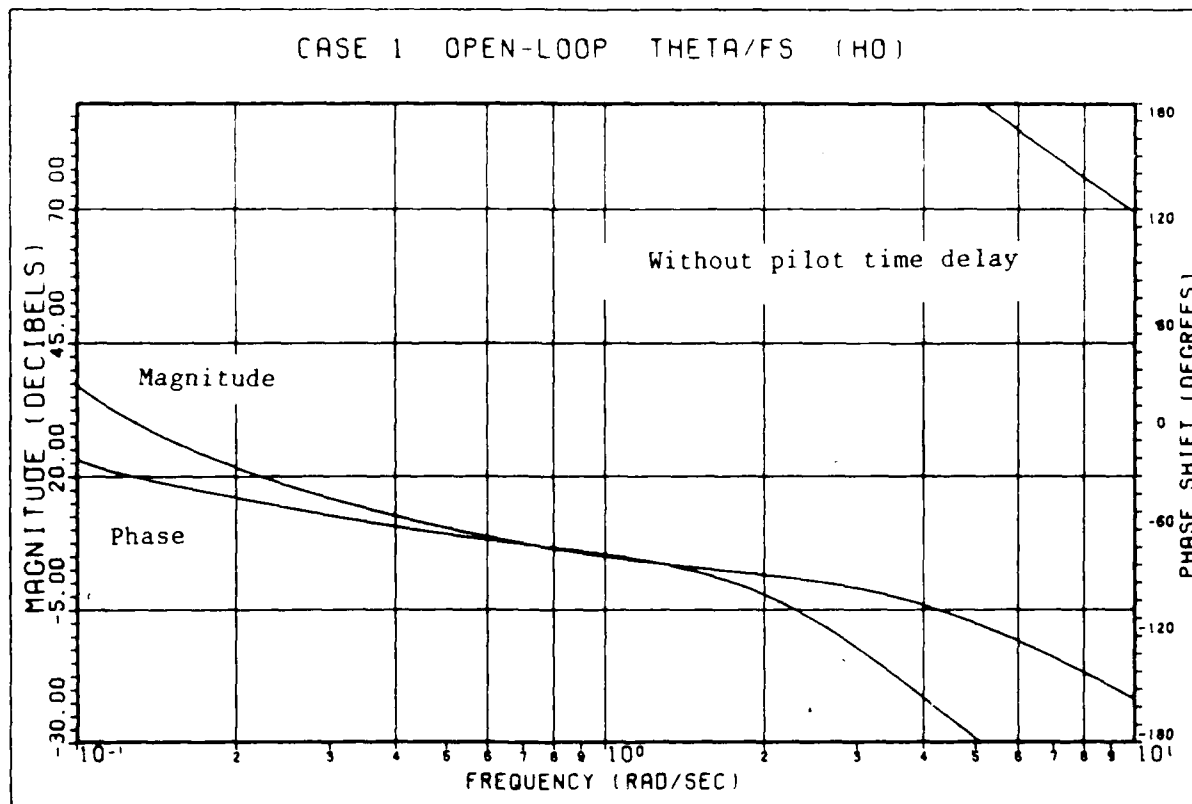Figure 12. Case 1, Low-Order Bode Plots

52

Figure 13.   Case 1, High-Order Bode Plots

53

At this point the simplified criteria was applied to
both the higher-order and lower-order systems. For the lower

order system, $\dfrac{d|\theta/F_s|}{d(\log \omega)} = -33$ db/dec, $\dfrac{d(ARG\ \theta/F_s)}{d(\log \omega)} = -230$ deg/dec

and $(ARG\ \theta/F_s)_{BW_{min}} = -136$ deg. Therefore, $ARG_{ad} = -196$

degrees and $(dA/dARG)_{ad} = +.0895$ db/deg. From Figure 9, this
predicts Level 2 handling qualities. Similarly for the
higher-order system, $ARG_{ad} = -200.2$ deg and
$(dA/dARG)_{ad} = +.0786$ db/deg. These numbers correspond to
Level 2/Level 3 handling qualities from Figure 9. Thus, the
simplified criteria indicates that the system which was
designed to yield good handling qualities may in fact be
Level 2 or worse. Clearly the higher-order effects and pilot
time delay have taken their toll on the system performance.

Next, $K_p$, $\tau_{p_1}$, and $\tau_{p_2}$ were found for the lower-order
system using the method described Reference 16, Section 6.6.
First, $K_p$ was adjusted to bring the open-loop amplitude-phase
curve up on the Nichol's chart so that it crossed the 0 db
line at -180 degrees of phase. Any further increase in $K_p$
would drive the system unstable. As can be seen from Figure
14, a value of 1.63 accomplishes this. It is clear that lead
compensation by the pilot can be used to bring the curve to
the right in order to meet the bandwidth criteria ($-90°$ of
phase at $\omega = 3.5$ rad/sec). As pointed out by Neal-Smith, it
is desirable to have the phase at $\omega = 3.5$ rad/sec near -130
degrees in order to have low resonance [16:55]. From Figure
14, the phase at $\omega = 3.5$ rad/sec was $-198°$. Therefore, the
pilot would have to provide $68°$ of phase lead at $\omega = 3.5$
rad/sec. From Figure 15, taken from the Neal-Smith report, a
phase lead of $68°$ corresponds to $\tau_{p_1}\omega \approx 2.6$ ($\tau_{p_2} = 0$), or
$\tau_{c_1} = 0.74$ sec. Therefore, the pilot model would look like

54

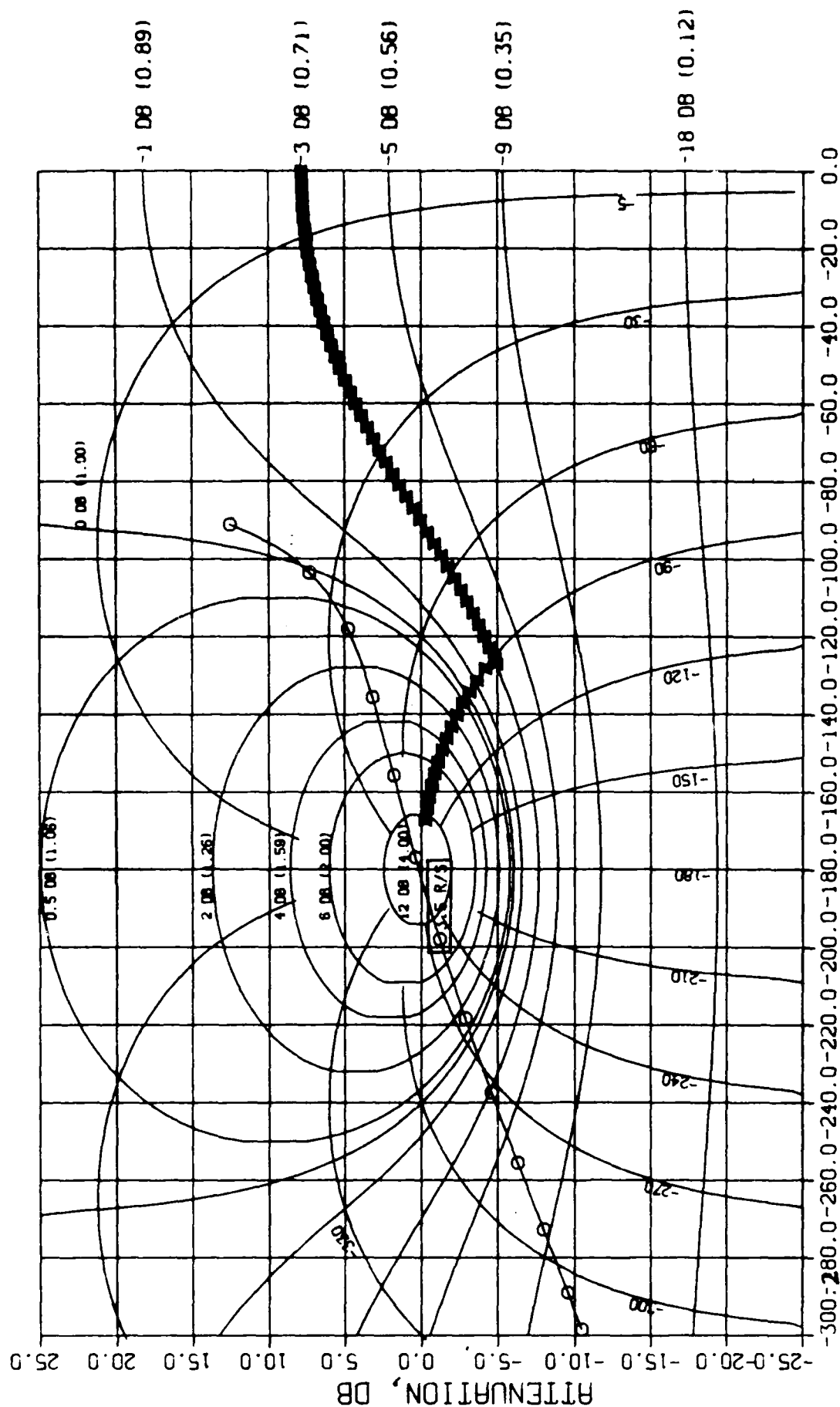CASE 1  KP=1.6,  TP1=TP2=0.0  (LO)



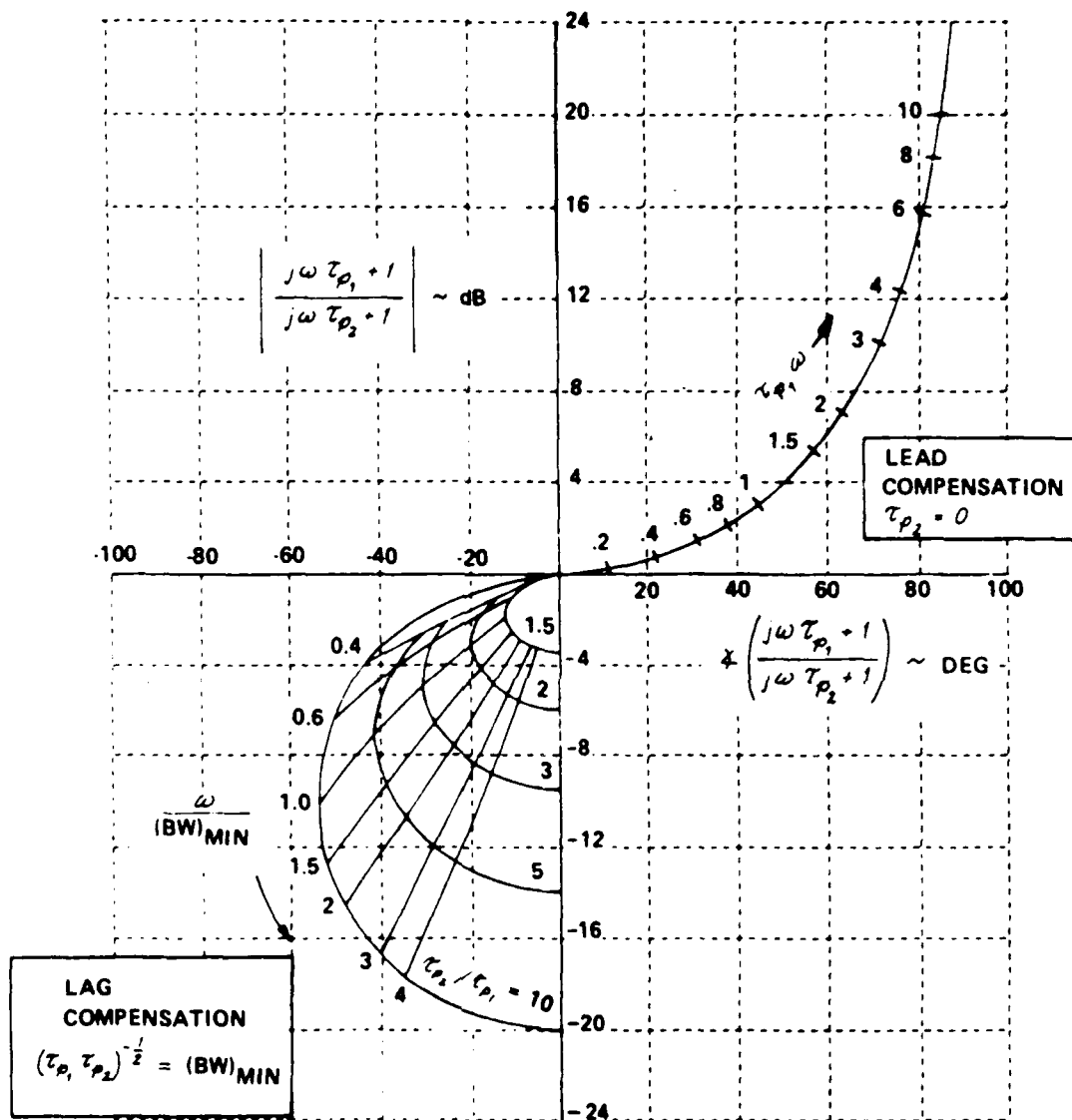Figure 14.  Case 1, Nichol's With No Pilot Equalization

55

Figure 15. Amplitude-Phase Curves for "Optimum" Pilot Compensation

$$G_p = (1.63)e^{-.3s}(0.74s + 1) \tag{5.4}$$

However, when this new pilot model was included in the $\theta/\theta_e$ transfer function and plotted on the Nichol's chart, the performance standards were not quite met. An iterative process began until the correct values of $K_p = 0.82$ and $\tau_{p_1} = 0.42$ are found.

The resulting Nichol's chart and closed-loop Bode diagram are shown in Figures 16 and 17 respectively. The amount of pilot phase added at $\omega = 3.5$ rad/sec was $56°$ and $|\theta/\theta_e|_{max} = 5.4$ db. Therefore, from Figure 8, the aircraft would exhibit Level 2 handling qualities, as the simplified criteria predicted. This gives us some faith in appling the simplified criteria to the higher-order systems.

Case 5. Figures 18 and 19 show the Bode plots for the lower and higher order systems, respectively. The phase and gain margins indicate that they are all unstable systems. Figure 20 shows the Nichol's chart for the lower-order system with a value for $K_p$ of 0.35. Several attempts were made to meet the performance standards using pure lead ($\tau_{p_2} = 0$) but no configuration was found. When both $\tau_{p_1}$ and $\tau_{p_2}$ were adjusted, slightly better results were obtained. A value of $K_p = 0.06$, $\tau_{p_1} = 5.0$, and $\tau_{p_2} = 0.005$ was used to produce the Nichol's chart in Figure 21 and the closed-loop Bode diagram in Figure 22. The value of $\tau_{p_1}$ used here is unreasonable. The amount of pilot phase added was $86°$ and $|\theta/\theta_e|_{max} = 4.4$ db. The maximum low-frequency droop was 6.25 db. This is probably a Level 3 system as seen in Figure 8.

Appling the simplified criteria to the higher-order system resulted in $(ARG)_{ad} = -254$ deg and $(dA/dARG)_{ad} = .18$ db/deg. Figure 9 shows this to be Level 3, almost Level 2.

57
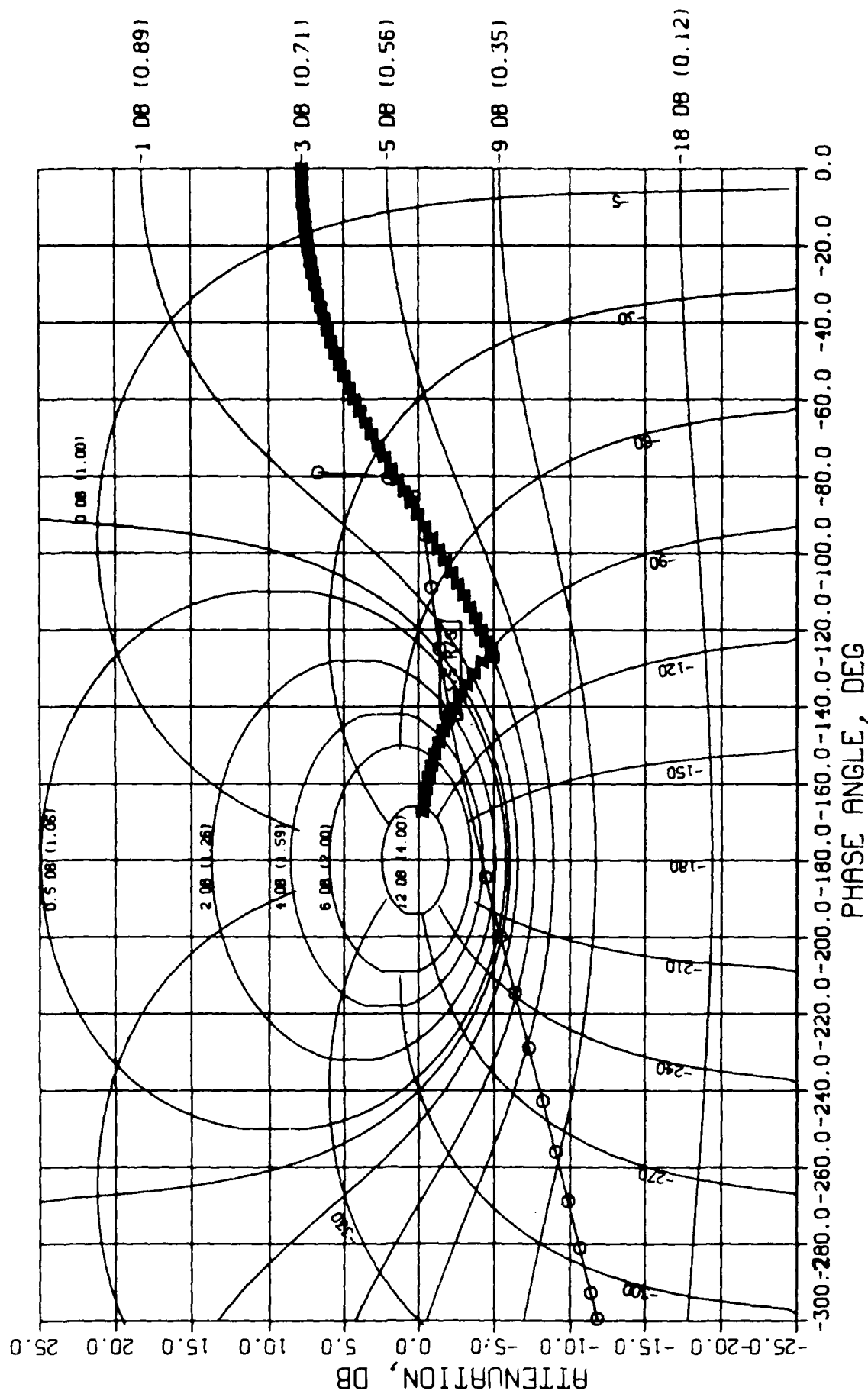
Figure 16. Case 1, Nichol's Chart With Pilot Equalization

CASE 1  KP=.82, TP1=.43 TP2=0.0 (LO)

CASE 1 CLOSED-LOOP KP=.82 TP1=.43 TP2=0. (LO)
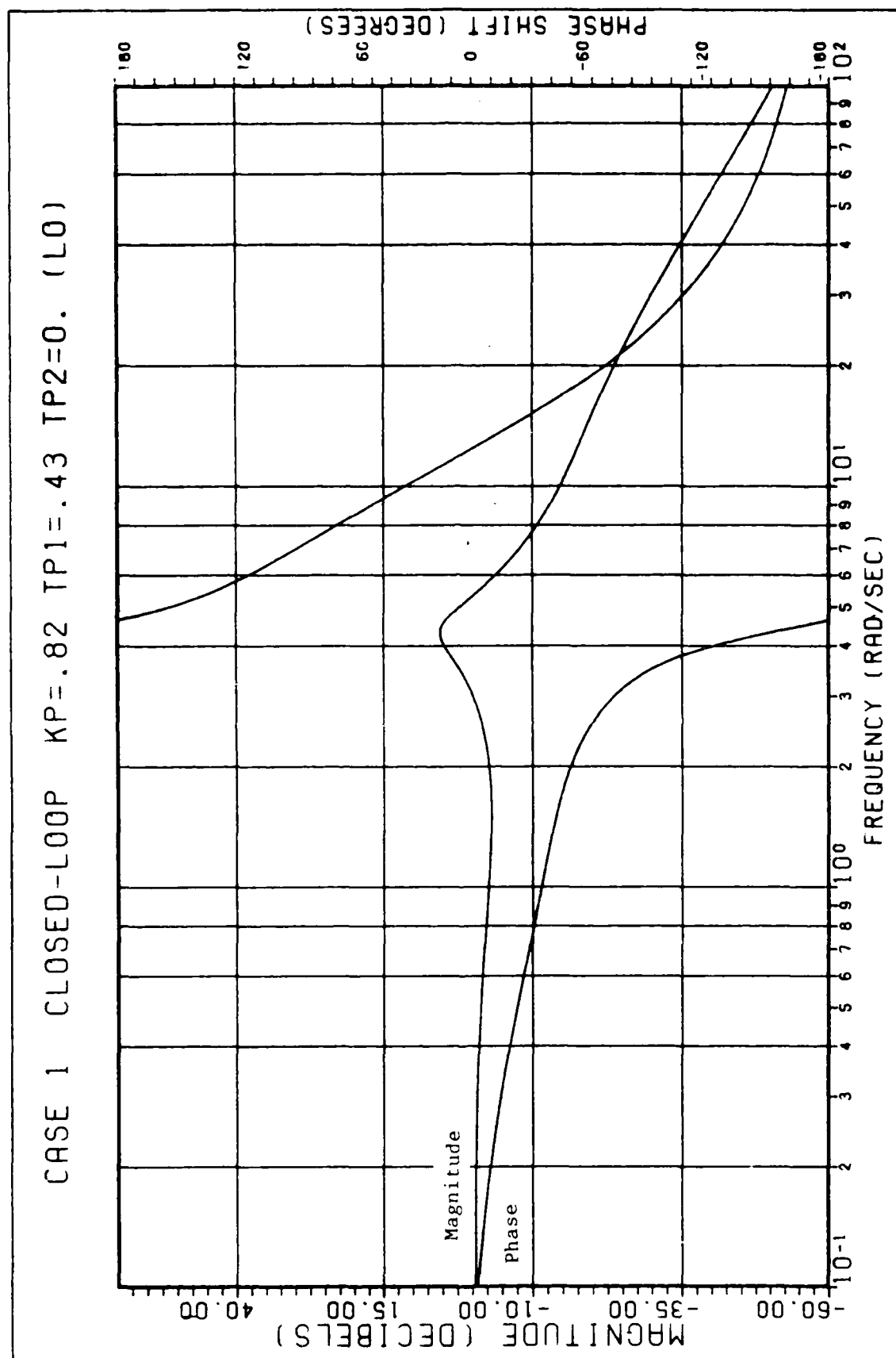
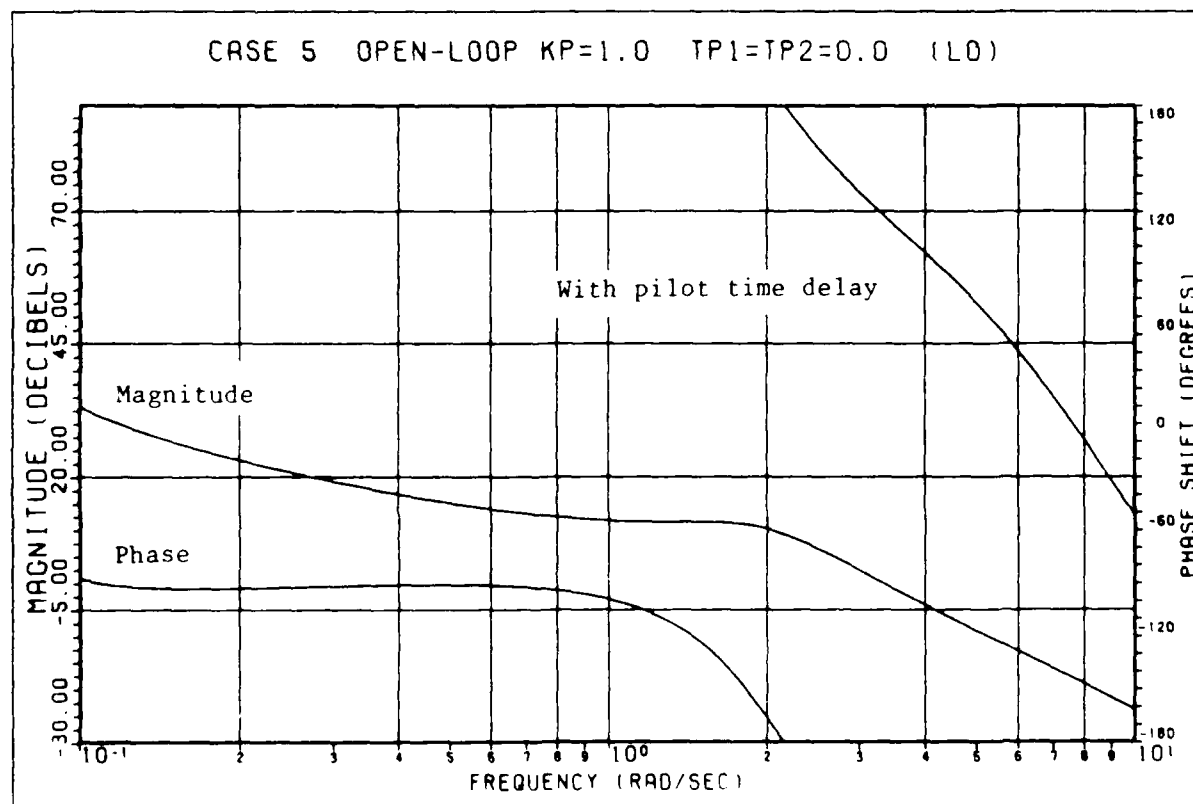Figure 17. Case 1, Closed-Loop Bode Plot With Pilot Equalization

59
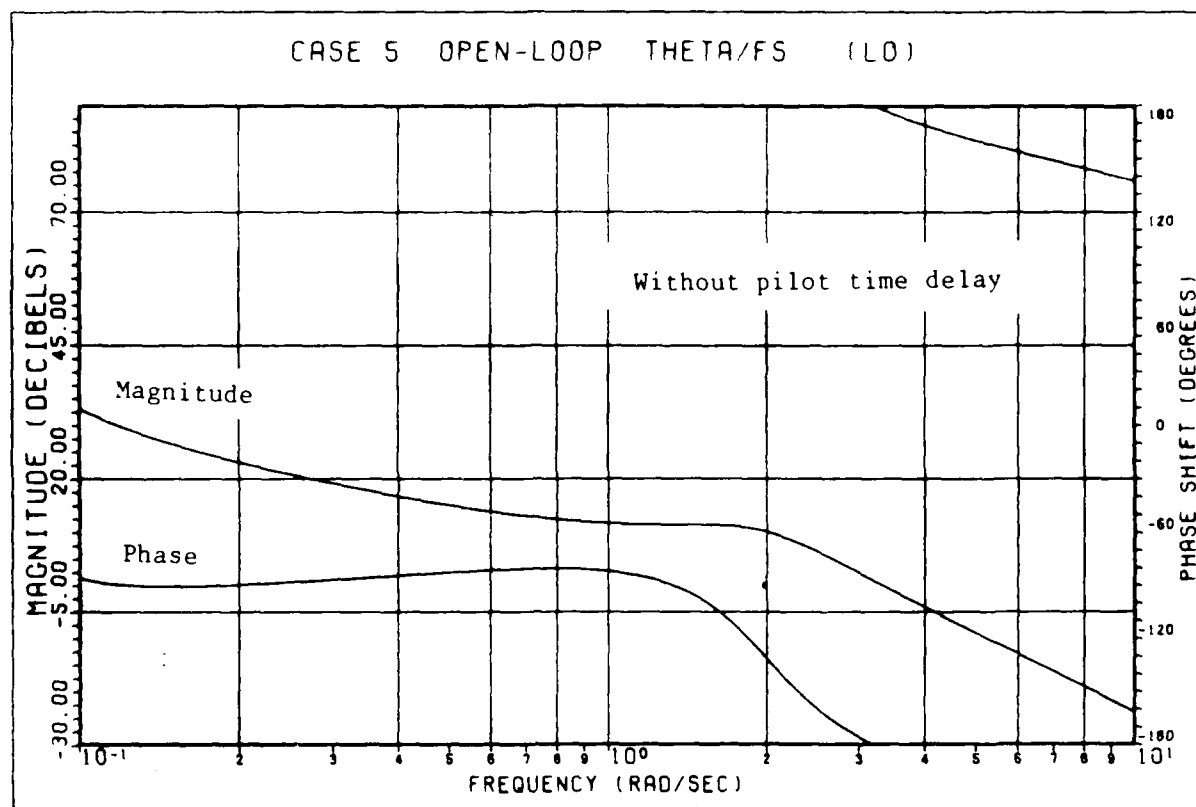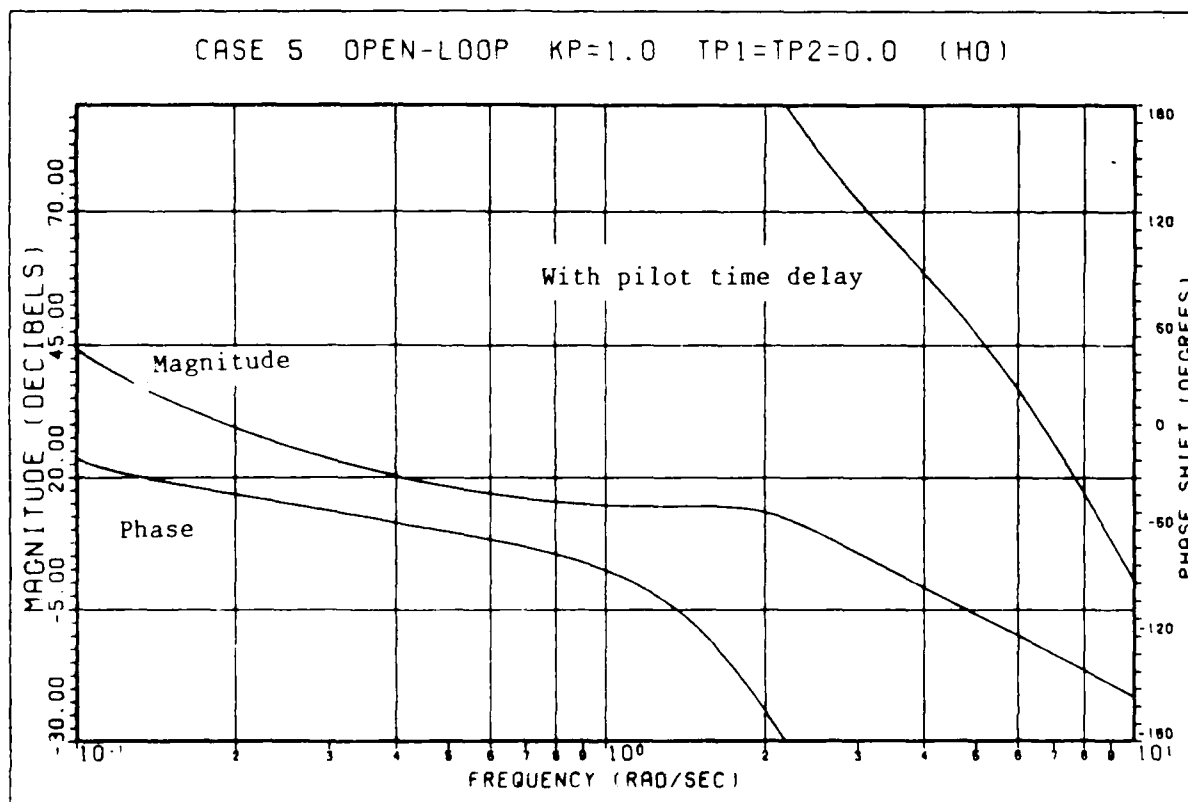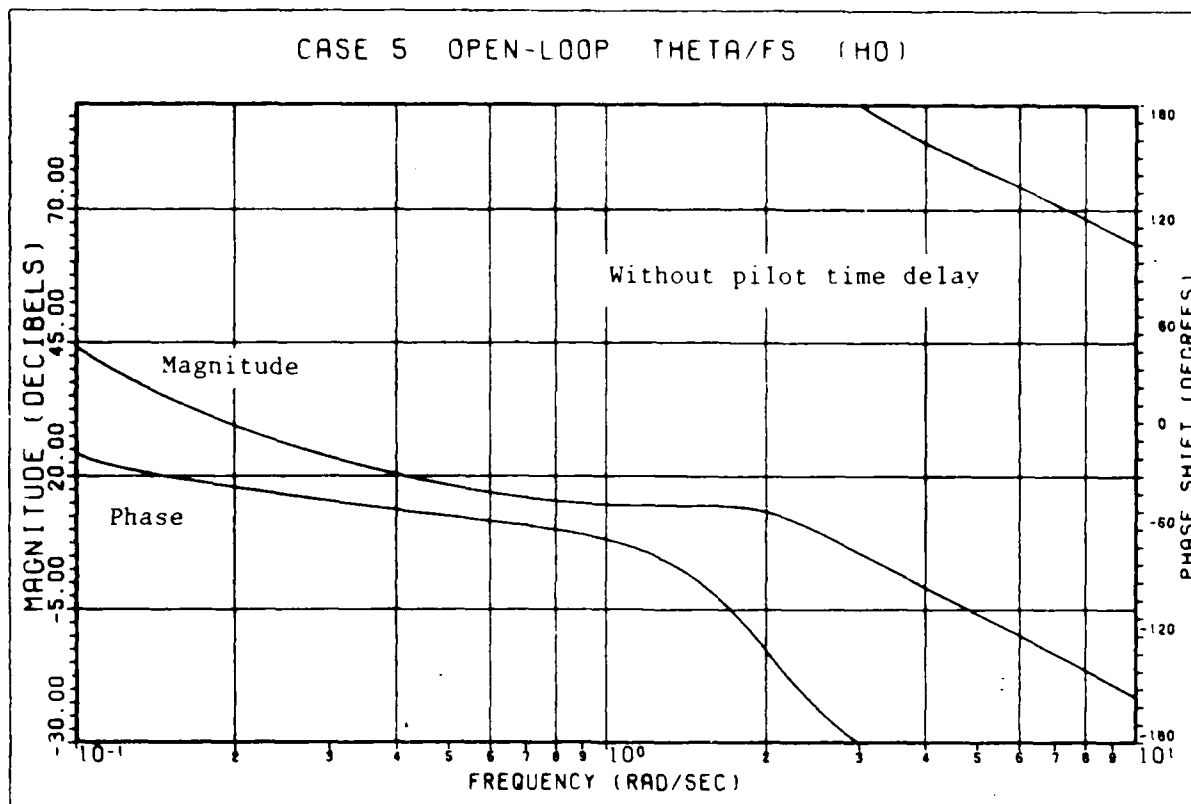
Figure 18.   Case 5, Low-Order Bode Plots

Figure 19.   Case 5, High-Order Bode plots

61
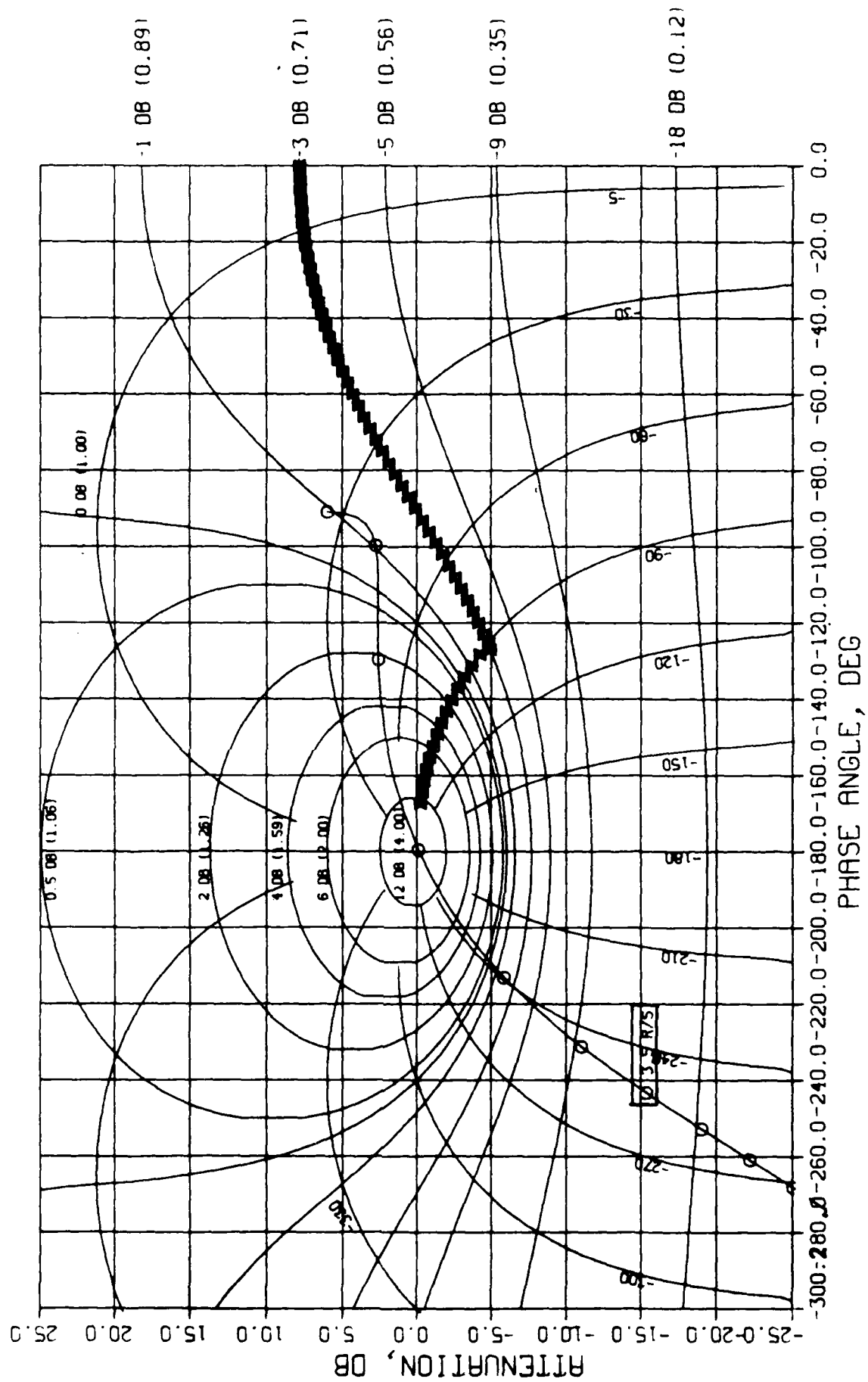
CASE 5  KP=.35,  TP1=0.0 TP2=0.0 (LO)

Figure 20.  Case 5, Nichol's Chart With No Pilot Equalization

62

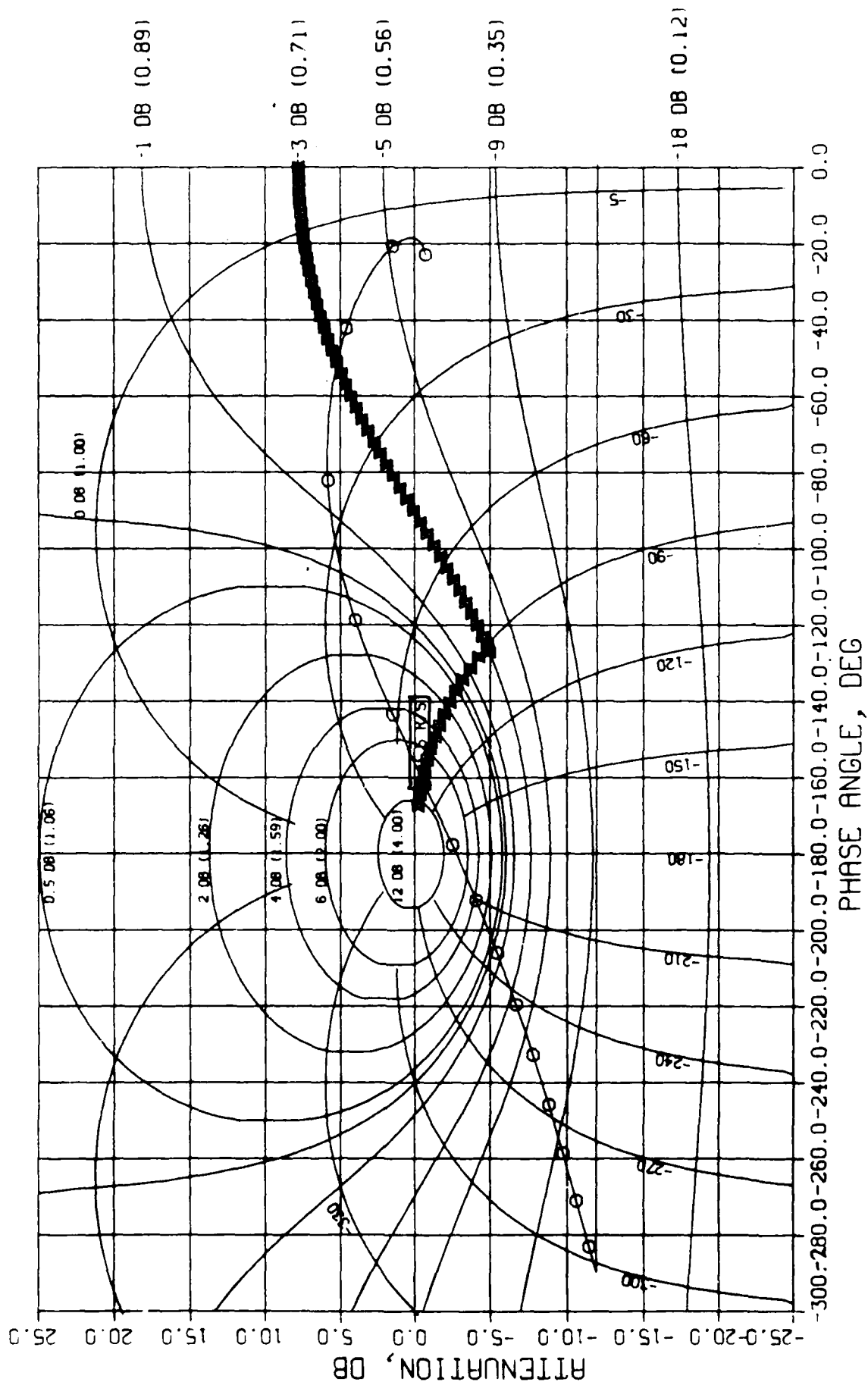CASE 5 KP=.06, TP1=5.0 TP2=.005 (LO)

Figure 21. Case 5, Nichol's Chart With Pilot Equalization
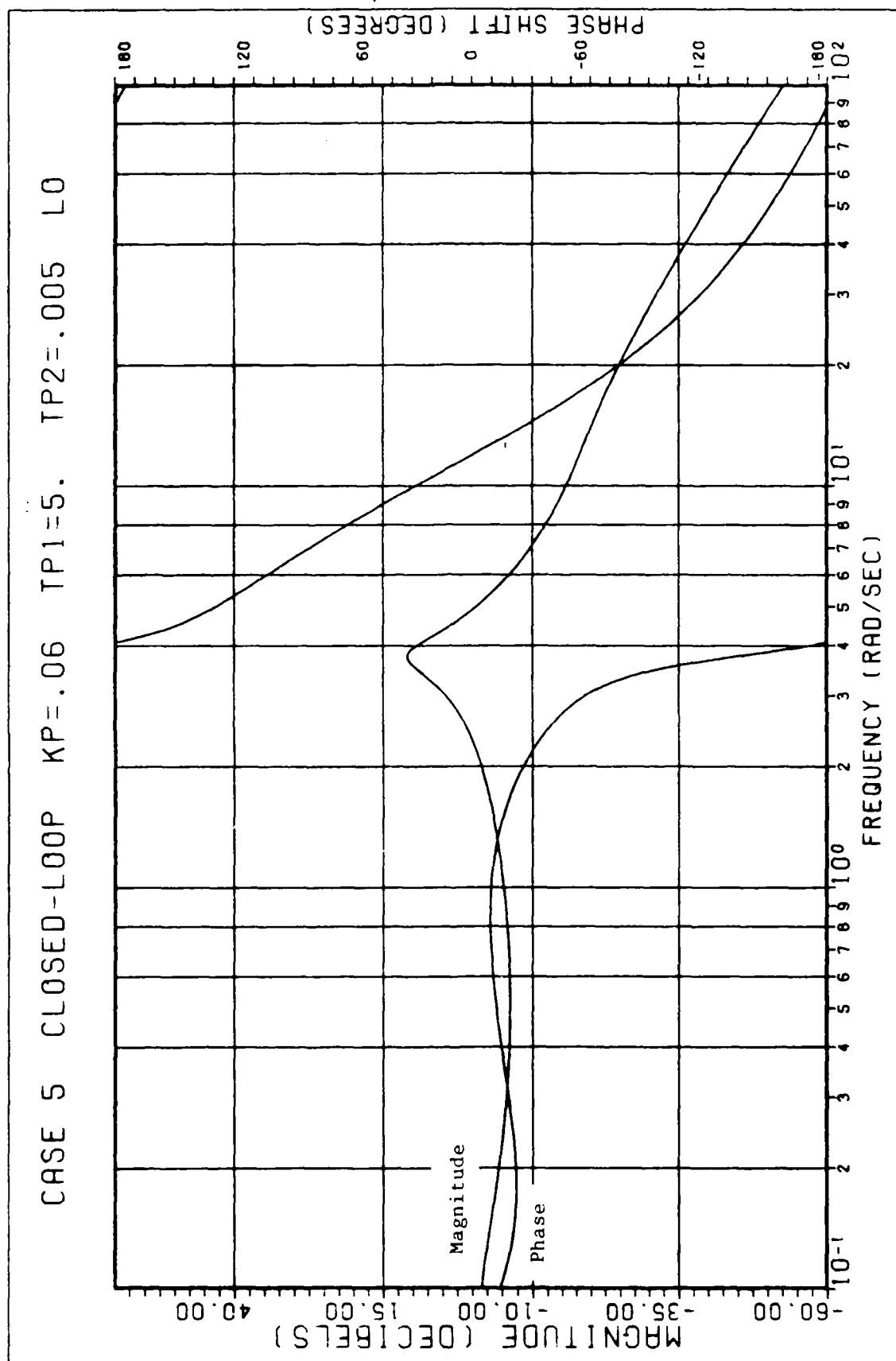
63

Figure 22. Case 5, Closed-Loop Bode Plot With Pilot Equalization

64

Case 9. Figures 23 and 24 are the Bode plots for the lower and higher-order systems, respectively. Again, the phase and gain margins indicate that the systems are unstable. Figure 25 is the Nichol's chart for the lower-order system with $K_p$ = 0.04. It is obvious that a good deal of compensation is required to meet the performance standards. A pilot model with $K_p$ = 0.03, $\tau_{p_1}$ = 10., and $\tau_{p_2}$ = 0.001 gave the closest agreement with the performance standards, as shown in Figure 26. The closed-loop Bode diagram is shown in Figure 27. The amount of pilot phase added was 88 and $|\theta/\theta_c|_{max}$ = 19.5 db. The maximum droop is 2.5 db. This is a Level 3 system with strong PIO tendancies, as seen in Figure 8.

Appling the simplified criteria to the higher-order system resulted in $(ARG)_{ad}$ = -280 deg and $(dA/dARG)_{ad}$ = .23 db/deg. From Figure 9, this is a Level 3 system.

Summary

The addition of even just the pilot delay and stick prefilter noticably degrades the performance of the systems. According to Neal-Smith, the system designed to be Level 1 is Level 2; the system designed to be Level 2 is almost Level 3; and the system designed to be Level 3 is very Level 3, possibly uncontrollable. The small values of $K_p$ could be helped by reducing the stick gain from 2.0 to 1.0. It was satisfying to see good correlation between the simplified criteria applied to the higher-order systems and the full pilot model analysis, applied to the lower-order systems. Pilot-in-the-loop evaluations will be examined in the next section.
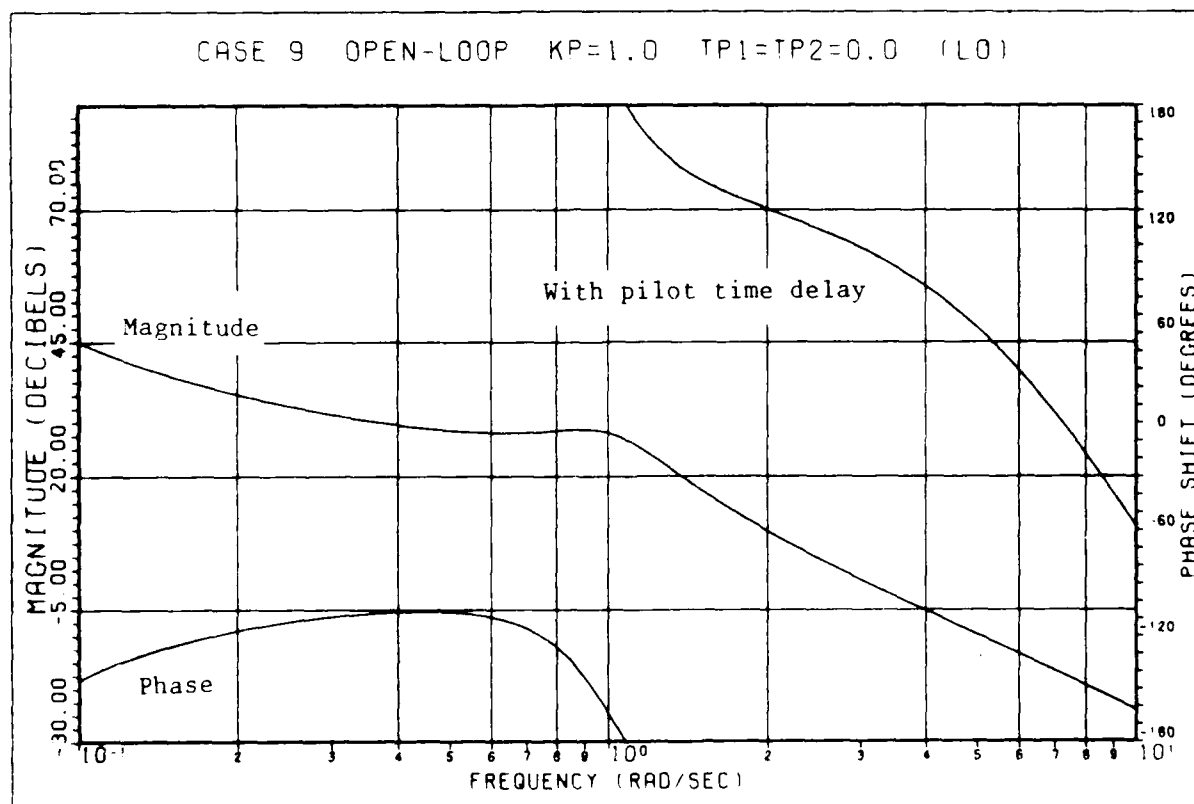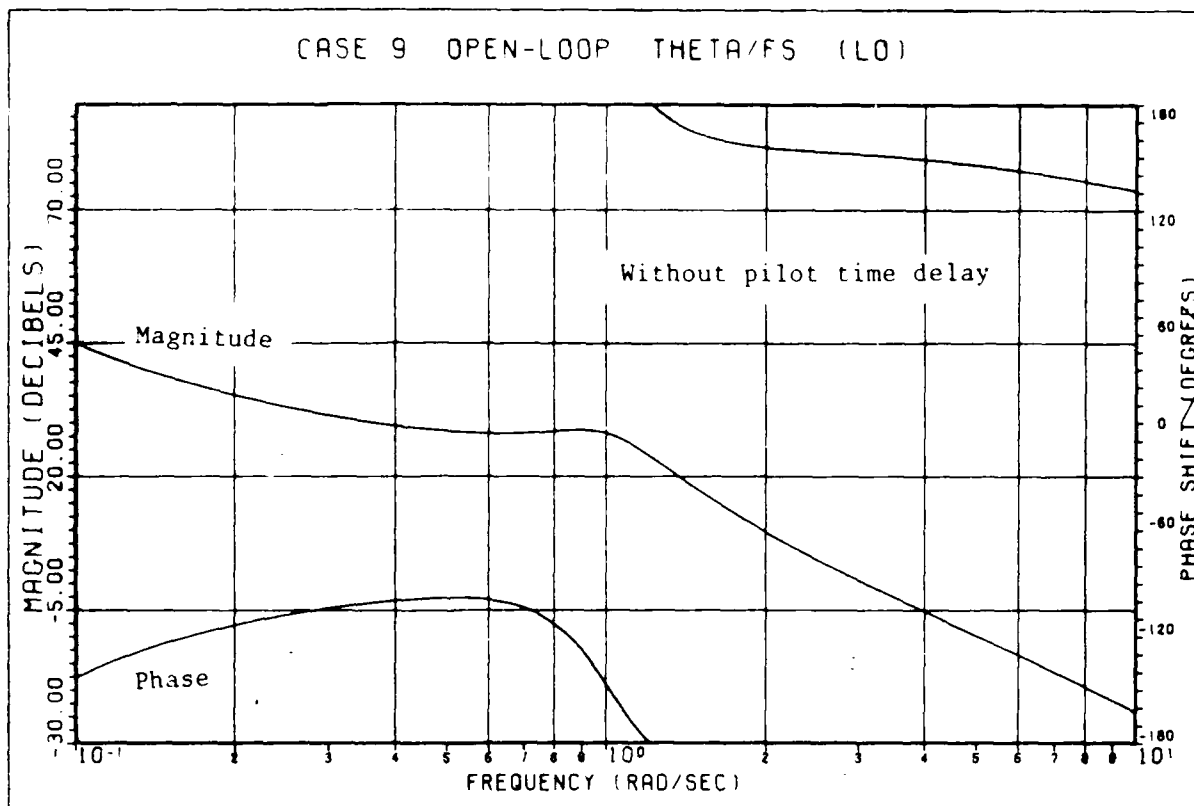
Figure 23.   Case 9, Low-Order Bode Plots

66

Figure 24. Case 9, High-Order Bode Plots
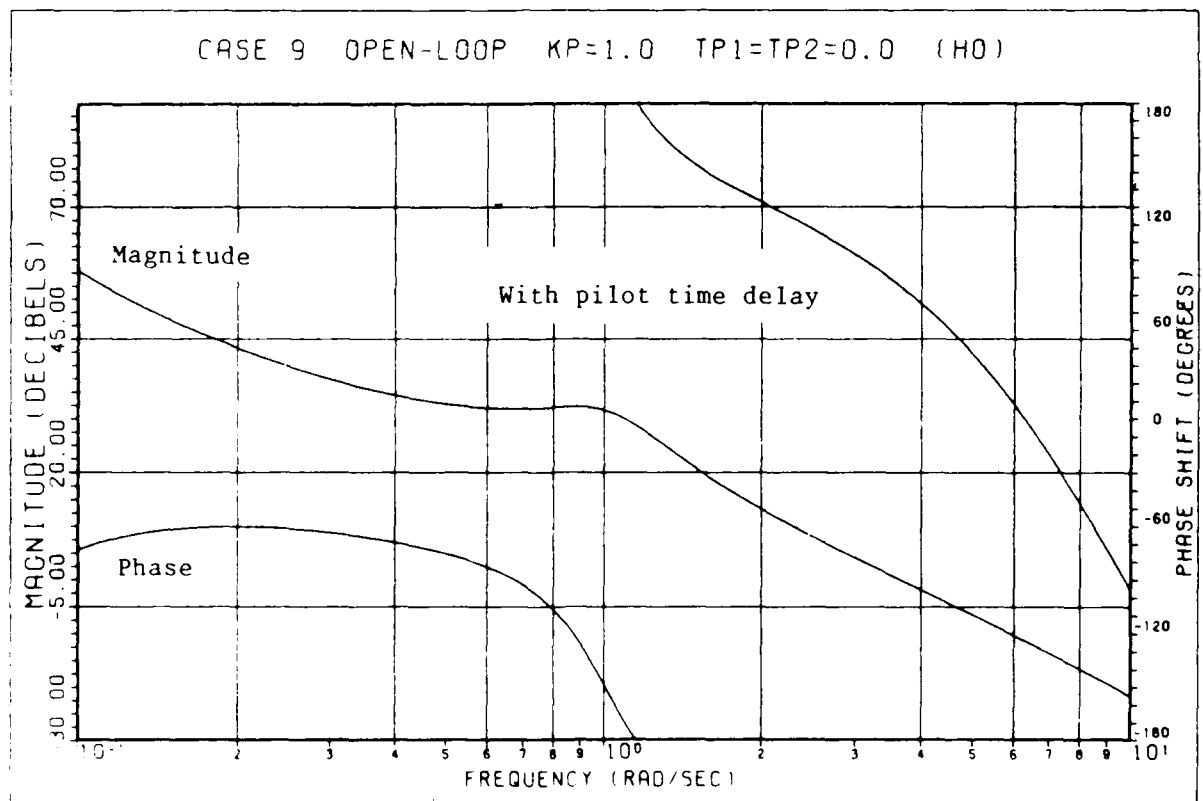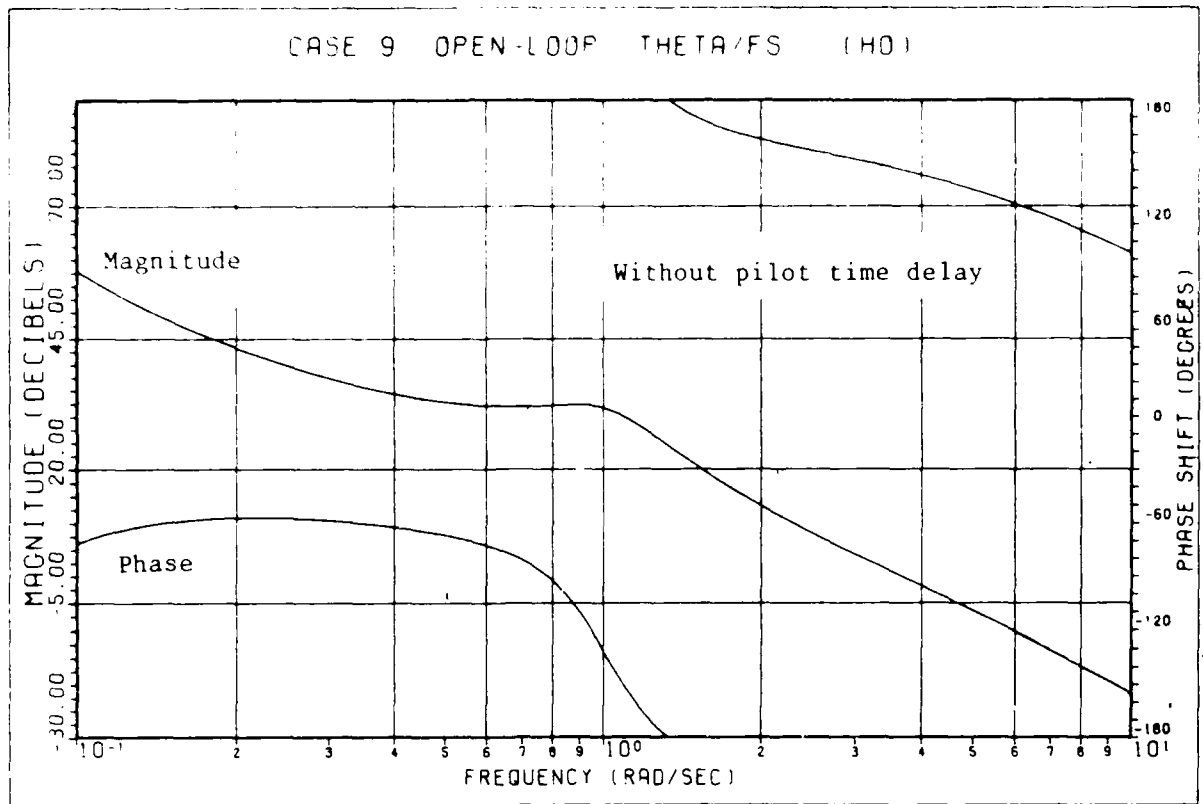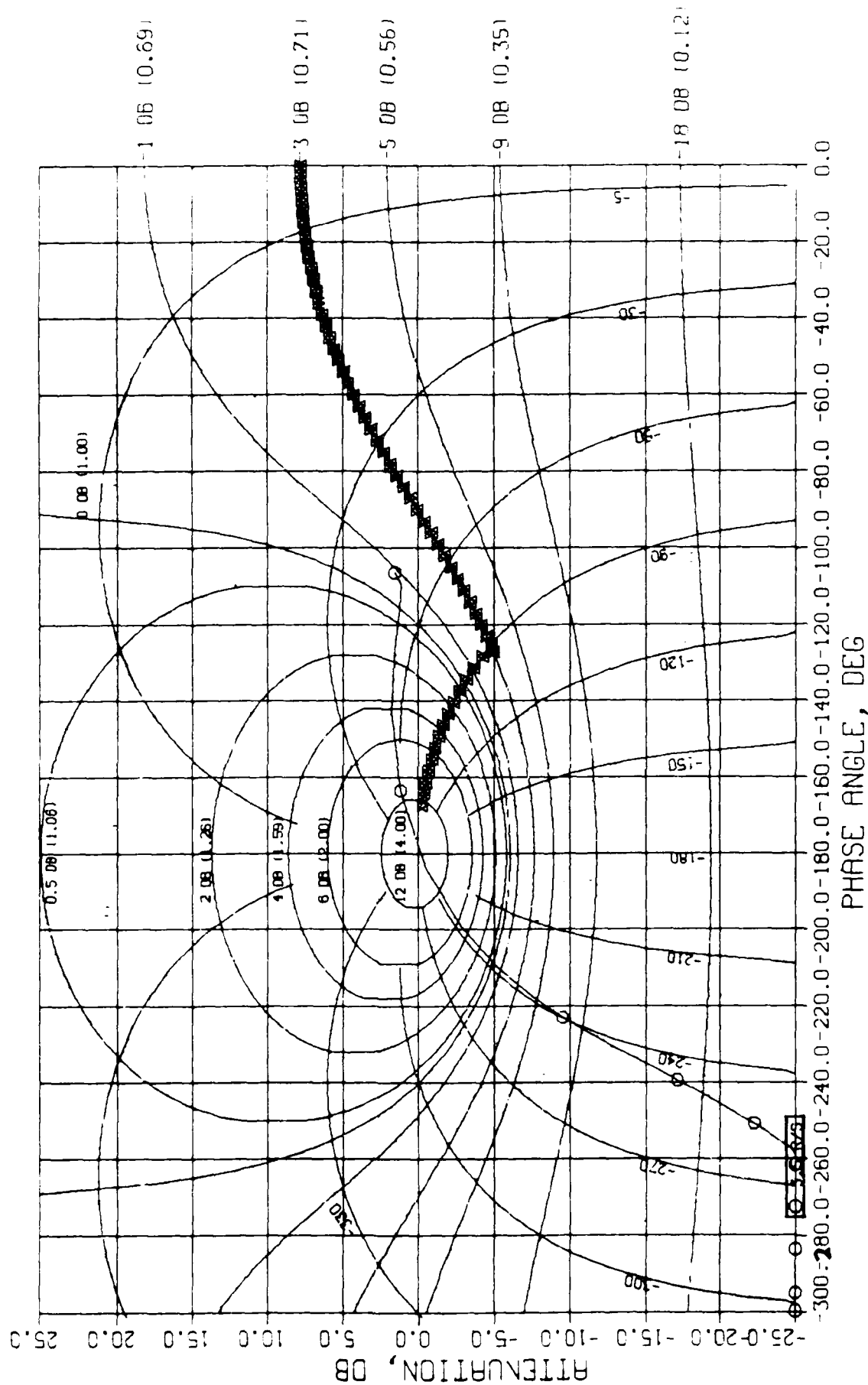
67

Figure 25. Case 9, Nichol's Chart With No Pilot Equalization

CASE 9 KP=.03, TP1=10. TP2=.001 (LO)
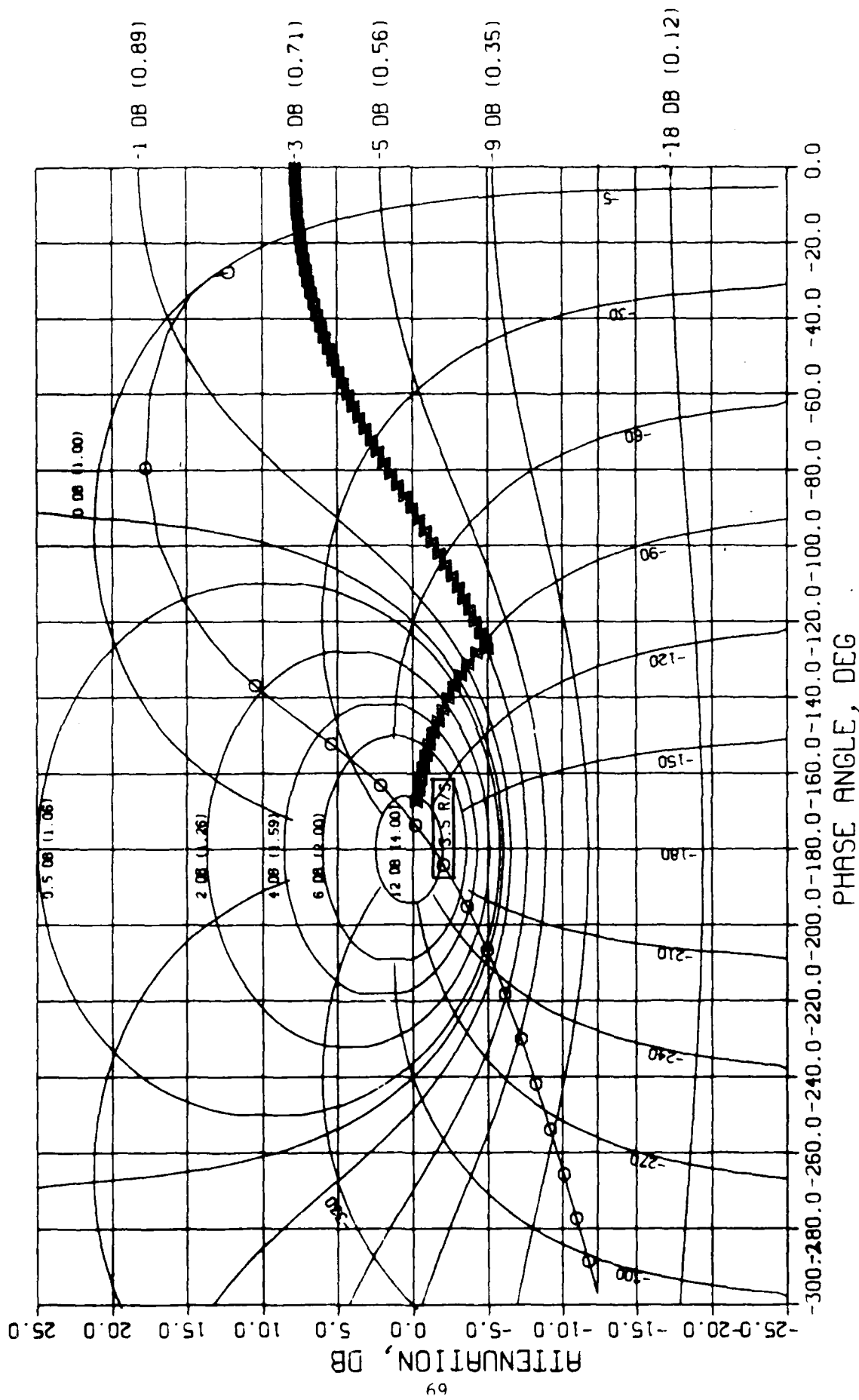


Figure 26.  Case 9, Nichol's Chart With Pilot Equalization
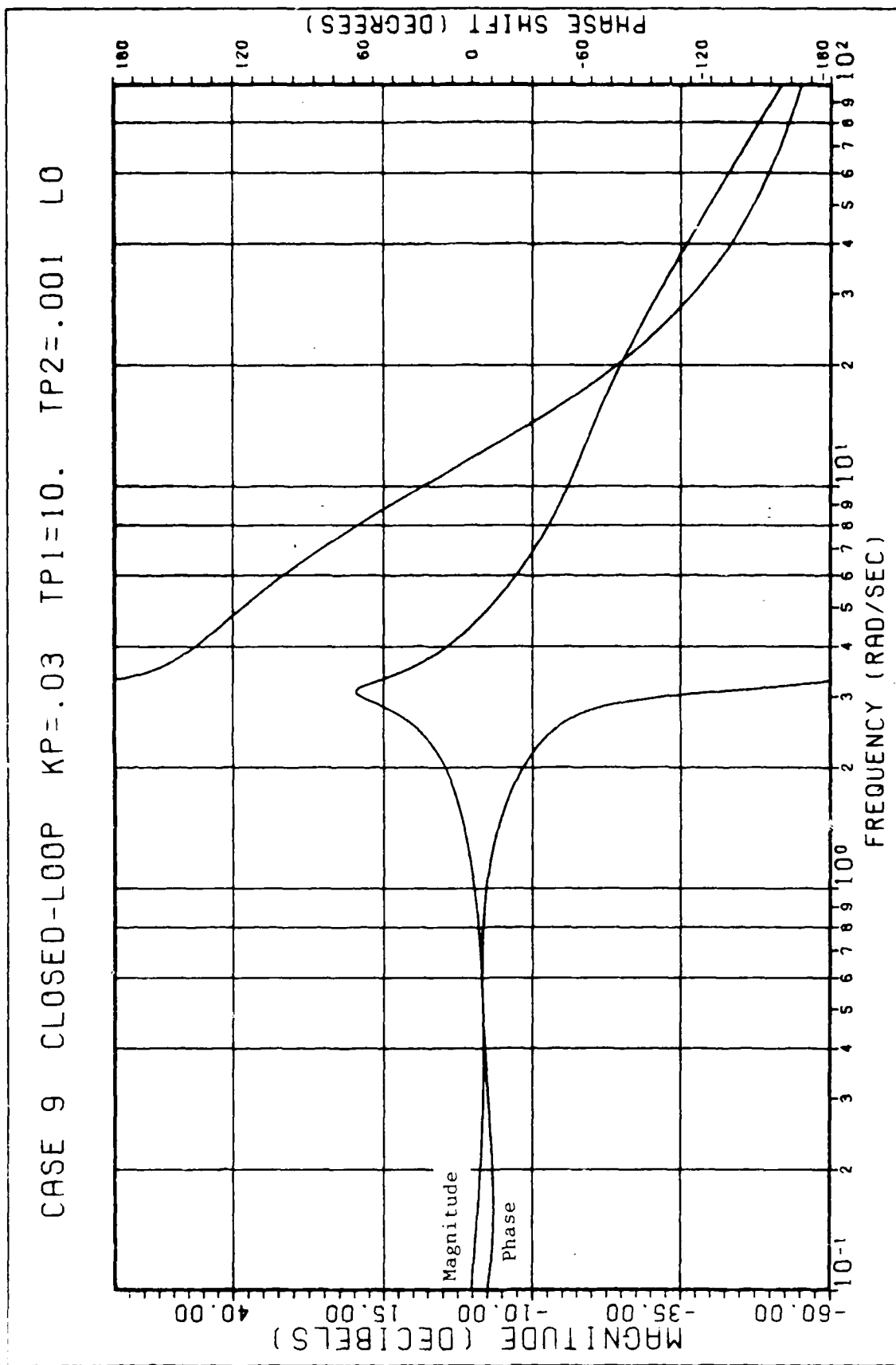
Figure 27. Case 9, Closed-Loop Bode Plot With Pilot Equalization

# VI.  Manned Simulation Analysis

The final step in the evaluation process was to integrate the full-state feedback control system into the LAMARS X-29A simulation and conduct man-in-the-loop evaluations for a pitch tracking task.  It is generally accepted that ground-based man-in-the-loop simulators are a very useful tool but should never be considered the final word on the acceptibility of a control system.  They are best utilized in the role of bridging the gap between paper analysis and flight test.

The LAMARS simulation of the X-29A received extensive scrutiny from government agencies and industry when it was used as the Air Force safety-of-flight evaluation simulator. It is recognized as being a superior simulation and therefore, the results of the current study should be valid within the restrictions of the control system design.  The most notable restrictions were the small perturbation assumption and the piecewise linearization of feedback gains throughout a limited flight envelope.

## Description of the Flight Control Development Laboratory

The Flight Control Development Laboratory (FCDL) is located within the Flight Control Division of the Flight Dynamics Laboratory.  The primary mission of the facility is to evaluate flight control system concepts in as realistic an environment as necessary through the use of several man-in-the-loop simulators.  The simulators include three motion-base, one static-base, and one manned combat station. A brief description of the hardware used in this study is presented below in order to give the reader a sense of the level of fidelity used for the study.

Hardware. The LAMARS, shown in Figure 28, provides high quality flight cues in a five degree-of-freedom (lateral, vertical, roll, pitch, and yaw), beam-type motion system. The 20-foot-diameter dome contains a single-seat fighter cockpit and spherical dome display. The LAMARS motion system consists of a 30-foot-long horizontal beam, gimbaled at the rear and driven by hydraulic actuators to provide ± 10 feet of both vertical and lateral motion to the cockpit. The cockpit gimbal system is mounted on the forward end of the beam and provides angular rotation of ± 25 degrees in pitch, roll, and yaw. The LAMARS motion system performance is summarized in Table V.

The transient motion cues provided by the LAMARS motion system were augmented by a g-suit which is programmed to provide positive, sustained cueing for load factor conditions above one gee.

The cockpit was configured as a generic fighter cockpit with a standard suite of up-front instruments, a head-up display (HUD), throttle, and a programmable feel system center-stick. A typical LAMARS cockpit configuration is shown in Figure 29. On the inside surface of the dome a 300 degree dynamic sky-earth image was projected to aid the test subject in visual cues. Also, artificial engine noise provided throttle setting feedback to the test subject and added to the overall environment realism.

At the heart of the simulation are four Gould SEL computers which communicate to each other through 1 MegaByte of shared memory. The computers' CPU's and IPU's are run in a parallel processor fashion. The SEL's are 32-bit digital machines with high-speed, real-time and scientific computing capabilities. A real-time hybrid clock provides the clock pulse to start each simulation cycle and initiate the

72
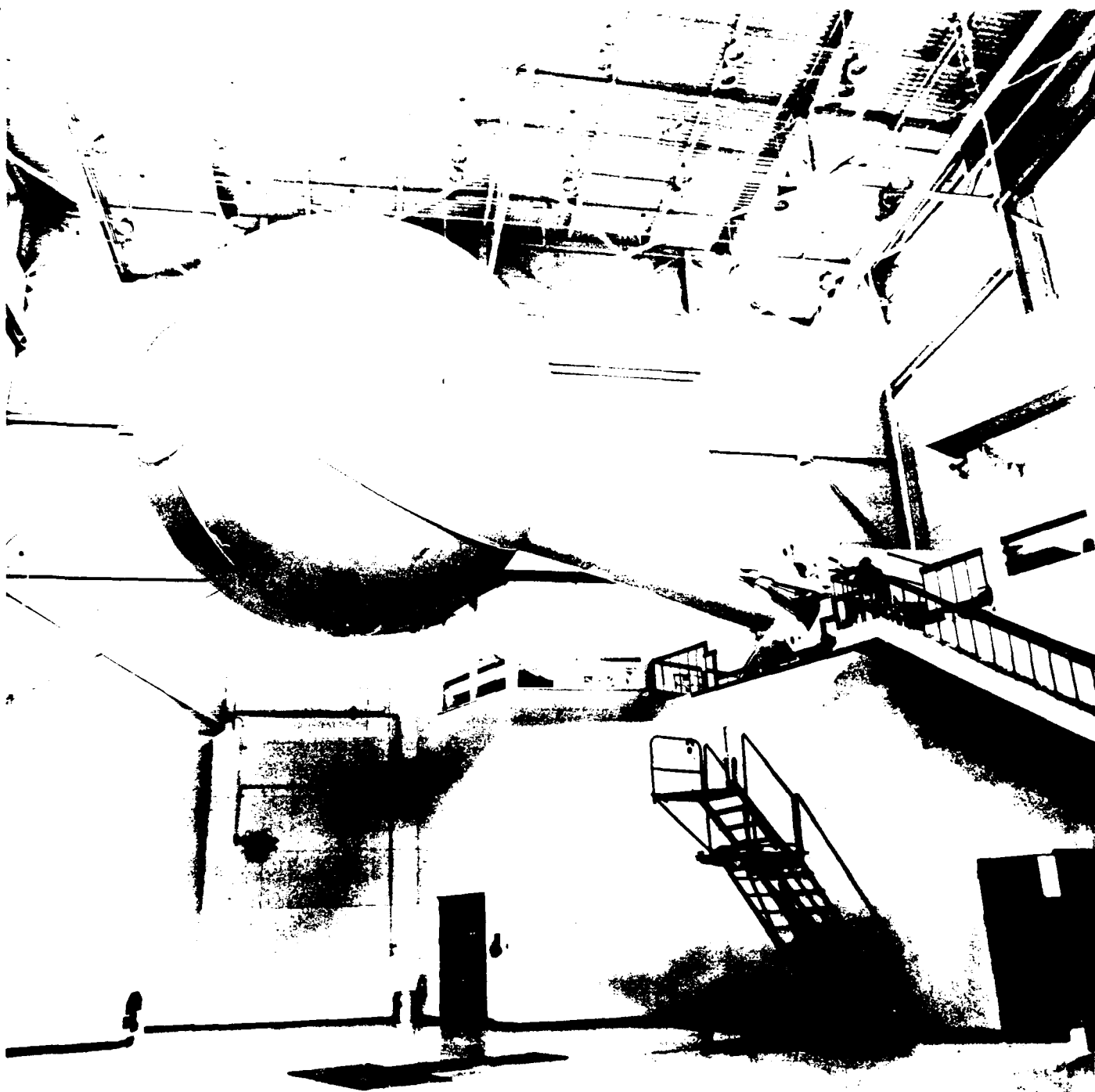
Figure 28.  LAMARS

TABLE V. LAMARS MOTION PERFORMANCE

| AXIS | DISPLACEMENT | ACCELERATION | VELOCITY | BANDWIDTH |
|------|--------------|--------------|----------|-----------|
| Vertical | ± 10 ft | ± 3 g's | 13 ft/sec | 25 rad/sec |
| Lateral | ± 10 ft | ± 1.65 g's | 10 ft/sec | 25 rad/sec |
| Pitch | ± 25° | ± 400°/sec$^2$ | 60°/sec | 25 rad/sec |
| Yaw | ± 25° | ± 200°/sec | 50°/sec | 25 rad/sec |
| Roll | ± 25° | ± 460°/sec$^2$ | 60°/sec | 25 rad/sec |

Figure 29. LAMARS Cockpit

75

digital-to-analog (DAC) and analog-to-digital (ADC) conversions. A 25 milli-second frame rate was used on this simulation. An EAI 781 analog computer was used to model the Analog Reversion mode of the X-29A flight control system and also the fourth-order actuator models. A CSPI array processor was used to perform table look-ups for the aerodynamic math model. Over 60,000 data points in breakpoint format were used in the data package.

An Interactive Machines Inc. (IMI) 455D stroke graphics system was used to generate the head-up display, shown in Figure 30. The IMI communicated to the SELs through an Ethernet system. There was virtually no time delay in the Ethernet/IMI system for this simple HUD. A Megatek Whizzard 7000 calligraphic system was used to provide the test conductor with a real-time display of pertinent simulator/aircraft data on a monitor adjacent to the test conductor's station.

The Master Control Console (MCC), shown in Figure 31, provides the ability for one simulation operator to monitor and control the entire simulation. A complete complement of aircraft instruments replicates those in the cockpit. Video monitors provide images of the HUD, LAMARS cockpit over-the-shoulder, and LAMARS bay. A joystick and set of potentiometers allows the simulation operator to fly the simulation during development and check-out. Thirty lighted, pushbutton switches provide the ability to control various aircraft subsystems, to switch between the standard AR mode and the modified control system, and to select the particular modified system to evaluate (Good, Fair, or Poor handling qualities). Several multichannel intercom units are available to provide communication between the test subject, LAMARS operator, simulation operator, and observers.
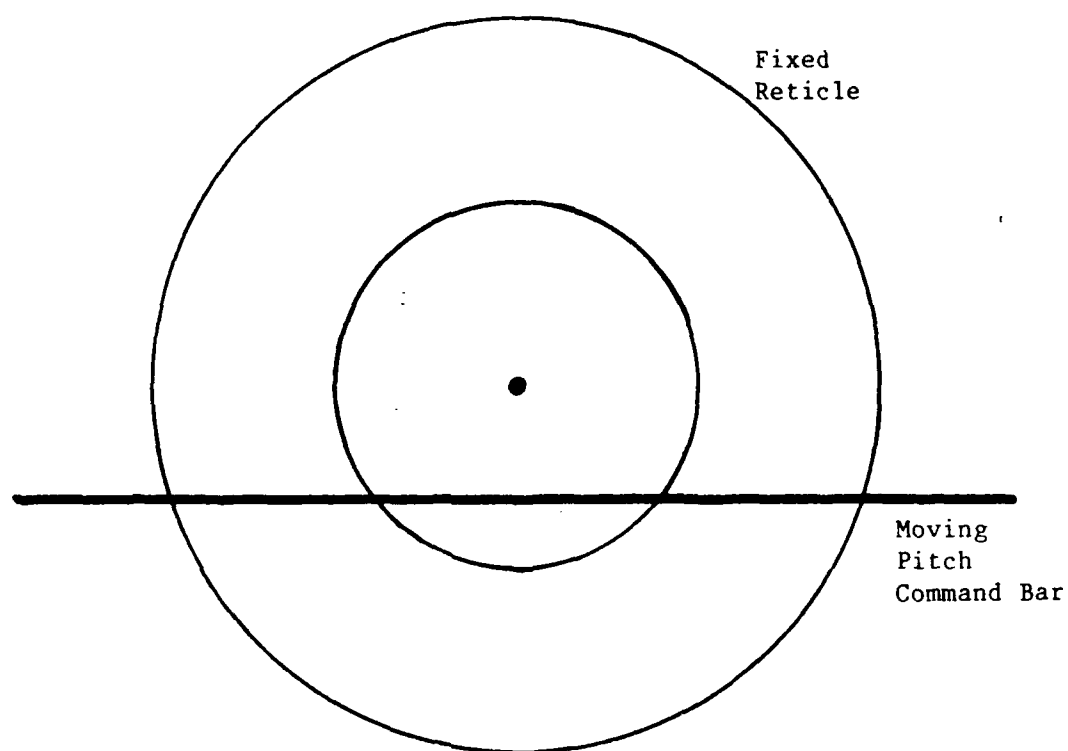
Figure 30. Head-Up Display

Figure 31. Master Control Console

Software. A complete description of the software used by the X-29A simulation is beyond the scope of this report. All of the software is coded in FORTRAN and written in-house. Relatively few changes were made to the simulation to carry out this study and they will be discussed later in this section.

## Modification of the X-29A Longitudinal Control Path

A three-step process was used to integrate the new control system into the simulation. Before discussing this process, an explanation needs to be made concerning the use of the word "controller". In this report, the word controller is meant to describe that portion of the flight control system which interprets the stick movements and creates four state perturbation signals for the twelve feedback gains. As will be seen, the design of the controller was an interesting problem.

The pitch-rate feedback, proportional plus integral longitudinal control path of the standard X-29A AR mode on the analog computer was replaced by the a simple full-state feedback system with no controller installed, as shown in Figure 32. Actually, the standard AR mode remained patched and a series of function relays activated by a single MCC button was used to switch between the standard AR path and the modified path.

Initial attempts to use this modified control path failed to keep the aircraft from diverging in pitch. The cause of the divergence turned out to be the added delay introduced by the fourth-order actuator models. Recall that the actuator time constants were not taken into account when the feedback gains were calculated. The penalty for this was made apparent by the diverging aircraft. When the actuator

79
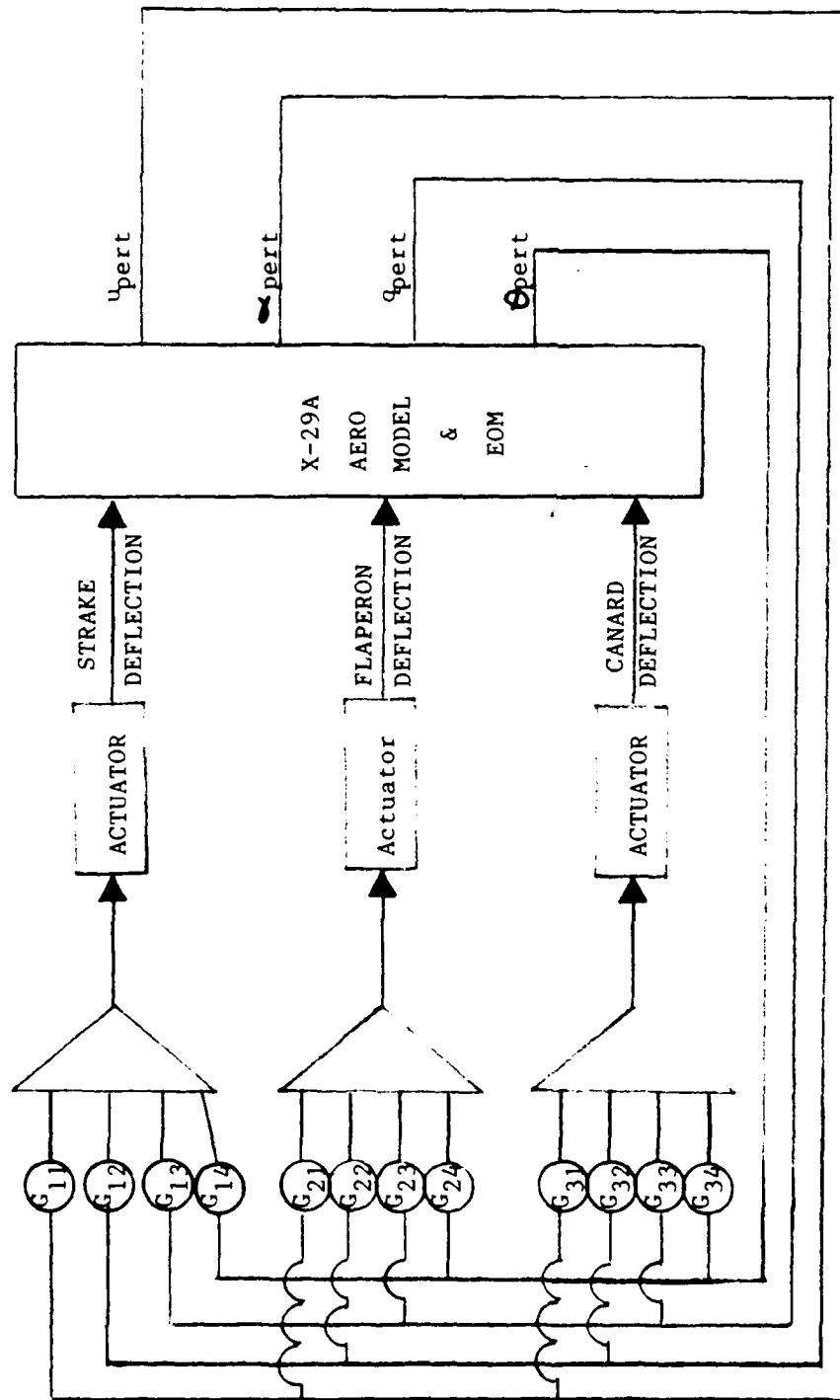
Figure 32. Modified Analog System, No Controller

models were bypassed on the analog computer, the aircraft remained very stable. One of the primary purposes of the flight control system was successfully completed: to make an unstable aircraft behave in a stable manner. A turbulence model was used to provide five ft/sec RMS of simulated turbulence and the aircraft handled it quite well, as seen in the time histories of Figure 33. This showed that a second advantage of feedback had been realized: reducing the effects of disturbances.

One of the attractive parts of the modified control system was that essentially only three summers on the analog computer were used to accomplish this design (keep in mind that the controller was not built yet). The feedback gains, which were now a function of dynamic pressure, were calculated on the digital computer, multiplied by the appropriate state perturbation variable, and sent out to the analog on DACs. The four feedback signals for each of the three control surfaces were summed together to formulate the control surface commands (which in the absence of the actuators were the deflections too). These three control surface commands were read back into the digital computer through ADCs. The commands were used by the aerodynamic model to compute the aerodynamic force and moment coefficients for the equations-of-motion.

In view of the simple nature of the aircraft stabilization system, it was decided to move the modified control path from the analog computer to the digital computer. This would permit a more flexible system to be used during debugging and check-out, allow digital recording of control system variables, and alleviate the magnitude scaling worries of the analog computer. The capability to switch between the standard AR mode and the modified path was

81
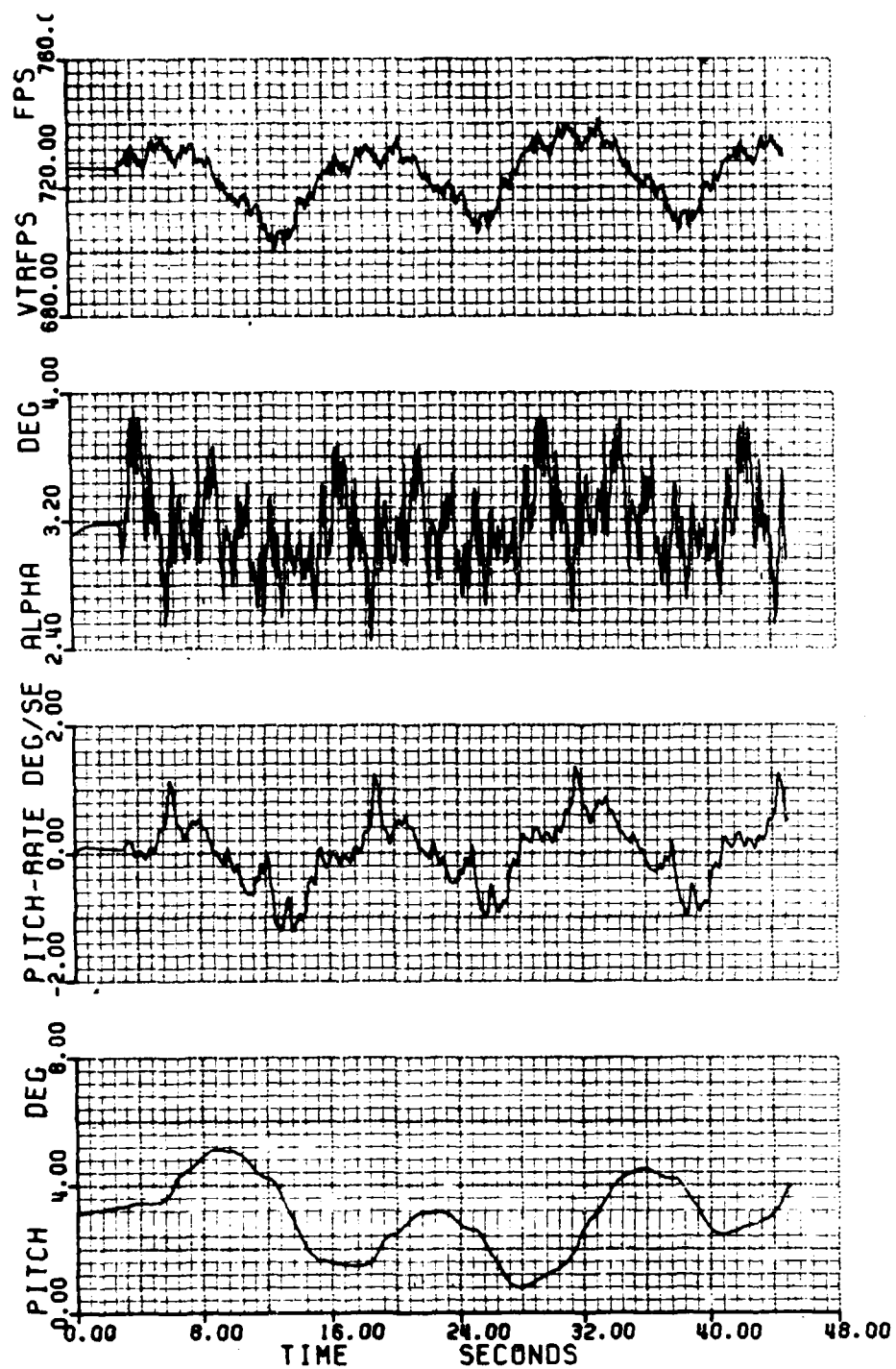
Figure 33. Turbulence Run with Modified Control System

retained, as well as the interface to the analog lateral/directional control path. This switch to the digital computer was the second of the three-step process.

The last step was to design a controller which would allow a pilot to maneuver the aircraft. The controller design was based on a search of the literature and discussions with flight control engineers in the Flight Control Division. Unfortunately, most work being done in the division focuses on the transfer function model, for instance $\theta/\delta_e$. The design of the controller is left to industry. Likewise, most papers on control system design seem to stop at an examination of the transfer functions. For this reason, a trial and error approach was used to design the controller.

Experience indicated that a pitch-rate command, attitude hold system was an appropriate controller to try. Therefore, the stick was made to provide an added pitch-rate perturbation for that particular feedback path. However, due to the large feedback gains on angle-of-attack, this pitch-rate command system had very little effect on the aircraft. Clearly the alpha feedback was providing the static stability for the aircraft and it would need some form of a command if the aircraft was to be successfully maneuvered.

Recall that $a_{z_{cg}} = \dot{w} - U q$ or $a_{z_{cg}} = U_(\dot{\alpha} - q)$. This provided an equation to determine an appropriate alpha command. A stick gradient for both normal acceleration and pitch-rate were devised based on standard X-29A time histories of stick pulses. Thus, a stick deflection resulted in both a normal acceleration command (AZCOM) and pitch-rate command (QCOM) from which an alpha-dot command was calculated

83

according to the equation

$$ALPDOTCOM = AZCOM/UFPS + QCOM \qquad (6.1)$$

ALPDOTCOM was integrated to give an alpha command to be used when calculating the alpha perturbation signal. The disadvantage of this scheme was that while the alpha-dot command would go to zero when the stick wasn't deflected, the alpha command would remain at whatever value it held when the rate went to zero. This would result in the aircraft continuing to change pitch attitude after the stick was released. This, of course, was undesirable. Therefore, logic was introduced into the controller which would integrate the alpha command to zero at a rate of 2 degrees-per-second if the stick was not deflected. The rate of integration was found by experimentation and balanced attitude overshoot (small rate) with pitch bobble (large rate). Since this was essentially an alpha feedback system, the reference for orientation stabilization was the relative wind, whereas for a conventional aircraft it would be the horizon. This resulted in a control system which handled disturbances by trying to maintain a constant angle-of-attack.

The forward velocity and theta perturbation command signals were less of a problem since they primarily provided phugoid stability. In fact, with the strong angle-of-attack feedback, the assumption that the phugoid motion occurs at constant angle-of-attack was even more valid than usual. It should be noted that forward velocity feedback provided very good speed stability. However, since the throttle was not one of the controllers, speed stability was accomplished by varying the total drag of the aircraft through control surface deflections. This feature became unruly when it came to commanded attitude changes and the capability to turn-off

84

the u feedback was added to the simulation.

An attitude hold feature was added for the theta feedback. This was accomplished by having a zero theta perturbation signal while the stick was deflected; when the stick was centered, theta was sampled and used as the reference value until another stick deflection. However, again due to the overwhelming alpha feedback, attitude hold was only marginally successful.

The flight control system appeared as shown in Figure 34. As can be seen, a stick prefilter and stick gain have been added so that the system more closely matches that used in the pilot-model analysis. Digitally controlled stick inputs were used to get aircraft time histories. The response to a four second, one inch stick input is shown in Figures 35-37 for each of the feedback gain sets. The most notable feature is the slow onset of pitch-rate compared to a more conventional design. This is because the system is essentially a position command system which is unusual for up-and-away flight. The difference in response between the three designs is evident. The system designed to yield fair handling qualities is more sluggish and oscillatory than the system designed to yield good handling qualities. As can be seen, the control system designed to give poor handling qualities is divergent in phugoid, as its eigenvalues predicted.

Test Procedure

In order to get the best correlation possible between the pilot-model analysis and the pilot-in-the-loop analysis, the same pitch tracking task used in the Neal-Smith study was used in this simulation [16:23]. Therefore, a series of pitch pulses lasting 110 seconds was programmed and used to

85

Figure 34. Final Flight Control System Configuration

86
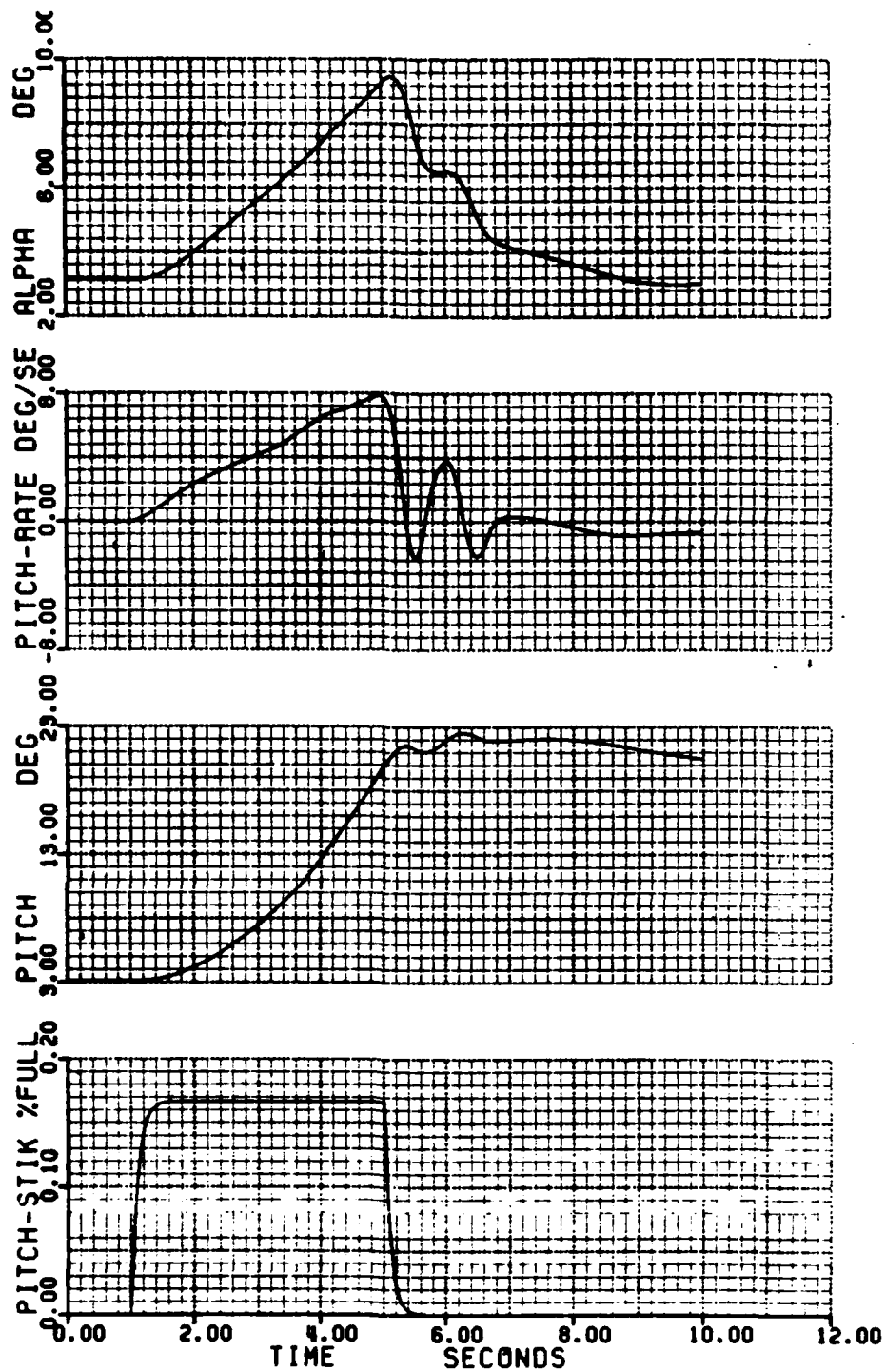
Figure 35.   "Good" System Stick Pulse Response (1 of 2)
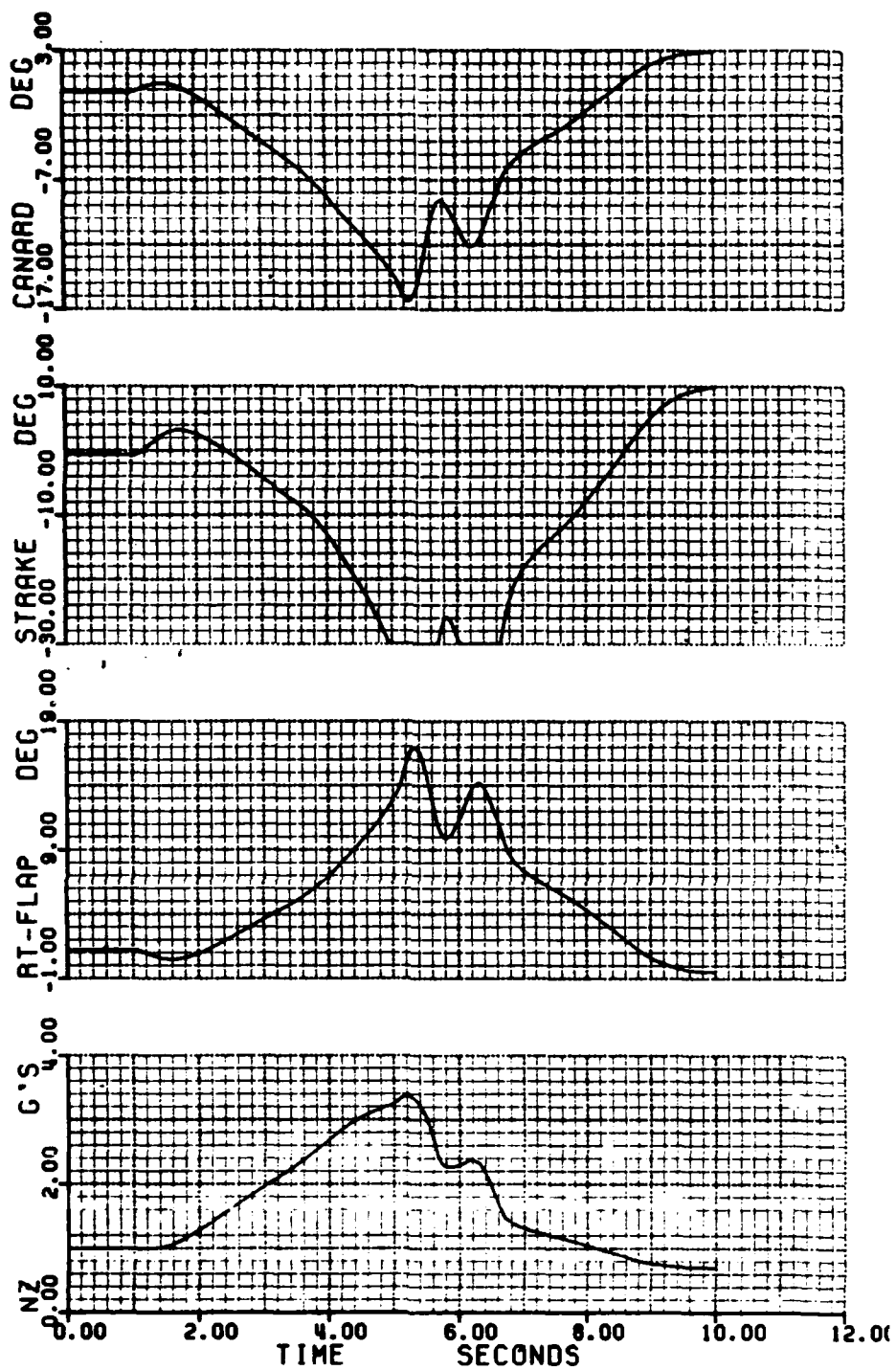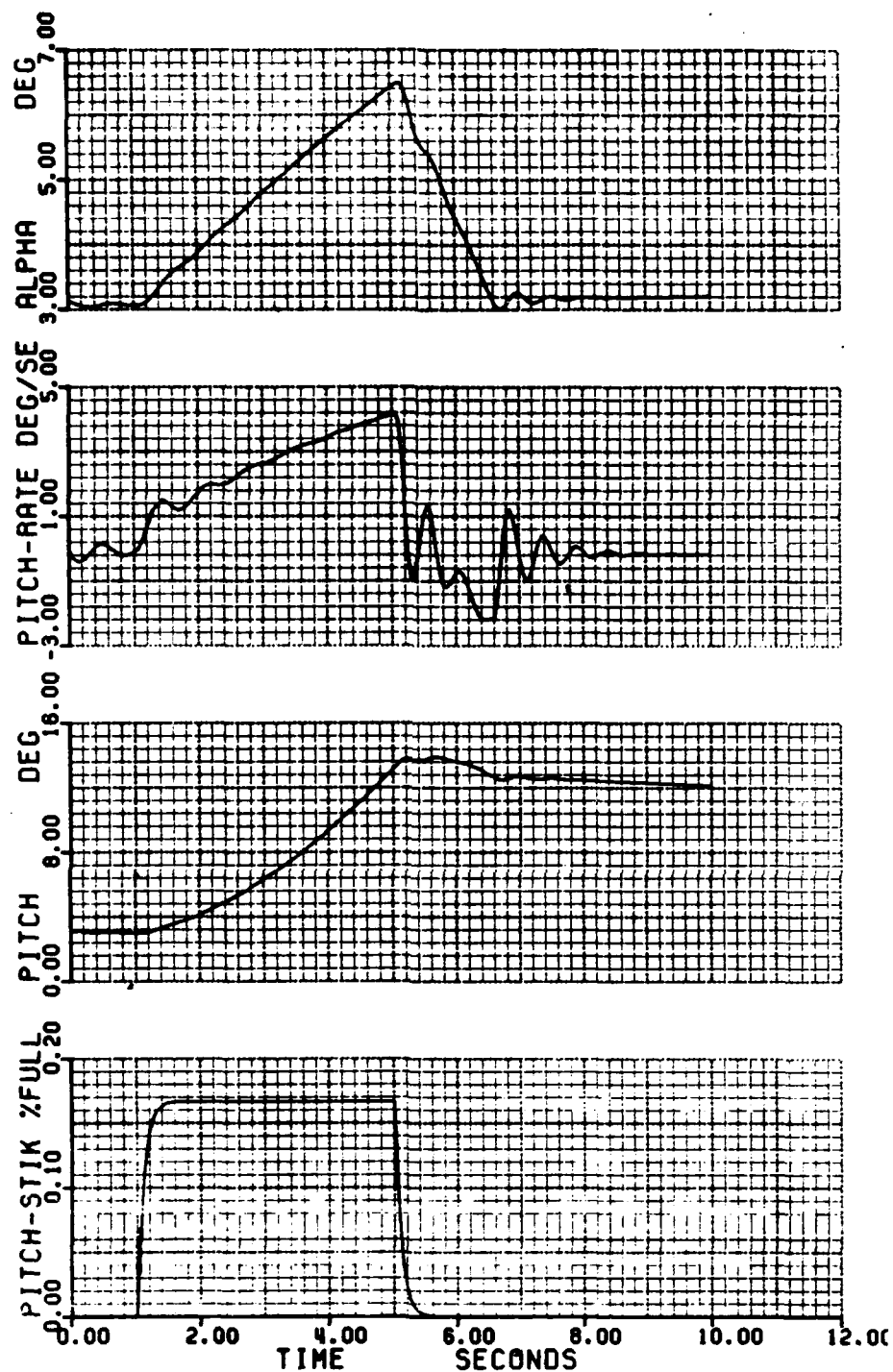
Figure 35. "Good" System Stick Pulse Response (2 of 2)

Figure 36. "Fair" System Stick Pulse Response (1 of 2)

89

Figure 36. "Fair" System Stick Pulse Response (2 of 2)

90
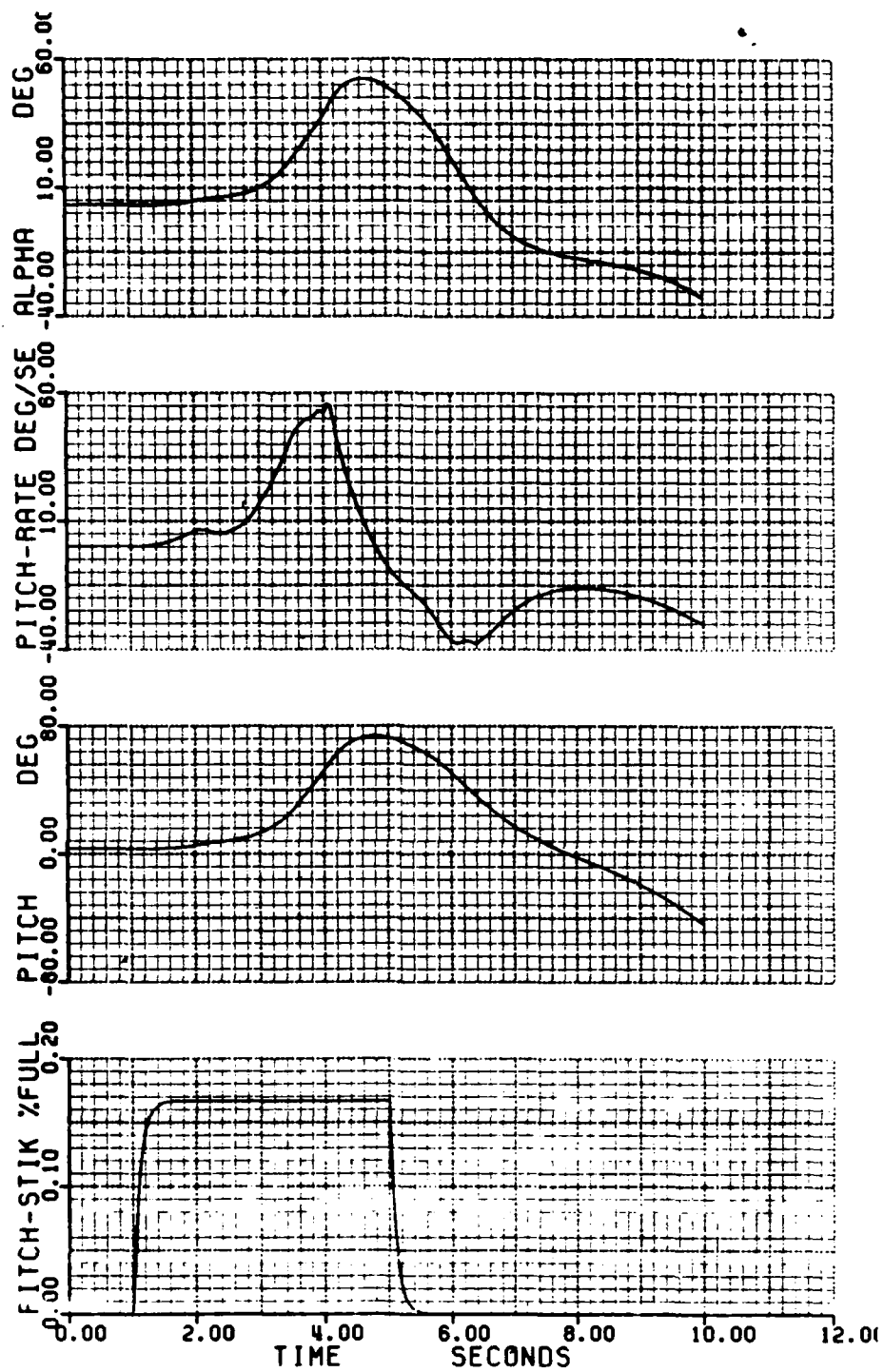
Figure 37. "Poor" System Stick Pulse Response (1 of 2)
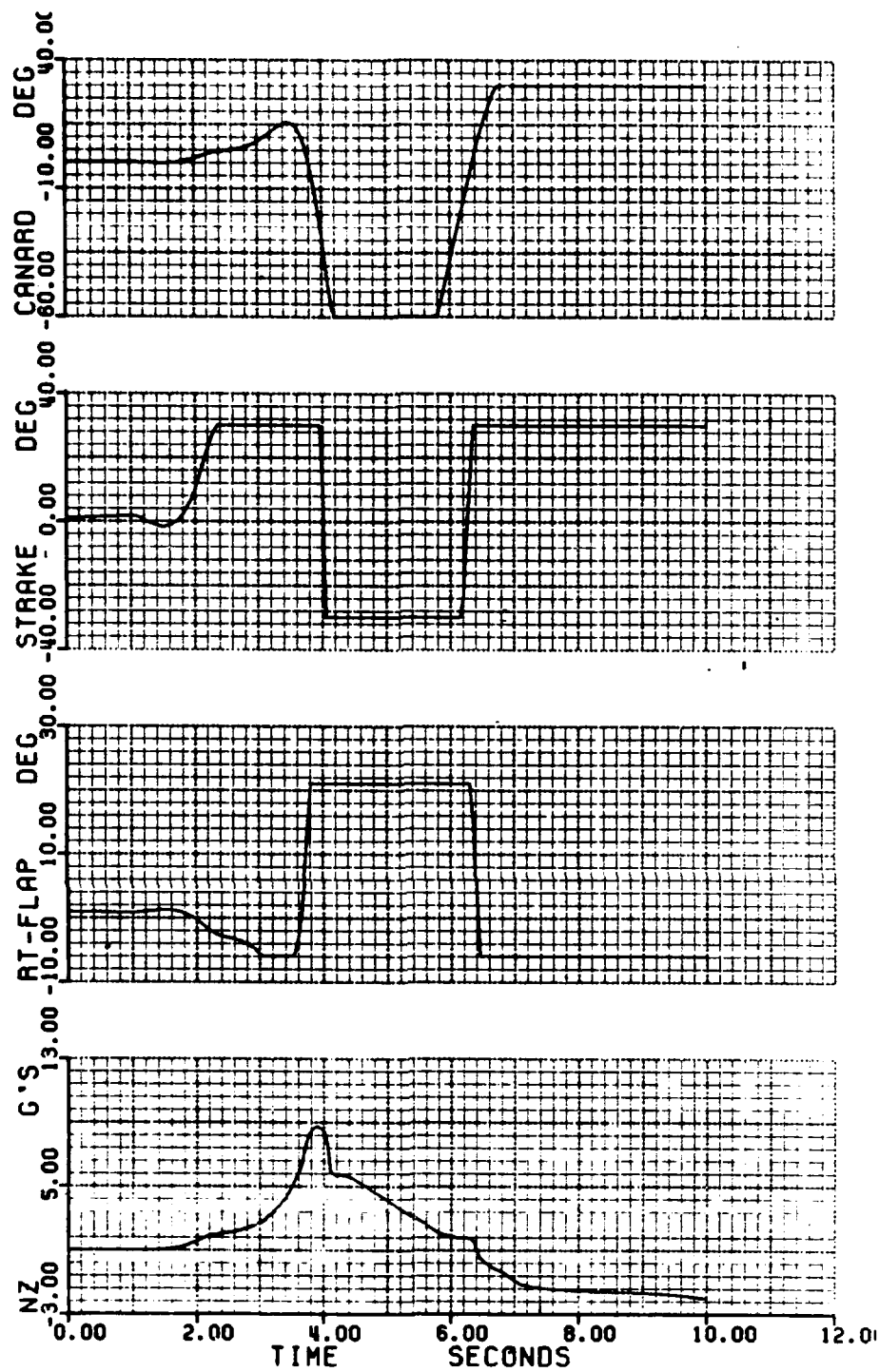
Figure 37. "Poor" System Stick Pulse Response (2 of 2)

drive the pitch command bar on the HUD. It was the test
subjects' task to zero out the error between the command bar
and the pipper. In order to help the test subject remain in
the longitudinal axis only, the lateral/directional
equations-of-motion were fixed. In addition, the test
subject was told to leave the throttle in the trim position
throughout the experiment. As a result, the test subjects
could concentrate on the pitch tracking task alone.

A test matrix was formed which randomized the two
control systems to be evaluated (the third was divergent).
As a control for the experiment, all the test subjects
evaluated the standard AR mode. This provided a baseline by
which to judge the test subjects. Next the subjects flew a
modified system with the u feedback engaged to show that this
configuration was not appropriate. Then the subjects flew
each of the modified systems twice and also each modified
system in turbulence, all without the u feedback. The test
matrix used is shown in Table VI. The test subjects were not
told which system they were evaluating.

Table VI
Test Matrix

| Subject 1 | Subject 2 | Subject 3 | Subject 4 | Subject 5 |
|-----------|-----------|-----------|-----------|-----------|
| AR | AR | AR | AR | AR |
| GOOD* | FAIR* | GOOD* | FAIR* | GOOD* |
| GOOD | FAIR | GOOD | FAIR | GOOD |
| FAIR | GOOD | FAIR | GOOD | GOOD |
| FAIR | GOOD | GOOD | GOOD | FAIR |
| GOOD | FAIR | FAIR | FAIR | FAIR |
| FAIR** | FAIR** | FAIR** | GOOD** | GOOD** |
| GOOD** | GOOD** | GOOD** | FAIR** | FAIR** |

* - flown with speed stability engaged
** - flown in moderate turbulence

93

After each test point, the test subject was asked to give a Cooper-Harper rating (Figure 38), a PIO rating (Figure 39), and any other comments. The comments were recorded by a tape deck interfaced into the intercom system so that they could be analyzed at a later time. Also, digital recording of pertinent simulation variables was made for each run. The results of the simulation study will be presented in the last section.

94

| ADEQUACY FOR SELECTED TASK OR REQUIRED OPERATION | AIRCRAFT CHARACTERISTICS | DEMANDS ON THE PILOT IN SELECTED TASK OR REQUIRED OPERATION | PILOT RATING | FLYING QUALITIES LEVELS |
|---|---|---|---|---|
| | Excellent Highly desirable | Pilot compensation not a factor for desired performance | 1 | |
| | Good Negligible deficiencies | Pilot compensation not a factor for desired performance | 2 | 1 |
| | Fair—some mildly unpleasant deficiencies | Minimal pilot compensation required for desired performance | 3 | |
| | Minor but annoying deficiencies | Desired performance requires moderate pilot compensation | 4 | |
| | Moderately objectionable deficiencies | Adequate performance requires considerable pilot compensation | 5 | 2 |
| | Very objectionable but tolerable deficiencies | Adequate performance requires extensive pilot compensation | 6 | |
| | Major deficiencies | Adequate performance not attainable with maximum tolerable pilot compensation. Controllability not in question. | 7 | |
| | Major deficiencies | Considerable pilot compensation is required for control | 8 | 3 |
| | Major deficiencies | Intense pilot compensation is required to retain control | 9 | |
| | Major deficiencies | Control will be lost during some portion of required operation | 10 | |

Is it satisfactory without improvement?

No — Deficiencies warrant improvement

Yes

Is adequate performance obtainable with a tolerable pilot workload

No — Deficiencies require improvement

Yes

Is it controllable

No — Improvement mandatory

Yes

PILOT DECISIONS

Figure 38. Cooper-Harper Rating Scale

95

| DESCRIPTION | NUMERICAL RATING |
|---|---|
| NO TENDENCY FOR PILOT TO INDUCE UNDESIRABLE MOTIONS | 1 |
| UNDESIRABLE MOTIONS TEND TO OCCUR WHEN PILOT INITIATES ABRUPT MANEUVERS OR ATTEMPTS TIGHT CONTROL. THESE MOTIONS CAN BE PREVENTED OR ELIMINATED BY PILOT TECHNIQUE. | 2 |
| UNDESIRABLE MOTIONS EASILY INDUCED WHEN PILOT INITIATES ABRUPT MANEUVERS OR ATTEMPTS TIGHT CONTROL. THESE MOTIONS CAN BE PREVENTED OR ELIMINATED BUT ONLY AT SACRIFICE TO TASK PER-FORMANCE OR THROUGH CONSIDERABLE PILOT ATTENTION AND EFFORT. | 3 |
| OSCILLATIONS TEND TO DEVELOP WHEN PILOT INITIATES ABRUPT MANEUVERS OR ATTEMPTS TIGHT CONTROL. PILOT MUST REDUCE GAIN OR ABANDON TASK TO RECOVER. | 4 |
| DIVERGENT OSCILLATIONS TEND TO DEVELOP WHEN PILOT INITIATES ABRUPT MANEUVERS OR ATTEMPTS TIGHT CONTROL. PILOT MUST OPEN LOOP BY RELEASING OR FREEZING THE STICK. | 5 |
| DISTURBANCE OR NORMAL PILOT CONTROL MAY CAUSE DIVERGENT OSCILLATION. PILOT MUST OPEN CONTROL LOOP BY RELEASING OR FREEZING THE STICK. | 6 |

Figure 39.   Pilot Induced Oscillation
             (PIO) Rating Scale

# VII.  Results and Recommendations

## LAMARS Results

The man-in-the-loop testing on the LAMARS was the final evaluation tool used in this study.  Five test subjects were selected with flying experience ranging from an Air Force Test Pilot School graduate to an aerobatics private pilot working in the flight controls field.  Four of the test subjects had previous experience flying the LAMARS and evaluating systems on it, and thus were more accustomed to the sensory feedbacks the LAMARS provides.  All testing was accomplished with the pilot "blind" to the particular control system being evaluated.  They were also unaware of total number of different control systems being evaluated.

An average Cooper-Harper rating and PIO rating is given in Table VII for the standard AR mode, the control system designed to yield good handling qualities, the control system designed to yield fair handling qualities, and the runs with turbulence.

Table VII

LAMARS Cooper-Harper and PIO Ratings

| | Standard AR | Good System | Fair System | Turbulence Good | Fair |
|---|---|---|---|---|---|
| Cooper-Harper | 2.6 | 7.5 | 4.3 | 7.5 | 4.0 |
| Standard Deviation | 2.56 | 1.18 | 0.82 | 1.0 | 1.73 |
| PIO | 1.4 | 3.4 | 1.9 | 3.7 | 2.0 |
| Standard Deviation | 0.55 | 0.73 | 0.88 | 0.96 | 0.0 |

Averaging the Cooper-Harper ratings is valid as long as the ratings are all given in the same handling quality level, which was the case for this study. The ratings for each configuration were very consistent, as seen by the standard deviation. Those pilots who flew the same configuration back-to-back showed a definite learning curve and usually gave a better rating the second time. The ratings for the standard X-29A AR mode, which reflects years of development put into the control system, provided a baseline by which to compare the modified control systems.

Comments on the "Good" System. As an overall system, this control law was rated as Level III with significant PIO tendancies. However, a close review of the pilot comments recorded during the testing revealed that for fine tracking the pilots liked the system. Only during the second half of each test run, when gross maneuvers were required, did the complaints of PIO surface. Some typical comments were:

"precise tracking is better...I get into a PIO on gross maneuvers which are almost unstable"

"large inputs are bad...have to add lead to get adequate performance"

"sluggish getting started...large captures are PIO prone"

When asked to give a separate rating for the fine tracking and the gross acqusitions, the fine tracking was given a Cooper-Harper rating in the 3-4 range, whereas the gross acquisition was given a rating in the 7-9 range, with the overall rating being the worse of the two. This disparity between fine tracking and gross maneuvering was discussed recently in a paper describing the AFTI/F-16 control modes [21]. In this paper, it was shown that a

98

deadbeat pitch rate response is best for fine tracking but lacks the quick normal acceleration response needed for gross acquisition. The pitch-rate response for the modified control system allowed very little pitch-rate overshoot and in addition, the normal acceleration build-up was slow. This is believed to have contributed to the PIO problem during large inputs.

Another possible source for the PIO was that the stick was more sensitive than the other control system evaluated. In other words, the system was running with a high gain. The value for the stick gain was selected as a compromise between the best values for the good and fair systems. It was felt that keeping the stick gain constant between the two configurations was necessary for comparison. However, this may have been too restrictive and a smaller stick gain should have been used on the good system.

The portion of the control system to blame for these short-comings is the controller, not the feedback gains arrived at by eigenstructure assignment. As mentioned in Section VI, the controller design was not conventional for an air-to-air tracking task. It is felt that the onset of normal acceleration was slow contributing to the PIO problems. One possible solution to the controller problem would be to force the feedback for static stability to be on pitch-rate instead of angle-of-attack by using output feedback. Then a controller could easily be devised to create a pitch-rate command which would be sufficient to maneuver the aircraft.

As seen by the Cooper-Harper ratings, the addition of a moderate level of turbulence did not significantly degrade the performance of the pilot. This was to be expected since state feedback should damp-out unwanted disturbances.

<u>Comments</u> <u>on</u> <u>the</u> "<u>Fair</u>" <u>System</u>.   This system was rated
Level II, which matched the handling quality level for which
it was designed.   Some of the comments made during the
testing by the pilots were:

"oscillatory...precision control difficult"

"more controllable for large commands"

"annoying bobbles when I stop the stick"

As expected, some of the comments centered on the poor
damping of the overall system.   However, better control over
gross acquisition kept the Cooper-Harper ratings in the
correct level for a system having minor deficiences.   It is
believed that the reason this system did not experience the
PIO problems of the good system was that the stick was less
sensitive.   This resulted in a response which was more
predictable.   Again, turbulence did little to effect task
performance for the fair control system.

As mentioned in an earlier section, the system designed
to give poor handling qualities was nearly divergent, even
without the actuator models.   Therefore this control system
was not evaluated by the test subjects.

## Conclusions

The culmination of this thesis project can be summarized
in four key results:

1) Optimal  A  matrices can be found for the longitudinal
   axis.   This matrix can be weighted toward specific tasks
   or handling quality levels by the judicious selection of
   the handling quality parameters.

2) Eigenstructure assignment with four states and three control surfaces produced an $\tilde{A}$ matrix which had nearly identical dynamic characteristics as the desired $A$ matrix. The necessary projection of the desired eigenvectors onto the range space of the $\tilde{A}$ matrix did not change the eigenvectors dramatically.

3) The Neal-Smith pilot-model analysis revealed that pilot delays, actuator models (especially fourth-order), and control system dynamics will degrade the overall system performance by approximately one handling quality level if these effects are not taken into account when calculating the feedback gains.

4) The LAMARS simulation backed-up the Neal-Smith prediction and the actuator models were removed to get the system performance back closer to that for which it was designed. The type of controller used, in this case an attitude command/attitude hold system, had a significant effect on the handling quality ratings For fine tracking, the Cooper-Harper ratings closely matched those for which the system was designed and moderate levels of turbulence had no significant effect.

Keep in mind that no compensation other than full-state feedback through a simple gain was used to attain these results. It is felt that the technique shows great promise.

Recommendations

A number of areas examined during this project warrant a more comprehensive study. In particular, the

101

man-in-the-loop analysis was abbreviated due to simulator availability. A careful analysis of the simulation could easily be the basis for a follow-on thesis. It would be interesting to apply some system identification techniques to the simulation to determine exactly what the total system dynamics are. A lower-order equivalent system approach could be used by examining some LAMARS time histories and determining whether the system displayed conventional dynamics. A frequency analyzer could be used to obtain Bode plots of the total system. This would show the system gain, bandwidth, phase margin, and gain margin.

A different type of controller could be developed which may yield better results. In particular, the stick gain could be optimized for specific tasks, or a non-linear stick gearing used to get different response rates. Or, as in the AFTI/F-16 paper, a blended controls mechanism could be employed which would require a separate prefilter for the normal acceleration and alpha command paths. Each prefilter would have its own gain which would vary.

Also, as mentioned earlier, output feedback could be used to force the pitch-rate feedback to contain the static stability augmentation. This would allow a more conventional controller to be developed which would permit more control over pitch-rate and normal accelearation commands and responses.

# Bibliography

1. Air Force Wright Aeronautical Laboratories, X-29 ADPO. X-29A Envelope Expansion & Flight Test Results: Industry Briefing. Wright-Patterson AFB OH, 1987.

2. Department of Defense. Military Specification-Flying Qualities of Piloted Airplanes. MIL-F-8785C. Washington: Government Printing Office, November 1980.

3. Moorehouse, D. J. and R. J. Woodcock. Background Information and User Guide for MIL-F-8785C, Military Specification-Flying Qualities of Piloted Airplanes. AFWAL-TR-81-3109. Air Force Wright Aeronautical Laboratories, Wright-Patterson AFB, July 1982.

4. Flight Dynamics Laboratory. Flying Qualities of Piloted Aircraft. Draft MIL-STD-0000. Wright-Patterson AFB, February 1986.

5. McRuer, D., I. Ashkenas, and D. Graham. Aircraft Dynamics and Control. Princeton NJ: Princeton University Press, 1973.

6. Elbert, T. F. Estimation and Control of Systems. New York: Van Nostrand Rheinhold Company, 1984.

7. Reid, J. G. Linear Systems Fundamentals. New York: McGraw-Hill Book Company, 1983.

8. Moore, B. C. "On the Flexibility Offered by State Feedback in Multi-Variable Systems Beyond Closed Loop Eigenvalue Assignment," IEEE Transactions on Automatic Control, 21 (5): 689-692 (October 1976).

9. Klein, G. and B. C. Moore. "Eigenvalue-Generalized Eigenvector Assignment with State Feedback," IEEE Transactions on Automatic Control, 22 (1): 140-141 (February 1977).

10. Srinathkumar, S. "Eigenvalue/Eigenvector Assignment Using Output Feedback," IEEE Transactions on Automatic Control, 23 (1): 79-81 (February 1978).

11. Sobel, K. M. and E. Y. Shapiro. "Design of Decoupled Longitudinal Flight Control Laws Utilizing Eigenspace Assignment," Proceedings of the 1984 American Control Conference, Volume I. 403-408. IEEE Press, New York, 1984.

12. Sobel K. M., E. Y. Shapiro, and R. H. Rooney. "Synthesis of Direct Lift Control Laws Via Eigenstructure Assignment," Proceedings of the IEEE 1984 National Aerospace and Electronics Conference, Volume I. 570-575. IEEE Press, New York, 1984.

13. Andry,Jr., A. N., E. Y. Shapiro, and J. C. Chung. "Eigenstructure Assignment for Linear Systems," IEEE Transactions on Aerospace and Electronics Systems, 19 (5): 711-729 (September 1983).

14. Stein, G. and A. Henke. A Design Procedure and Handling-Quality Criteria for Lateral-Directional Flight Control Systems. AFFDL-TR-70-152. Air Force Flight Dynamics Laboratory, Wright-Patterson AFB, May 1971.

15. Hopper, Capt Michael E. Multi-Input/Multi-Output Designated Eigenstructure (MODES): A Computer-Aided Control System Design Program. MS Thesis, AFIT/GAE/AA/87M-2. School of Engineering, Air Force Institute of Technology (AU), Wright-Patterson AFB Ohio, March 1987.

16. Neal, T. P. and R. E. Smith. An In-Flight Investigation To Develop Control System Design Criteria for Fighter Airplanes. AFFDL-TR-70-74, Vol I. Air Force Flight Dynamics Laboratory, Wright-Patterson AFB, December 1970.

17. Cooper, G. and R. Harper Jr. The Use of Pilot Rating in the Evaluation of Aircraft Handling Qualities. NASA TN-D-5153. April 1969.

18. Gera, J. and others. <u>Linear Analysis of the X-29A Airplane Control Laws in the Limited Envelope</u>. X-84-009. Dryden Flight Research Facility, Ames Research Center, National Aeronatics and Space Administration, October 1984.

19. Etkin, B. <u>Dynamics of Atmospheric Flight</u>. New York: John Wiley & Sons, Inc., 1972.

20. Roskam, J. <u>Airplane Flight Dynamics and Automatic Flight Controls</u>. Lawrence, KA: Roskam Aviation and Engineering Corp., 1979.

21. Toles, R. D. and others. "Application of AFTI/F-16 Task-Tailored Control Modes in Advanced Multirole Fighters," <u>Active Control System - Review, Evaluation and Projections</u>, AGARD-CP-384. Flight Mechanics Panel Symposium, Toronto, Canada, October 1984.
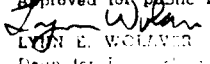
## VITA

Daniel G. Goddard

_entered the University of Cincinnati, majoring in Aerospace Engineering. While participating in the cooperative education program in the engineering college, he spent his work quarters in the Air Force Wright Aeronautical Laboratories at Wright-Patterson AFB, Ohio. In June 1983, he received the degree of Bachelor of Science in Aerospace Engineering and was employed at Wright-Patterson AFB in the Flight Controls Division. Here he worked with man-in-the-loop simulation and was involved in flight control related testing on the X-29A and F-16 LANTIRN programs. In the fall of 1984, he began to take part-time courses at the Air Force Institue of Technology. In January of 1987, he began three quarters of full-time study under the civilian Long-Term, Full-Time training program. He is a member of the American Institute of Aeronautics and Astronautics.

# REPORT DOCUMENTATION PAGE

Form Approved
OMB No. 0704-0188

| 1a. REPORT SECURITY CLASSIFICATION | 1b. RESTRICTIVE MARKINGS |
|---|---|
| UNCLASSIFIED | NONE |

| 2a. SECURITY CLASSIFICATION AUTHORITY | 3. DISTRIBUTION/AVAILABILITY OF REPORT |
|---|---|
| | Approved for public release; |
| 2b. DECLASSIFICATION/DOWNGRADING SCHEDULE | distribution unlimited. |

| 4. PERFORMING ORGANIZATION REPORT NUMBER(S) | 5. MONITORING ORGANIZATION REPORT NUMBER(S) |
|---|---|
| AFIT/GAE/AA/87S-2 | |

| 6a. NAME OF PERFORMING ORGANIZATION | 6b. OFFICE SYMBOL (If applicable) | 7a. NAME OF MONITORING ORGANIZATION |
|---|---|---|
| School of Engineering | AFIT/ENG | |

| 6c. ADDRESS (City, State, and ZIP Code) | 7b. ADDRESS (City, State, and ZIP Code) |
|---|---|
| Air Force Institute of Technology (AU) Wright-Patterson AFB OH 45433-6583 | |

| 8a. NAME OF FUNDING/SPONSORING ORGANIZATION | 8b. OFFICE SYMBOL (If applicable) | 9. PROCUREMENT INSTRUMENT IDENTIFICATION NUMBER |
|---|---|---|
| | | |

| 8c. ADDRESS (City, State, and ZIP Code) | 10. SOURCE OF FUNDING NUMBERS | | | |
|---|---|---|---|---|
| | PROGRAM ELEMENT NO. | PROJECT NO. | TASK NO | WORK UNIT ACCESSION NO. |
| | | | | |

11. TITLE (Include Security Classification)

APPLICATION OF EIGENSTRUCTURE ASSIGNMENT TECHNIQUES IN THE DESIGN OF A LONGITUDINAL FLIGHT CONTROL SYSTEM

12. PERSONAL AUTHOR(S)
Daniel G. Goddard

| 13a. TYPE OF REPORT | 13b. TIME COVERED | 14. DATE OF REPORT (Year, Month, Day) | 15. PAGE COUNT |
|---|---|---|---|
| MS Thesis | FROM _____ TO _____ | 1987, September | 120 |

16. SUPPLEMENTARY NOTATION

| 17. COSATI CODES | | | 18. SUBJECT TERMS (Continue on reverse if necessary and identify by block number) |
|---|---|---|---|
| FIELD | GROUP | SUB-GROUP | Flight Control Systems, Eigenvalues, Eigenvectors, |
| 01 | 04 | | Flight Simulation, Sweptforward Wings |

19. ABSTRACT (Continue on reverse if necessary and identify by block number)

Thesis Advisor:  Capt Daniel Gleason

Approved for public release: IAW AFR 190-1/.

LYNN E. WOLAVER                 2Y Feb 87
Dean for Research & Professional Development
Air Force Institute of Technology (ATC)
Wright-Patterson AFB OH 45433

| 20. DISTRIBUTION/AVAILABILITY OF ABSTRACT | 21. ABSTRACT SECURITY CLASSIFICATION |
|---|---|
| [X] UNCLASSIFIED/UNLIMITED   [ ] SAME AS RPT   [ ] DTIC USERS | UNCLASSIEFIED |
| 22a. NAME OF RESPONSIBLE INDIVIDUAL | 22b. TELEPHONE (Include Area Code) | 22c. OFFICE SYMBOL |
| Capt Dan Gleason, Instructor | (513) 255-2362 | AFIT/ENY |

**DD Form 1473, JUN 86**          Previous editions are obsolete.          SECURITY CLASSIFICATION OF THIS PAGE

UNCLASSIFIED

ABSTRACT

The use of eigenstructure assignment techniques has received wide attention as a tool for designing flight control systems for aircraft with multiple control surfaces. One drawback for using this technique is a lack of handling quality guidelines to apply when selecting the eigenvalues and eigenvectors of the closed-loop system. This lack of specific eigenstructure requirements means that some uncertainty will remain as to whether the augmented control system will meet the MIL-F-8785C specifications.

Therefore, development of a method for choosing the desired eigenstructure of the augmented, closed-loop system which would meet the handling qualities specifications was examined. This method consisted of forming an "optimal" plant matrix which possessed desirable dynamic characteristics and performing a spectral decomposition of this matrix. The resulting eigenstructure was used as the desired eigenvalues and eigenvectors during the full-state feedback, eigenstructure assignment process. The resulting feedback gain matrix was used in the control system.

As an example, this process was performed on a model of the X-29A using the canard, flaperon, and strake flap control surfaces. The resulting augmented system was evaluated using the Neal-Smith pilot-model analysis and also using an X-29A man-in-the-loop simulation. The results show that the method is very promising, although care must be taken that all anticipated control system dynamics are considered when forming the optimal A matrix.